Considerations in the Selection of the Operating Regimes for Microfiltration

Andrew Fugard Swart

Submitted in fulfillment of the
academic requirements for the degree of
Master of Science
Faculty of Engineering
in the
Department of Chemical Engineering
University of Natal

Durban, December 1993

Abstract

The two distinct operating modes of microfiltration are dead-end and cross-flow. The choice of operating mode is made on the basis of minimum power and area cost as well the quality of the permeate that is produced. The power cost of operation in the dead-end mode is less than in the cross-flow mode due to the lower tangential velocities. The parameter that was thus investigated was the area cost which was given by the relative quantity of permeate produced.

A suspension made up of equal proportions of bentonite and kaolin was used to investigate the operating modes of microfiltration at feed concentrations less than 1 000 mg/ℓ. Flux and permeate quality data are presented and the relative quantities of permeate produced are evaluated.

Operation in the dead-end mode was shown to give a significant enhancement over cross-flow in the low concentration range (< 300 mg/ℓ) provided the operation in the dead-end mode was preceded by precoating in the cross-flow mode with a limestone suspension. The dissertation does not determine the exact cross-over point nor does it develop a model for determining the operating regime. Rather, it outlines observed experimental trends and develops the *modus operandi* for a more precise determination of the economic choice of operating mode.

This dissertation is dedicated to my parents

Preface

I hereby declare that this dissertation is my own work, unless stated to the contrary in the text, and that it has not been submitted in part, or in whole to any other University or Institution. The research was carried out at the University of Natal, Durban in the Department of Chemical Engineering. The supervisor for the work was Prof. C.A. Buckley. The work was carried out as part of the Water Research Commission Project No. 238, Research on the Design Criteria for Cross-flow Microfiltration.

A.F. Swart

December 1993

Acknowledgements

This dissertation has been more than simply completing a project. It has been a time of growth and development, a time where I have learnt as much about a new and growing field as I have about myself. All of this however, would not have been possible or as rewarding were it not for the following people or organisations.

(i) I am first and foremost indebted to Professor Chris Buckley for all his guidance, help, encouragement and trust throughout the project. I thank him for the opportunities and atmosphere that he created in the research group, that made the project and time spent so worthwhile.

(ii) Dr Lingam Pillay, for his advice and help throughout the study. I thank him for making the time spent in the Department thoroughly rewarding and enjoyable. I must also thank him for the many intellectual conversations that were held after hours and which undoubtedly led to the final success of this project.

(iii) Mr Chris Brouckaert for his wisdom and direction. I must also thank him for writing the regression software and his help throughout.

(iv) Dr Gunter Rencken, for his help, assistance and time.

(v) Explochem for the use of equipment and help in obtaining the fabric tubes. In particular mention must be made of Mr Kevin Treffry-Goatley, who provided a great deal of assistance.

(vi) Ms Karen Mitchley for her patience and support during this study. I must thank her for accommodating my odd time schedules, spending so many hours with me in the department and putting up with my frustrations during many parts of the project.

(vii) My parents for their continued interest and encouragement.

(viii) The staff of the department of Chemical Engineering Workshop for their assistance in constructing the experimental apparatus.

(ix) The secretaries of the Pollution Research Group, Mrs N Kissoon and Mrs M Thotharam for their work behind the scenes which is often overlooked but never forgotten. Thank you!

(x) The Water Research Commission for funding the project.

(xi) Anglo American Corporation of SA Ltd for allowing me to continue my studies. I must also thank them for the financial assistance that was provided. It is my sincere hope that the Corporation will allow other students to do the same, it was a time of invaluable study and I am sure that in the long term the Corporation will reap the benefits of their investment.

(xii) The Computing Centre for Water Research, University of Natal, Pietermaritzburg for the use of their computing facilities.

(xiii) The patrons of Scully Hall, in particular Mr James Trinder for putting me on the *right track* so many times during the study. Many process and design problems were solved at this venue and credit must go to these late night owls.

(xiv) My fellow postgraduate students, who made the time spent exceedingly interesting and enjoyable. I am sure that the artistic flare developed during this time will stand me in good stead.

(xv) The academic and services staff of the Department of Chemical Engineering, for helping me in so many ways, directly and indirectly.

(xvi) Dr Norton de Benito, for challenging many aspects of the establishment and serving as an inspiration to postgraduates past and present.

(xvii) Finally, to my friends outside the department without whom none of this would have been worthwhile. I would like to especially single out Mrs Sarah Wright, the residents of Ridgeview Heights and patrons of the Bulldog, thank you and may our paths cross again.

Table of Contents

CHAPTER 3 : SUSPENSION AND FABRIC CHARACTERIZATION

CHAPTER 4 : EXPERIMENTAL WORK

List of Figures

CHAPTER 3

CHAPTER 4

CHAPTER 5

APPENDIX A

APPENDIX B

APPENDIX C

List of Tables

List of Symbols

a	area (m^2)
A	regressed constant in the CFMF regression model (-)
b	constant (s/m^2)
B	regressed constant in the CFMF regression model (-)
c	concentration (g/ℓ)
c_b	particle concentration in the bulk suspension - polarization model (g/ℓ)
c_f	concentration of the feed (g/ℓ)
c_i	concentration at the inlet of the tube (g/ℓ)
c_o	concentration of the reject (g/ℓ)
c_s	mass of dry solids per unit volume of suspension (kg/m^3)
c_w	particle concentration at the membrane surface - polarization model (g/ℓ)
C	regressed constant in the CFMF regression model (-)
d	internal tube diameter (m)
d_{50}	arithmetic mean particle size (μm)
D	regressed constant in the CFMF regression model (-)
f_1	function of v, c, p, l, t_c (ℓ/m^2h)
F_F	feed flowrate (m^3/h)
F_O	reject flowrate (m^3/h)
F_P	permeate flowrate (m^3/h)

F_R	recycle flowrate (m^3/h)
J_{CFMF}	average CFMF flux along the tube length ($\ell/m^2.h$)
J_{DEMF}	average DEMF flux along the tube length ($\ell/m^2.h$)
$k(x)$	local mass transfer coefficient between the bulk suspension and the concentrated regime next to the wall (m/s)
$k_m(x)$	effective diffusion coefficient - Zydney and Colton (m/s)
k_o	coefficient of earth pressure at rest (-)
K	local permeability of the filter cake or sediment (m^2)
l	tube length (m)
P	operating pressure (gauge) during the filtration cycle (Pa)
p_i	inlet pressure of the tube (Pa)
p_L	liquid pressure in Rencken's model (Pa)
p_s	solids compressive pressure in Rencken's model (Pa)
P	pressure drop across the filter cake (Pa)
Q	overall volumetric flowrate of liquid (filtrate) per unit length of filter tube in Rencken's model ($m^3/m.s$)
r	radial distance in Rencken's model (m)
r_p	particle radius (m)
R_m	resistance of the filter cloth (1/m)
SDI_T	silt density index (-)
t	time (s)
t_c	cycle time (s)
t_d	down time (s)
t_{dp}	time to deposit a mass w_c of cake (s)
t_f	time required to collect 500 mℓ of SDI permeate after an elapsed test time of T (s)

t_i	initial time required to collect 500 mℓ of permeate from the SDI apparatus, (s)
t_o	time from the beginning of the cycle (s)
t_p	production time (s)
t_{perm}	the time taken to measure a quantity of permeate (s)
T	total elapsed flow time for the SDI (min)
v	superficial suspension velocity (m/s)
v_i	superficial inlet velocity (m/s)
V_a	volume of filtrate per unit medium area (m^3/m^2)
V_t	tank volume (m^3)
$V(t, l)$	volume of permeate produced on a tube of length l and up to a time t (m^3)
w_c	total mass of dry cake solids deposited per unit medium area (kg/m^2)
x	axial distance co-ordinate along the tube (m)
X	regressed constant in the DEMF regression model (-)
Y	regressed constant in the DEMF regression model (-)
Z	regressed constant in the DEMF regression model (-)
α_{av}	average specific filtration resistance of the cake (m/kg)
$\Delta_{FLUX,l}$	difference in permeate volume produced per area of the DEMF relative to the CFMF (ℓ/m^2)
$\Delta_{\%}$	relative % improvement of the permeate volume produced per area of the DEMF relative to the CFMF
ϕ	instantaneous flux at a point along a tube ($\ell/m^2.h$)
τ	integration variable (-)
τ_w	shear rate at the wall (1/s)
μ	viscosity of the liquid filtrate (Pa.s)

List of Abbreviations

CFMF	Cross-flow Microfilter
DEMF	Dead-end Microfilter
TFP	Tubular Filter Press
C-P	Compression-permeability
SDI	Silt Density Index
UF	Ultrafiltration

CHAPTER

ONE

Introduction

1.1 INTRODUCTION

The Cross-flow Microfilter (CFMF) and the Tubular Filter Press (TFP), as developed by RENOVEXX Technology Ltd[1]. have different applications. Although both the CFMF and the TFP enable the removal of solids from suspensions, the CFMF has been used as a clarifier or thickener while the TFP has conventionally been used to de-water concentrated suspensions and produce a spadeable cake.

Despite the differing applications, the two processes share much in common. Both the CFMF and the TFP use the same tubular woven polyester fabric support and it will be shown that the TFP represents an extreme operating condition of the CFMF. The two processes will first be introduced and then the focus of the thesis set out.

1.1.1 The Cross-flow Microfilter

A process where species in solution or suspension are passed tangential to a barrier or membrane, resulting in a retention of those species, is termed a *cross-flow separation process*. Cross-flow microfiltration is distinguished from ultrafiltration and reverse osmosis, by the size of the rejected species (Fig. 1.1). In microfiltration, discrete particles are retained as opposed to reverse osmosis and ultrafiltration where dissolved salts and macromolecules respectively, are retained.

1 RENOVEXX Technology Ltd, Kitty Brewster Industrial Estate, Blyth, Northumberland, NE2457B, UK

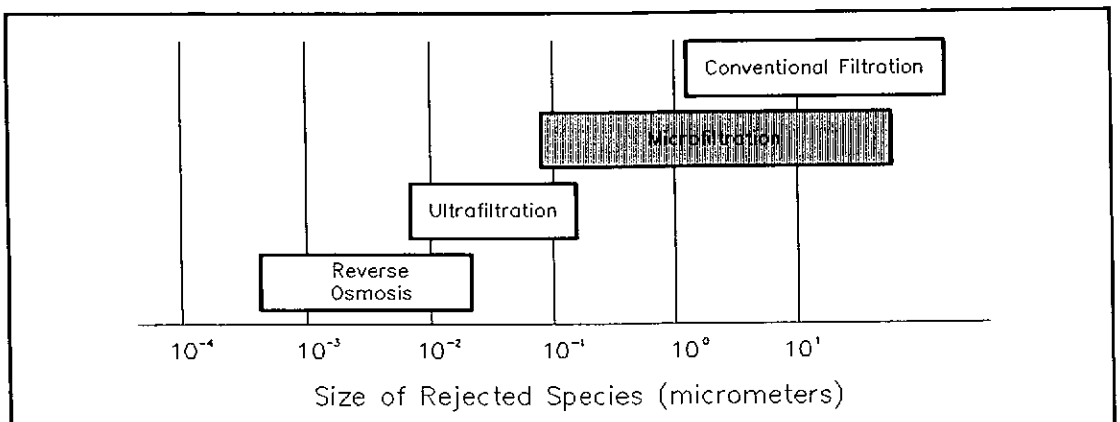

Figure 1.1 : Diagram showing the differentiation between cross-flow processes on the basis of the size of the rejected species. The diagram was reproduced from Schneider & Klein [1982]

Cross-flow microfiltration is a means of clarifying or thickening a suspension. A number of cross-flow microfiltration systems [Zaidi *et al.*, 1992] utilising a range of membranes and supports are currently available. The most common system uses a manufactured synthetic membrane on a porous support. The system that was investigated in this thesis, is the EXXFLOW Cross-flow Microfilter which uses a woven polyester tube as the membrane support and the deposited solids as the dynamic membrane [Pillay, 1992a; Squires, 1992].

A slurry is pumped into the array of horizontal collapsible fabric tubes. Suspended solids are deposited onto the inside tube wall, forming a cake which acts as a filtration barrier or membrane (See Fig. 1.2). The thickness of the cake increases initially as solids are deposited, but is limited by the tangential shearing action of the bulk suspension. A clarified liquid, driven by the pressure difference across the barrier, permeates through the tube wall and a thickened stream is rejected. The permeate flux is initially high, but decreases as the hydraulic resistance of the cake increases with time.

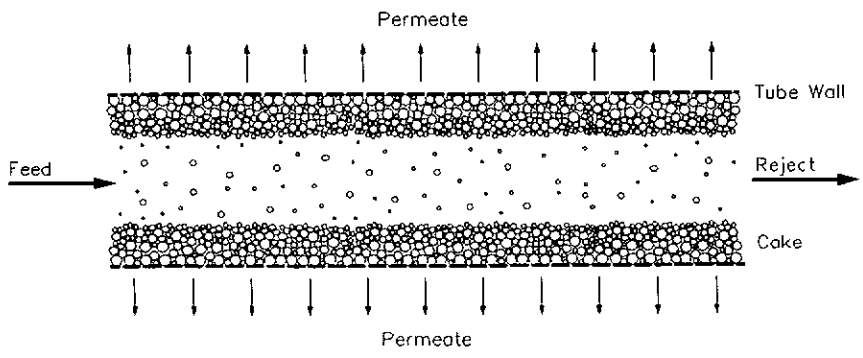

Figure 1.2 : Illustration of cross-flow microfiltration in a porous tube, where a cake is deposited along the tube wall

A schematic diagram of the CFMF system is shown in Fig. 1.3.

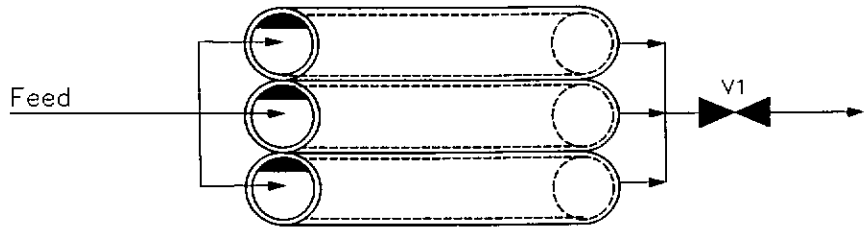

Figure 1.3 : Illustration of the EXXFLOW Cross-flow Microfiltration System

After passing through the array of tubes, the thickened stream can either be continuously purged from the system or thickened further by returning the reject stream to the feed. The valve V1 acts as a back-pressure valve.

The declining flux may be restored by a number of cleaning methods. Pinch-roller, spray or brush cleaning methods are used to dislodge the fouling layer from woven fabric tubes. In Fig. 1.4, the pinch roller method is illustrated where rollers are engaged, squeezing the tube, causing a venturi effect. The cake is then scoured off the fabric as the feed is pumped through the restriction and the rollers move along the length of the curtain. Backflushing, flow pulsating or sponge ball cleaning are commonly employed for other rigid membrane systems.

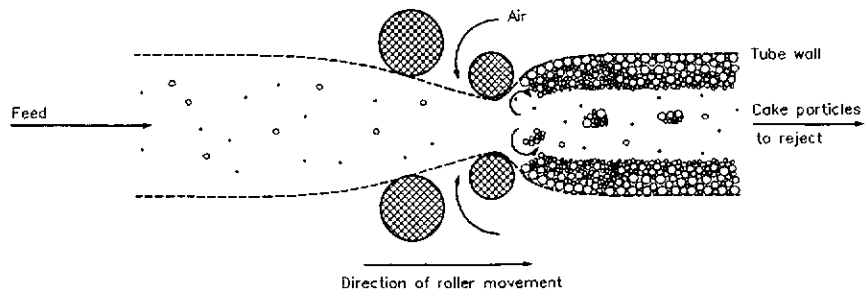

Figure 1.4 : Illustration of the pinch-roller method of cleaning woven tubes

1.1.2 The Tubular Filter Press

The EXXPRESS Tubular Filter Press (TFP) is a dead-ended filtration process. It was developed by the Pollution Research Group, University of Natal, under a Water Research Commission grant [Treffry-Goatley & Buckley, 1987]. The TFP was developed as a cake recovery process.

It should be stressed that the difference between the CFMF and the TFP is that the TFP is operated in a dead-end mode with V1 closed (Fig. 1.3) as opposed to the CFMF where V1 is open. The TFP process, like the CFMF, is characterised by two cycles, a cake deposition and a cleaning cycle. During the cake deposition cycle, the slurry is fed into the array of porous fabric tubes. The valve V1 is closed and the cake is deposited on the inside tube wall. When the filtration rate has declined to a set level, the cleaning cycle is started. The valve V1 is then opened and pieces of the cake are dislodged by a roller device (Fig. 1.4), a spray cleaner or brushes and hydraulically transported out of the tubes.

The TFP may be viewed as a limiting case of the CFMF where the cross-flow velocity is close to zero.

1.1.3 Previous Applications of Cross-flow Microfiltration and the Tubular Filter Press

The areas of application have been different for the two processes; the CFMF has been used to clarify suspensions and act as a thickener with a view to producing a high quality permeate, while the TFP has been used as a cake recovery process.

Cross-flow filtration has found application in a diverse range of industries such as the treatment of municipal and industrial wastewater streams, biotechnology and water treatment (Table 1.1).

The use of conventional dead-end and depth filtration is a widely documented subject. Literature on the tubular filter press is however limited to work undertaken at the University of Natal and by EXXPRESS Technology Limited[2]. Some documented applications of the TFP have been to de-water sludges from a power station and a waterwork's sludge [Rencken, 1992; Treffry-Goatley *et al.*, 1987].

2 Enquiries to RENOVEXX Technology Limited

Application	Reference
Municipal Waste Water	
Concentration of waste activated sludge	Bindoff *et al.*, 1988
Treatment of primary sewage	Perona *et al.*, 1974
Biotechnology	
Separation of bacteria, cell debris and micro-organisms from growth media and natural waters	Eriksson, 1985 Kuwabara & Harvey, 1990 Mackay & Salusbury, 1988 Tanny *et al.*, 1982
Separation of particulate matter and proteins from cheese whey	Hanemaaijer, 1985 Tanny *et al.*, 1982
Retention of biomass in biological reactors	Pillay, 1992b Saw *et al.*, 1985
Recovery of beer tank bottoms	Le, 1987 Shackleton, 1987
Applications in the food industry	Van der Horst & Hanemaaijer, 1990
Industrial Wastewater Streams	
Recovery of heavy metals	Gassel & Ripperger, 1985
Removal of heavy metals	Squires, 1992
Recovery of crystalline material from electronic industry waste streams	Klein & Hoelz, 1982
Concentration and washing of magnesium hydroxide	Klein & Hoelz, 1982
Concentration of nickel hydroxide sludge from an ion exchanger	Klein & Hoelz, 1982
Recovery of dispersed catalyst particles	Gassel & Ripperger, 1985
Separation of oil/water emulsions	Murkes, 1986 Tanny & Hauk, 1980
Treatment of Water	
Removal of algal blooms from sea-water	Holdich & Zhang, 1991
Removal of hardness from brackish water	Sheppard & Thomas, 1974

Table 1.1 : Applications of cross-flow microfiltration filtration in various industries

1.1.4 Project Background

The CFMF and the TFP are both processes for the removal of solids from suspensions. The CFMF operates at a high velocity and is used to clarify dilute suspensions. The TFP operates in a *dead-ended cross-flow* mode, and has previously been used to de-water concentrated suspensions and produce a spadeable cake.

The University of Natal has performed various investigations [Pillay, 1992a; Pillay, 1992b; Rencken, 1992; Treffry-Goatley *et al.*, 1987] on both the CFMF and the TFP using various concentrated suspensions (10 to 100 g/ℓ). Tubular woven polyester supports were used in these studies. At these concentrations the permeate production rates from the CFMF were significantly higher than the TFP. Hence, for suspensions with high

suspended solids (10 to 100 g/ℓ), the CFMF would be the preferred process for maximum permeate production. It should also be noted that the hydraulic power required by the TFP is less than that for the CFMF due to the lower operating velocities.

At low solids concentrations typical of river water (10 to 1 000 mg/ℓ), it was thought that the permeate production rates of the TFP and the CFMF might be of similar magnitude. Under these circumstances it might be feasible to operate the tubular filter in a dead-end mode or what has been termed the TFP. It would then be necessary to optimise the filter to produce a clear permeate as opposed to maximising the recovery of suspended solids.

It would be incorrect to label this process as a TFP and hence it will be referred to as a Dead-end Microfilter or DEMF. As stated previously, the DEMF should be seen as a limiting case of the CFMF where the cross-flow velocity is close to zero.

The choice between the processes (CFMF and DEMF) would be resolved according to the performance, namely the permeate quality, the required area and the hydraulic power.

1.1.5 Project Objectives

The aims of the project were as follows :

i) To obtain flux and permeate quality data for the CFMF and the DEMF, using a low suspended solids water (< 1 000 mg/ℓ)

ii) To compare the performance of the two processes and to develop criteria for their selection.

1.1.6 Thesis Outline

The remainder of the dissertation is divided into five chapters.

Chapter Two first deals with past attempts to model CFMF and the TFP. This chapter serves as background to concepts or theories that are mentioned later. The chapter then deals with specific operating modes of the CFMF. The theoretical basis to these operating modes are developed to show the inter-dependence of the variables and also to lay down the basis for choosing the operating mode of the CFMF.

Once the theory has been developed, the study focuses on the experimental system itself. Before the experimental procedure is outlined, the basis for choosing the specific suspension is documented in **Chapter Three**. In order to provide some insight into the mechanisms and the peculiarities of fabric tubes, information is provided about the manufacture and preparation of the experimental tubes. A great deal of work went into optimising the experimental tube itself, and documenting it in this way provides insight into the experimental results that are presented in Chapter Five.

Chapter Four deals with the experimental system and procedure. It covers the start-up and operational procedure as well as outlining the method used to control and measure the experimental variables. **Chapter Four** also deals with error estimation.

The experimental results are presented in **Chapter Five.** The results for CFMF and DEMF are first presented separately, before they are compared on common graphs. The results are discussed and compared with work done by other researchers. The results are then taken and a simple model is developed which establishes the trends for the selection of the CFMF or the DEMF.

Chapter Six concludes the study.

CHAPTER

TWO

Theory

The objectives of the project were not to model the CFMF or the DEMF, but to evaluate comparatively the performance of the processes at low suspended solids concentrations. There is merit however, in outlining various attempts that have been made to model the phenomena associated with the two processes in order to highlight the important variables. The modelling of the DEMF will be set out in terms of the tubular filter press, since, although the aims of the DEMF and the TFP are different, the mechanisms associated with each process are similar.

2.1 TUBULAR FILTER PRESS

2.1.1 Simplified Model

The simplest way to model the TFP process is to assume that the cake formed in the tube is thin compared to the internal diameter of the tube, so that the filtration equations for a planar configuration are valid.

The following conventional planar filtration equation for both a compressible and incompressible cake has been derived in a variety of texts [Coulson & Richardson, 1978; Rencken, 1992].

$$\frac{dV_a}{dt} = \frac{P}{\mu(\alpha_{av} w_c V_a + R_m)} \tag{2.1}$$

where P = pressure drop across the filter cake, (Pa)

R_m = resistance of the filter cloth, (1/m)

t = time, (s)

V_a = volume of the filtrate per unit medium area, (m^3/m^2)

w_c = total mass of dry cake solids deposited per unit medium area, (kg/m^2)

α_{av} = average specific filtration resistance of the cake, (m/kg)

μ = viscosity of the liquid filtrate, (Pa.s)

If it is assumed that the resistance of the filter cloth, R_m is negligible in relation to the resistance of the cake then Eqn. (2.1) may be rewritten as :

$$\frac{dt}{dV_a} = \frac{\mu \alpha_{av} w_c}{P} \tag{2.2}$$

Now, if the quantity of solids in the permeate is negligible in comparison to the bulk feed concentration and the volume of water in the cake is negligible compared to the filtrate volume, then w_c may be rewritten in terms of V_a as :

$$w_c = c_s V_a \tag{2.3}$$

where c_s = mass of dry solids per unit volume of suspension, (kg/m^3)

Now, rewriting Eqn. (2.2) :

$$\frac{dt}{dV_a} = \frac{\mu \alpha_{av} c_s V_a}{P} \tag{2.4}$$

The specific cake resistance may be determined from the slope of a plot of dt/dV_a against V_a using the results from a constant pressure filtration test.

The time to deposit a mass of solids on the filter cloth can be obtained by integrating Eqn. (2.4) with respect to V_a. Integration with C_s constant yields :

$$t = \frac{\mu \alpha_{av} c_s V_a^2}{2P} \tag{2.5}$$

Substituting Eqn. (2.3) into Eqn. (2.5) gives :

$$t_{dp} = \frac{\mu \alpha_{av} w_c^2}{2 P c_s} \tag{2.6}$$

where t_{dp} = time to deposit a mass w_c of cake, (s)

In this study the optimum recovery of suspended solids was not considered; rather the production of a high quality permeate was the primary concern. It was therefore useful to develop a general form for the flux - time relationship.

If it is assumed that μ, α_{av}, c_s and P are constant then Eqn. (2.5) is reduced to

$$t = b V_a^2 \tag{2.7}$$

where b is a constant, (s/m^2)

Differentiating with respect to V_a yields

$$\frac{dt}{dV_a} = 2bV_a \tag{2.8}$$

Re-arranging and substituting Eqn. (2.7) into Eqn. (2.8)

$$\frac{dV_a}{dt} = \frac{1}{2b\sqrt{t/b}} \tag{2.9}$$

Eqn. (2.9) serves as a basis for the development of a more general form of the flux - time curve for the TFP and DEMF and this will be developed and discussed in **Chapter 4**.

2.1.2 Cylindrical Model

Rencken [1992] found the simplified model to be severely limited when dealing with a concentrated (50 g/ℓ) waterworks sludge. Rencken found that for the waterworks sludge, the model was unable to predict the variation of internal cake diameter with filtration time accurately. Rencken went on to develop an internal cylindrical model for dead-end constant pressure filtration.

One of the reasons why Rencken developed a dead-end internal cylindrical compressible cake filtration model was to predict the internal cake diameter in order to predict and prevent tube blockages in the press. It should be noted however, that the suspended solids content of the feed that was used in this study was two orders of magnitude lower than that used by Rencken. Furthermore, experiments on the DEMF have shown that after 36 h of operation, at a feed concentration of 150 mg/ℓ using a mixed clay suspension, the cake thickness is 50 times smaller than the internal tube diameter. Thus tube blockages are not likely to be a problem and a simple model may suffice for dilute suspensions. The model developed by Rencken will however be discussed briefly.

Rencken modified the external cylindrical compressible cake filtration model by Tiller & Yeh [1985] for an internal cylindrical medium. The basis of Rencken's model are two differential equations which relate the solids compressive pressure and the liquid pressure as functions of the radius :

$$\frac{dp_L}{dr} = -\frac{\mu Q}{2\pi r K} \tag{2.10}$$

and

$$\frac{dp_s}{dr} = \frac{\mu Q}{2\pi r K} - (1-k_o)\frac{p_s}{r} \tag{2.11}$$

where : p_L = liquid pressure, (Pa)

p_s = solids compressive pressure, (Pa)

r = radius, (m)

Q = overall volumetric flow rate of liquid (filtrate) per unit length of filter tube, ($m^3/m.s$)

K = local permeability of cake or sediment, (m^2)

k_o = coefficient of earth pressure at rest, (-)

Rencken used a waterworks sludge to evaluate the model. The cake that was formed by the filtration of the sludge had to be characterized and since it was compressible in nature, compressibility and porosity data were obtained over a wide range of solids compressive pressures.

A compression-permeability (C-P) cell and a settling technique were used to obtain cake permeability and porosity data. The data were used to obtain empirical constants for the equations relating permeability and porosity to solids compressive pressure. These equations were used in the internal cylindrical filtration model.

Rencken found that the model was able to predict the total volume of filtrate, the average cake dry solids concentration, the filtrate flux and the internal diameter of the cake within the limits of experimental uncertainty.

2.2 CROSS-FLOW MICROFILTRATION MODELS

Attempts at modelling cross-flow microfiltration have followed four basic approaches and can be categorized as diffusion models, force-balance models, axial convection models and scour or erosion models. A comprehensive review of recent cross-flow modelling attempts was undertaken by Pillay [1992a]; the pertinent aspects of that review are presented here.

All the models that have been proposed have their short-comings. The models are to a large extent specific to the suspensions that were used, with the result that no particular model is able to account for all the observed phenomena associated with CFMF.

2.2.1 Diffusion Models

The simplest attempts to model CFMF are based on the concentration polarization theory which was developed by Blatt *et al.* [1970] for ultrafiltration of macromolecules. In a CFMF system particles in a suspension are retained at the wall, while the suspending liquid permeates through the wall. Local steady-state mass transfer dictates that the rate of convective transport of particles to the wall, must be balanced by an equal rate of transport (diffusive or convective) of particles away from the surface. This condition can only be met if the there is a higher concentration of particles at the wall than in the bulk suspension. This is known as the concentration polarization phenomenon. The governing equation is :

$$\frac{dV_a}{dt} = k(x) \ln\left(\frac{c_w}{c_b}\right) \tag{2.12}$$

where dV_a/dt = permeate flux, (m/s)

c_w , c_b = particle concentrations at the membrane surface and in the bulk suspension respectively, (g/ℓ)

$k(x)$ = local mass transfer coefficient between the bulk suspension and the concentrated regime next to the wall, (m/s)

Investigators such as Fane *et al.* [1982] have empirically derived values for the mass transfer coefficient, $k(x)$.

The concentration polarization concept has been extended by others, such as Zydney & Colton [1986] to include a shear enhanced diffusion. They proposed that when a suspension is exposed to a shear field, the particles within each streamline, interact in a random nature causing them to be displaced into neighbouring streamlines. This they proposed could be characterised by an effective diffusion coefficient, $k_m(x)$,

$$k_m(x) = 0,052\left(\frac{r_p^4}{x}\right)^{\frac{1}{3}}\tau_w \qquad (2.13)$$

where r_p = particle radius, (m)

x = axial distance co-ordinate along the tube, (m)

τ_w = shear rate at the wall, (1/s)

$k_m(x)$ = effective diffusion coefficient, (m/s)

Extending the diffusion model, Davis & Leighton [1987] proposed that the deposition of particles into the polarised layer was balanced by the tangential flow of this fluidised layer of particles. The shear exerted by the bulk suspension on the concentrated layer of particles, causes particle-particle interactions to occur, thus displacing particles from their time-averaged streamlines. These particles then migrate in the direction of decreasing concentration. This process is called *shear induced hydrodynamic diffusion* or *viscous resuspension of particles.*

Other workers such as Hunt [1987] and Flemmer *et al.* [1982] proposed that particles in turbulent CFMF systems were transported down concentration gradients by turbulent eddies. Hunt's model is based on the simultaneous solution of the steady-state mass balance and the hydraulic resistance equations. The model has four regressed parameters.

Pillay [1992a], proposed that after the formation of a cake, the particles are sheared off the surface and the concentration of the layer adjacent to the cake (pre-cake) increases above the bulk concentration. A concentration profile is thus established. The particles in the pre-cake are then transported into the turbulent core by back diffusion. Pillay developed a mathematical model which correlated well with his experimental results.

2.2.2 Force-Balance Models

Belfort in a series of papers [Altena & Belfort, 1984; Green & Belfort, 1980; Belfort & Nagata, 1985] proposed an *inertial lift* or *lateral migration* model. The model theorises that the diffusion of particles from the concentrated layer into the bulk suspension was augmented by a lateral migration away from the wall due to an inertial lift force. Each particle, is subjected to two forces, a fluid drag force which corresponds to a permeation velocity (towards the wall) and a lift force corresponding to a lift velocity (away from the wall). Cake growth is limited when the lift velocity exceeds the permeation velocity.

A *critical force-balance* model was proposed by Rautenbach & Schock [1988] and Fischer & Raasch [1986]; conceptually the two models are similar. They proposed that a critical force balance condition existed for particle stability on the cake surface. Below this critical condition the particle deposits on the cake surface, while above this condition it will be destabilised or remain in suspension.

2.2.3 Axial Convection Models

This model, suggested by Leonard and Vassilieff [1984] and subsequently extended by Davis and Birdsell [1987], proposes that the cake layer adjacent to the tube wall flows axially, offsetting the deposition of particles onto this layer.

2.2.4 Scour/Erosion Models

These models have been adapted from the fields of sedimentation and slurry transport in pipelines. The models tend to be correlations rather than mechanistic interpretations of cross-flow microfiltration.

2.3 CONSIDERATIONS IN THE SELECTION OF THE CROSS-FLOW MICROFILTER AND THE DEAD-END MICROFILTER

It was discussed in Sec. 1.1.2 that the essential difference between the CFMF and the DEMF is in the mode of operation. It was further stated that the DEMF should be considered as a limiting case of the CFMF as the cross-flow velocity is close to zero.

To date the TFP and the CFMF (as a cake recovery process) have been modelled independently and these have been discussed in Sec. 2.1 and Sec. 2.2. The CFMF models outlined are steady state models which are concerned with a period where the flux remains more or less constant after an initial period of flux decline (Fig. 2.1). These models predict the steady state flux of the system based on various mechanistic interpretations of the interaction between the cake and the bulk suspension. In practice however, the period of initial decline cannot be ignored and the shape of the flux-time curve (as will be shown) becomes very important.

It is usually the case that filtration in the dead-end mode (in operations such as plate and frame presses) yields a flux-time curve with a greater rate of decline than operation in the cross-flow mode (Fig. 2.1); and hence that operation in the cross-flow mode is more desirable for a high volumetric permeate production rate.

As stated in Sec. 1.1.5 one of the aims of this project is to test that postulate at low solids concentrations on the tubular woven filters, namely the DEMF and the CFMF.

In order to select the operating mode of the tubular fabric filter (namely the CFMF or DEMF) economic variables need to evaluated. These variables will be influenced by the operating characteristics of the two processes, as well as the dependent and independent variables governing the physical and design equations. These equations will be developed in Sec. 2.3.1 and Sec. 2.3.2.

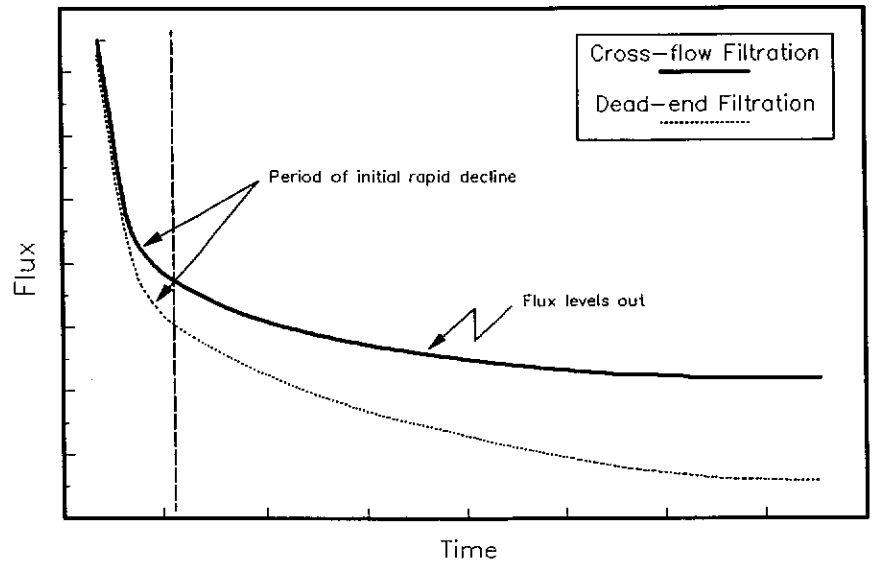

Figure 2.1 : **A comparison between the generally assumed flux-time curves for CFMF and the DEMF. The CFMF has two distinct periods, an initial period of rapid flux decline followed by a period where the flux levels out. For the DEMF the second period is generally assumed to have a much faster rate of flux decline than the CFMF and not showing a levelling out of the flux.**

2.3.1 Operating Characteristics of the Cross-flow Microfilter and the Dead-end Microfilter

The CFMF operational cycle can be divided into two stages namely a *down or non-production time*, t_d and a *filtration* or *production time*, t_p where the sum of the two periods is the *cycle time*, t_c. A typical CFMF cycle is illustrated in Fig. 2.2.

The *down time* is further divided into a number of stages which could include a cleaning, precoating and *dead time*. Each cycle would commence with cleaning where the rollers, brushes or sprays are engaged onto the fabric and the cake layer removed. The nature of the suspension might warrant the use of a precoat to alter the pore size of the fabric or to enhance the flux. Precoating of the fabric would take place after the cleaning cycle. After the introduction of the suspension into the tube, a certain period of time lapses before a permeate of acceptable quality[1] is obtained, this is known as the dead time. The production cycle then commences.

1 The quality might be measured in terms of turbidity, conductivity, bacterial plate counts etc.

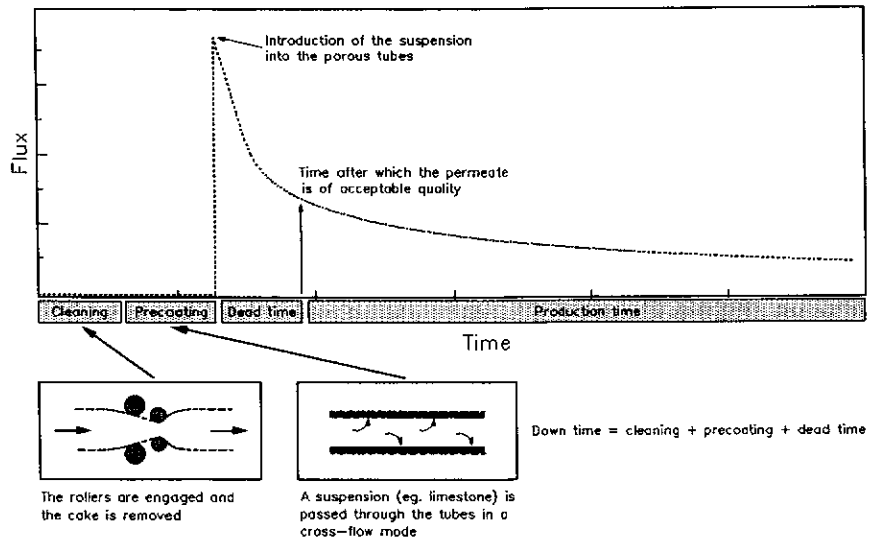

Figure 2.2 : **A profile of a typical CFMF cycle. The cycle starts with a cleaning time where the cake is removed from the fabric tubes. This is followed by a precoating time where a dynamic membrane is laid down. Note that in some instances the use of a precoat would not be necessary. The suspension is then introduced into the tubular array, and for an initial period termed the dead time, the quality of the permeate is unacceptable. The filter then goes into a production time where the permeate is drawn off and utilised.**

In the operation of a CFMF, the instantaneous flux at any point along the filter tube may be expressed as,

$$\phi(c, p, v, t) \tag{2.14}$$

where ϕ = instantaneous flux, (ℓ/m^2h)

c = suspension concentration, (g/ℓ)

p = point pressure difference across the tube wall, (Pa)

v = superficial suspension velocity, (m/s)

t = time, (s)

The variables c, p and v will themselves be functions of t and the position along the tube, x hence the flux can be written as $\phi(x, t)$. For $t < t_d$, $\phi(x, t) = 0$.

The quantity which is of interest in the economic evaluation of a design is the volume, $V(t, l)$ of permeate produced by the tubes over their length, l and over the time from the start of an operating cycle, t that is,

$$V(t, l) = \frac{a}{l} \times \frac{1}{3\,600\,000} \times \int_0^t \int_0^l \phi(x, \tau)\, dx \cdot d\tau \tag{2.15}$$

where a = area of the tubes, (m^2)

l = length of the tubes, (m)

V = volume produced by the tubes over their length l up to time, t , (m^3)

the numerical factor is for the conversion of the volumetric and time units into consistent dimensions

The relationship between V and t for a particular tube length l is illustrated in Fig. 2.3.

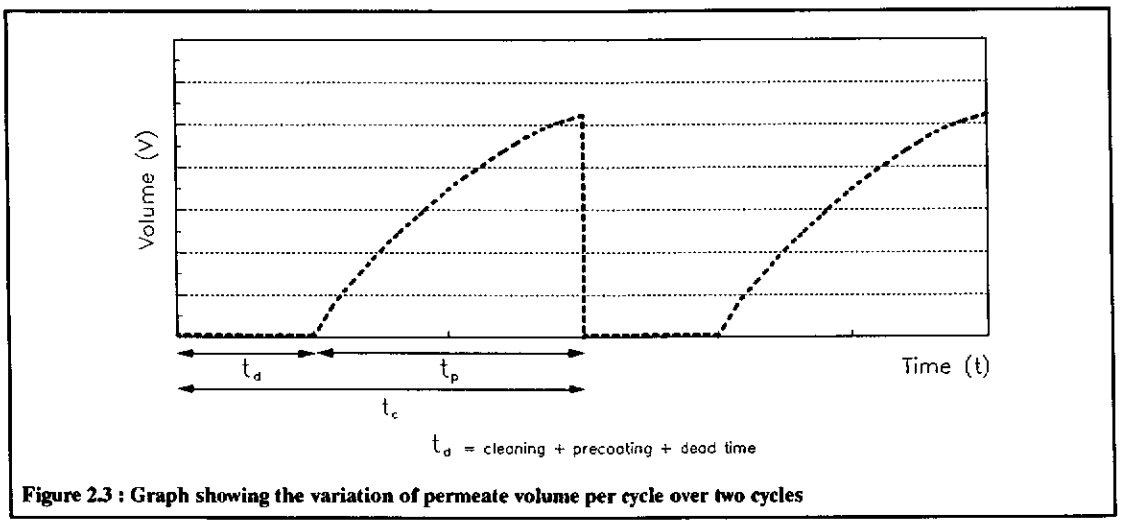

Figure 2.3 : Graph showing the variation of permeate volume per cycle over two cycles

In the context of design, the average permeate flux, J , over the cycle is more useful and is defined as :

$$J(c, p, v, t_c, l) = \frac{V}{a \cdot t_c} = \frac{\int_0^{t_c} \int_0^{l} \phi(x, \tau)\, dx \cdot d\tau}{t_c \cdot l} \qquad (2.16)$$

where J = average permeate flux, (ℓ/m^2h)

2.3.2 Economic Design Basis

It should be noted that the equations that are presented in this section were developed symbolically for conceptual purposes and not pursued in numerical detail.

The operation of the CFMF and the DEMF will be determined by a number of site specific factors. These include the permeate production rate and quality, the feed nature and concentration, and the required water recovery.

There are a number of methods of characterising water quality, which might include turbidity, bacterial plate counts and concentration of heavy metals. Turbidity is a very convenient way of establishing the quality of the permeate and could be related to the quantity of suspended solids and water-borne bacteria.

Two situations can be distinguished with respect to required water recovery. The first is where water is scarce and the maximum recovery of water is of overriding concern, while the other is where water is more plentiful and maximising the recovery of water, is of lesser importance.

The economic considerations in the selection of the CFMF and the DEMF can be classified in terms of *physical* and *design* relationships. The *physical* relationships are specific to the suspension in question and these must be determined experimentally. They would include for instance the flux-time profile as well as the effects of concentration, velocity and pressure on flux.

With respect to the *design* relationships, the two major cost-determining factors that need to be considered are the *membrane area* and the *power* requirements of the CFMF or the DEMF. The *membrane area* reflects the physical size of the plant, and most capital items are roughly proportional to it. The *power* reflects the pumping requirement, and has capital and operating cost components associated with it. The cost determining factors, *membrane area* and *power*, are obtained from the design relationships which are governed by the mode of operation of the CFMF.

A continuous CFMF configuration with a recycle will be considered where the reject is continually purged as shown in Fig. 2.4. Two other configurations will be discussed later.

Cross-flow with continuous purge

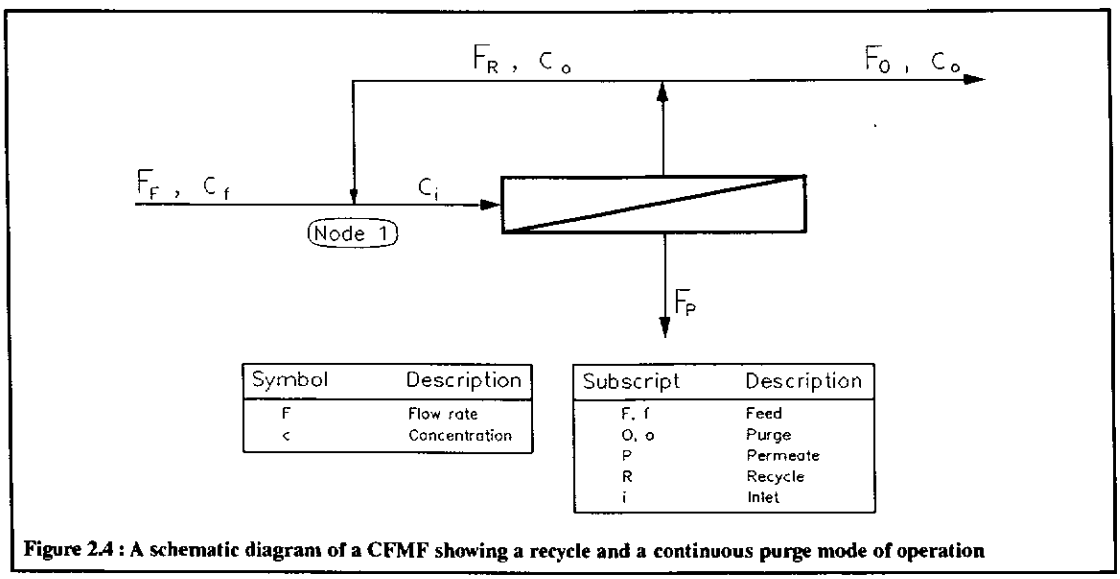

Figure 2.4 : A schematic diagram of a CFMF showing a recycle and a continuous purge mode of operation

The two principal design equations of the CFMF are :

$$\text{Power} = \text{pressure} \times \text{inlet flowrate} = p \times (F_P + F_R + F_O) \qquad (2.17)$$

where F_P, F_O and F_R are time dependent and have units of (m^3/h).

and

$$\text{Membrane area} = \frac{\text{Volume of permeate per cycle}}{\text{Average flux} \times \text{Cycle time}} = \frac{V(t_c, l)}{J \cdot t_c} \qquad (2.18)$$

The average flux in the denominator of Eqn. (2.18) is determined by Eqn. (2.16) where,

$$J = f_1(c, p, v, t_c, l) \qquad (2.19)$$

The point values of concentration, velocity and pressure which are required for the evaluation of Eqn. (2.19) are related to the inlet values c_i, v_i, p_i through the differential material and momentum balances governing the filtration in the tube. The physical relationships which are embodied in Eqn. (2.19) cannot be determined *a priori*, but must be found experimentally.

The *inlet velocity*, v_i for a tube of internal diameter, d is given by :

$$v_i = \frac{F_P + F_R + F_O}{\text{flow area}} \qquad (2.20)$$

where : flow area = filtration area $\times$ $[d/4l]$, (m^2)

The *inlet concentration*, c_i can be obtained by a material balance (see Appendix A) over Fig. 2.4,

$$c_i = c_f \times \left[\frac{F_P + F_O}{F_P + F_R + F_O}\right] \cdot \left[1 + \frac{F_R}{F_O}\right] \qquad (2.21)$$

where c_i = inlet concentration, (g/ℓ)

c_f = feed concentration, (g/ℓ)

In this problem the *permeate rate*, F_P is an external design factor. The feed concentration, c_f is similarly fixed, and hence the variables that will determine the optimum solution are F_R, F_O and t_c. A rigourous optimal economic design will involve the best choice of the *membrane area* and *power* subject to a simultaneous solution of Eqns. (2.15) to (2.21) as outlined above.

Cross-flow operated in a semi-batch mode

Another way of operating the CFMF is in a semi batch mode of operation as shown in Fig. 2.5. In this mode of operation the tank is maintained at a constant level by the inflow of feed.

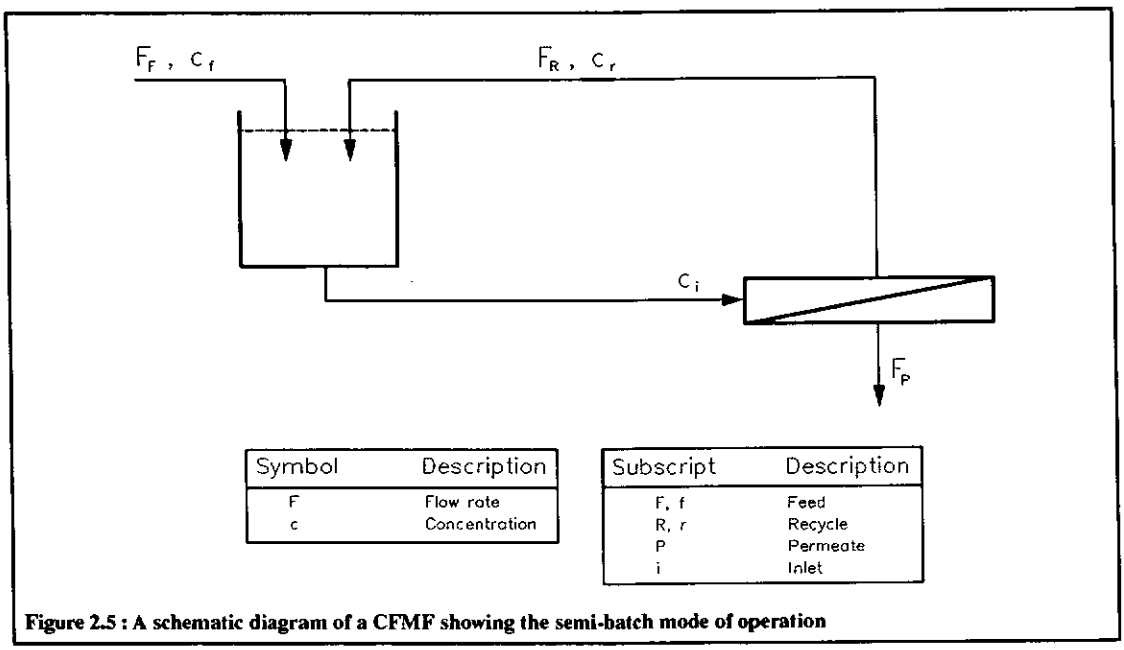

Figure 2.5 : A schematic diagram of a CFMF showing the semi-batch mode of operation

Since there is no continuous purge from the system, Eqn. (2.17) the power design equation, reduces to :

$$\text{Power} = \text{pressure} \times \text{inlet flowrate} = p \times (F_P + F_R) \qquad (2.22)$$

and the inlet velocity Eqn. (2.20) reduces to,

$$v_i = \frac{F_P + F_R}{\text{flow area}} \qquad (2.23)$$

In the case of semi-batch operation, the volume of the tank becomes another variable which will determine the tube inlet concentration. Eqn. (2.21) is thus replaced by (see Appendix A for derivation) :

$$c_i = c_f \times \left[1 + \frac{F_p \cdot t_c}{V_t}\right] \qquad (2.24)$$

where V_t = the tank volume, (m^3)

Again, the *permeate rate*, is a fixed external design factor. The feed concentration into the system is similarly fixed, and hence the variables that determine the optimum solution are F_R, V_t and t_c. A rigourous optimal economic design would involve the best choice of the *membrane area* and *power* subject to a simultaneous solution of Eqns. (2.15), (2.16), (2.18), (2.19), (2.22), (2.23) and (2.24).

The limiting case of the DEMF

The operation of the DEMF is a limiting case of the CFMF in which F_R and F_O in Fig. 2.4. are fixed at zero. The schematic diagram is reduced to Fig. 2.6.

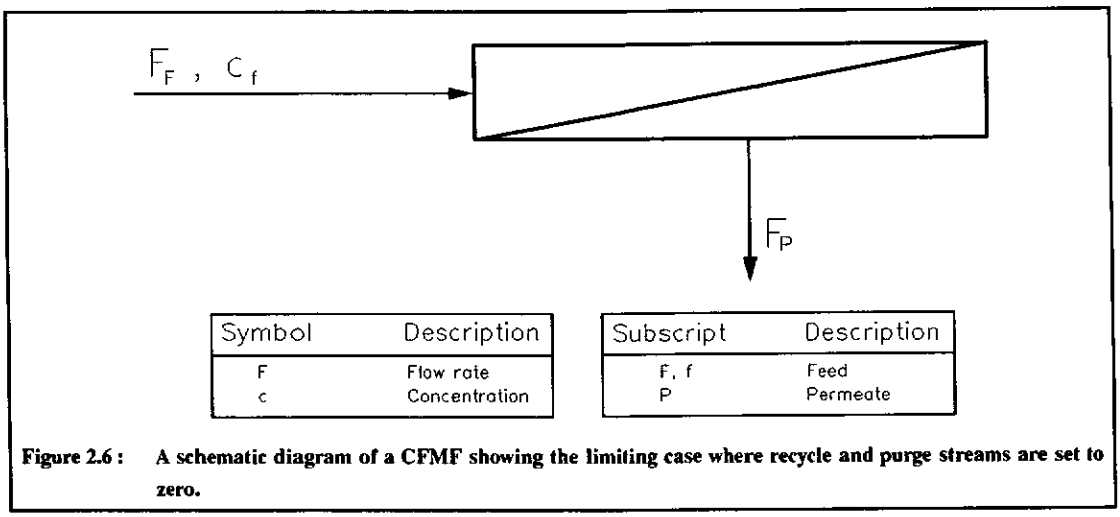

Figure 2.6 : A schematic diagram of a CFMF showing the limiting case where recycle and purge streams are set to zero.

The power, Eqn. (2.17), is reduced to,

$$\text{Power} = \text{pressure} \times \text{inlet flowrate} = p \times F_P \tag{2.25}$$

Similarly, since the cross-flow velocity tends to zero in the dead-end mode, the average flux, Eqn. (2.19), reduces to,

$$J = f_1(c, p, t_c, l) \tag{2.26}$$

The inlet velocity Eqn. (2.20) would also reduce to,

$$v_t = \frac{F_p}{\text{flow area}} \tag{2.27}$$

while the concentration at the tube inlet, c_i is the feed concentration, c_f, which is fixed.

The only variable that then needs to be optimised is t_c, and the optimal economic design would involve the best choice of area and power subject to a simultaneous solution of Eqns. (2.15), (2.16), (2.18), (2.25), (2.26) and (2.27).

CHAPTER

THREE

Suspension and Fabric Characterization

3.1 SUSPENSION CHARACTERIZATION

A reproducible dilute suspension which had similar properties (mineralogical and fouling) to river water was required for this research. A precise modelling of river water was not essential, since the task was not to compare cross-flow to conventional water treatment systems, but rather to compare the relative performance of two filtration processes on suspensions with low suspended solids (< 1 000 mg/ℓ).

3.1.1 Suspension Component Selection

To model river water, one has to match the formulation of the suspension to a particular river. The nature of the suspended material varies from one source to another and even the composition of water from one source varies from region to region. Kemp [1963], in a hydrobiological survey of the Umgeni River, Natal, found that the dissolved inorganic material in various tributaries of the river showed differences in composition. Kemp attributes these differences to the fact that the tributaries drained catchment areas formed from rocks of different geological formations.

Various researchers have attempted to model natural waters. Wall and Wilding [1976] endeavoured to characterise the suspended sediment material that is seasonally transported down the Maumee River, Ohio (USA). The suspended material was settled, fractionated and analysed by X-ray diffraction. The study showed that the suspended material was made up of a clay and silt fraction. The clay content was found to represent 80 % of the suspended load.

The characterization of natural water is complex; authors such as Eppler *et al.* [1975] attempted re-create the suspended and liquid phases of natural waters. The suspended phases they cited consisted of an organic and inorganic phase. The inorganic phase consists of kaolinite, illite, montmorillonite, silicon dioxide and aluminium oxide, all with a particle size less than 20 μm. The organic phase was made up by adding six strains of micro-organisms. Finally the liquid phase was re-created by adding the above to samples of river water (previously frozen) filtered through 100 nm membrane filters.

An attempt was made to use actual river suspended solids for this study. A 10 kg sample of silt/clay material was collected from the Nagle Dam area on the Umgeni River. The sample was successively wet screened from 2,00 mm down to 53 μm. The undersized particles were then passed through a Cyclosizer and the -10 μm fraction was retained. This fraction was in the form of a very dilute suspension. The suspension was then passed through a SORVALL continuous flow centrifuge at 15 000 rpm and the solid material retained. The wet solids were then dried in a vacuum oven at 30 °C. Despite the obvious merits of this method, it was found that less than 10g of -10 μm solids were recovered, which was a fraction of what was actually required to undertake this investigation.

It was clearly not feasible for the purposes of this project, to model river water in this detail, not only from the point of physical impracticality, but also the project would have been specific to a particular river, region and season.

Other researchers, who have attempted to characterise river water, without being concerned about the exact source, have done so by adding a commercial clay to distilled water to make up the desired concentration of suspended solids. Vlasova *et al.* [1989], Ahsan *et al.* [1991] and Teselkin *et al.* [1988] used fine (<10 μm) kaolin while Milisic & Bersillon [1986] used bentonite to characterise the fouling properties of river water in cross-flow processes.

Since the exact nature of the suspension was not important and the main criterion was that it be repeatable, it was decided to use a blend of commercial clays to simulate the suspended matter. There was also little to suggest that anything more would be gained by using actual suspended solids as opposed to a blend of commercial clays. The types and proportions of clay to be added to make up the suspension needed to be determined.

The suspended material in river water is mainly composed of clays and colloids, and in the case of the Umgeni catchment area, the clay fraction is predominantly kaolinitic [Kemp, 1963]. Another clay type that is commonly found in natural waters is montmorillonite of which bentonite is an example. Both clays are commercially available, and it was decided to use a blend of these.

The particle size of the clay fraction was also in question. Most of the size analyses done on suspended solids of river water [Wall & Wilding, 1976; Teselkin *et al.*, 1988; Vlasova *et al.*, 1989; Kirk, 1985; Crowley *et al.*, 1985; Beckett *et al.*, 1988] are reported to be below 10 μm.

The two clays were commercially available as SERINA ULTRAFINE KAOLIN and OCEAN BENTONITE. Both clays had particle sizes less than 10 μm. In order to determine the proportions of kaolin and bentonite to be added, an adaptation of the technique known as the Silt Density Index (SDI) [ASTM D 4189-82, 1990] was used. The SDI is a measure of the fouling propensity of the suspended material in a low turbidity water. The aim of both the CFMF and the DEMF is to retain suspended

material in the feed suspension, the correlation between the proportions of clay and the fouling characteristics of the suspension can obtained by using a technique such as the SDI.

3.1.2 Suspension Formulation

The aim of using the modified SDI test was to establish the proportions of bentonite and kaolin that would have to be added to water to simulate the fouling characteristics of a real river water suspension of the same concentration. It should be stressed that the aim was not to establish a river water standard or to model river water from a particular source, but simply to obtain similar behaviour in filtration tests.

The silt density index (SDI) was used as an indication of the quantity of particulate matter in water. This method is applicable to relatively low turbidity waters eg. well water, filtered water and clarified effluent samples. The actual test will be described as well as the modification made to it.

Silt Density Index Test (based on ASTM D 4189-82, 1990)

A diagram of the SDI apparatus is illustrated in Fig. 3.1. The apparatus was flushed with the suspension to remove any entrained contaminants. The suspension to be tested (1 ℓ) was then introduced into the liquid cylinder (B) which was then pressurised to 207 kPa with compressed air. A 0,45 μm membrane filter [MILLIPORE HAWP 025] was carefully inserted into the membrane holder (D). A conical flask was placed on a Mettler balance which was interfaced with a computer in order to log the cumulative mass at regular intervals.

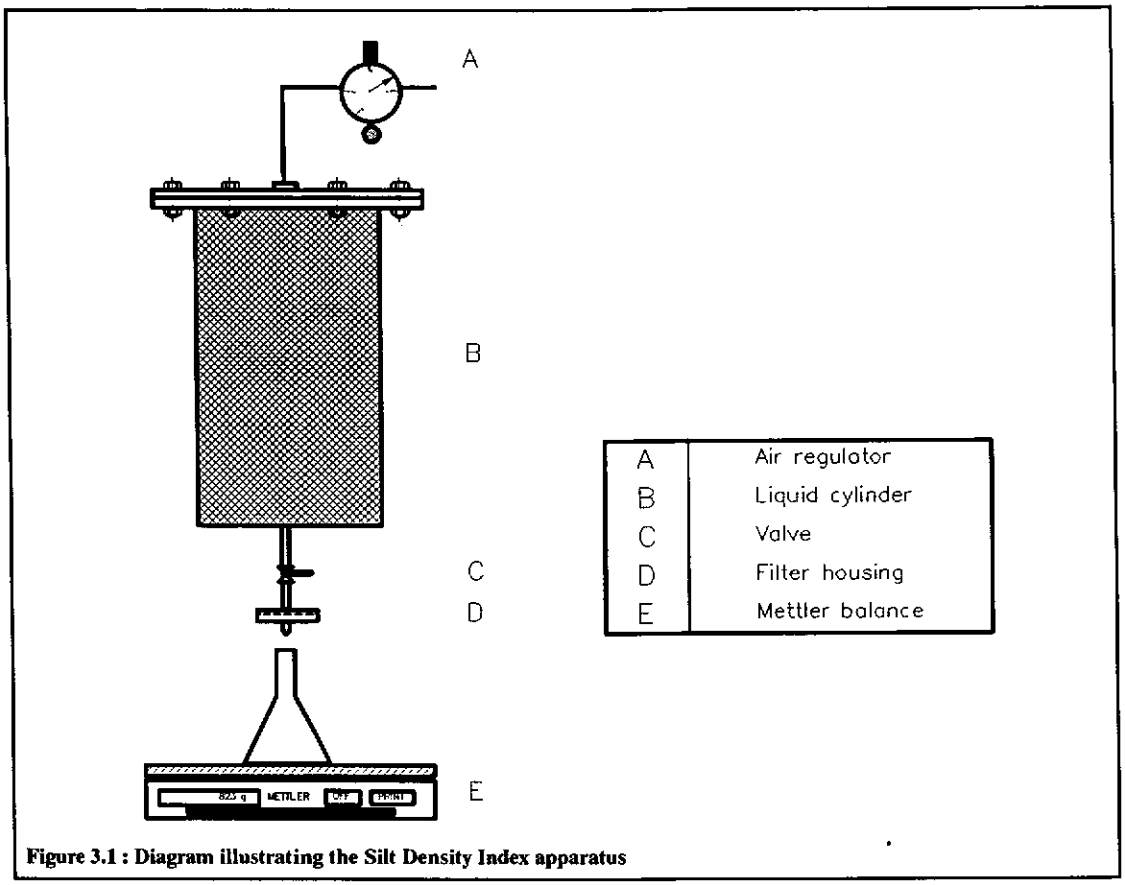

Figure 3.1 : Diagram illustrating the Silt Density Index apparatus

The valve (C) was then opened and the time (t_i) taken to collect 112,5 mℓ of filtrate recorded. After 15 min elapsed from the start of the test, the time (t_f) to collect a further 112,5 mℓ of filtrate was also recorded.

Calculation

The silt density index (SDI) is calculated from :

$$SDI_T = \frac{[1 - t_i/t_f] \cdot 100}{T}$$

where : T = total elapsed flow time, (min) [usually 15 min]

t_i = initial time required to collect 500 mℓ of sample, (s)

t_f = time required to collect 500 mℓ of sample after the test time T, (s)

The suspensions which were tested fouled the membrane rapidly and it was found that the test was unsuitable for poor water quality samples. It was found that t_f was much larger than t_i with the result that in most cases the equation simply reduced to :

$$SDI_T = \frac{100}{T}$$

making comparison of samples difficult. This is also noted by the ASTM standard which recognizes that the test is only applicable to *relatively low turbidity (<1,0 NTU) turbidity waters*. It was thus decided to rather use a graphical technique in order to compare different clay suspensions.

The computer was used to log the cumulative mass in the conical flask at regular intervals during each test. The cumulative volume of permeate collected versus the time was then plotted. This established a flux profile and the various suspensions were compared in this manner. All tests were performed at the same temperature, namely 22 °C.

Suspension Tests

A quantity of untreated Nagle Dam water was obtained from Durban Heights Water Treatment Plant on the 21 August 1991. A gravimetric analysis [ASTM 1888-78, 1990] of the water revealed a total solids content of 9,8 mg/ℓ. The modified SDI was first performed on the actual river water suspension and this acted as a baseline or the curve which had to be modelled. This is shown as curve A in Fig. 3.2. The test was also performed on distilled water and reverse osmosis permeate. These are shown as curves E and D respectively.

The distilled water was filtered through a 0,22 μm membrane filter [MILLIPORE GSWP 025] to produce a water which had a background turbidity of less than 0,05 NTU [ASTM D 1889-88A, 1990]. This water was used to make up the clay suspensions.

A suspension of kaolin was made up to a concentration of 9,8 mg/ℓ and the modified SDI test was performed. The fouling profile is shown as curve C. Clearly there is a large difference between curves C and A. The presence of bentonite in natural waters has been cited as a possible cause of fouling in membrane processes used to clarify natural waters [Milisic & Bersillon, 1986] and hence it was decided to make up proportions of bentonite and kaolin. It could be argued that bentonite simulates the colloid fraction in natural river water. Bentonite and kaolin were mixed in equal mass proportions to make up a suspended solids content of 9,8 mg/ℓ. The fouling profile is shown as curve B, which lies slightly above the actual river water suspension. It was found that if tap water was used instead of filtered distilled water to make up the 1:1 suspension, then the resulting curve coincided with A.

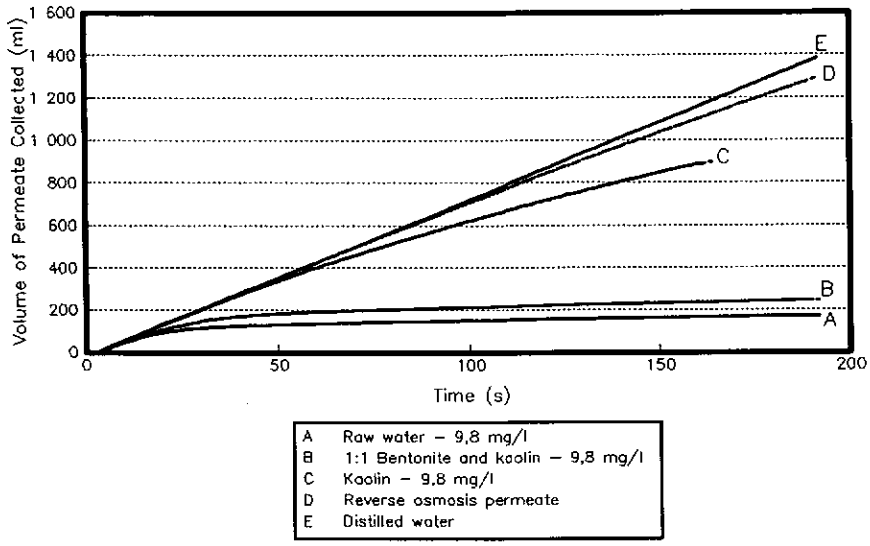

Figure 3.2 : Graph showing cumulative volume curves for Silt Density Index experiments

The suspension that was thus chosen for this project was a 1:1 bentonite : kaolin suspension made up in tap water. The arithmetic mean particle size of the suspension was determined with a HIAC/ROYCO PARTICLE COUNTER and found to be 8,46 μm (d_{50}). The cumulative-size curve and the size distribution is shown in **Appendix B**.

The suspension is not supposed to be a river water standard, rather it is a repeatable low suspended solids slurry which could have similar properties, both fouling and mineralogically, to some Natal waters. Since, the suspension was used to make a relative performance comparison between two filtration processes, the exact nature of the suspension was not essential.

Leger [1985] points out that the major disadvantage of the SDI, is that it does not simulate the cross-flow hydrodynamics. The suspension that is thus derived from the test or modification thereof might thus only approximate a river water suspension in conditions where the shear component is zero. This is clearly less of a concern in the case of the TFP where the hydrodynamics are characterised by a planar filtration model. It could however pose a problem in the case of the CFMF.

3.2 FABRIC PROPERTIES AND SET-UP OF EXPERIMENTAL FABRIC TUBES

The fabric medium used in both the EXXFLOW Cross-flow Microfilter and the EXXPRESS Tubular Filter Press is unique. Since it plays such an important role in both processes, the properties of the fabric and the weave will be outlined. Various problems that were encountered in the experimental set-up of the fabric tubes will also be discussed as well as methods of overcoming those difficulties.

3.2.1 Tubular Fabric Characterization

The fabric is woven to form a longitudinal array of filter tubes which is referred to as a tube curtain. The curtain construction is such that continuous and isolated tubes are formed from a single homogeneous cloth, as an array of side-by-side tubes in the warp direction. This is done by an interleaving weave pattern. When pressurised the collapsible array swells, forming the array of tubes as illustrated in Fig. 3.3.

The number of tubes in parallel, the tube diameter, and the length of the tube can be manufactured to suit the application. Typical values are shown in Table 3.1.

	Tube Diameter	
	13 mm	25 mm
Curtain length (m)	8 to 12	8 to 12
Number of tubes in parallel	44	20

Table 3.1 : Table showing typical manufactured sizes of the tube curtains

The curtain of tubes is conveniently positioned by suspending it from a rail as illustrated in Fig. 3.3. The ends of tubes are manifolded into a resin block which can be configured to form a multipass system in order to increase recovery along the curtain length.

The cloth is manufactured from a high tenacity multifilament polyester yarn and woven in a 2×2 twill weave.

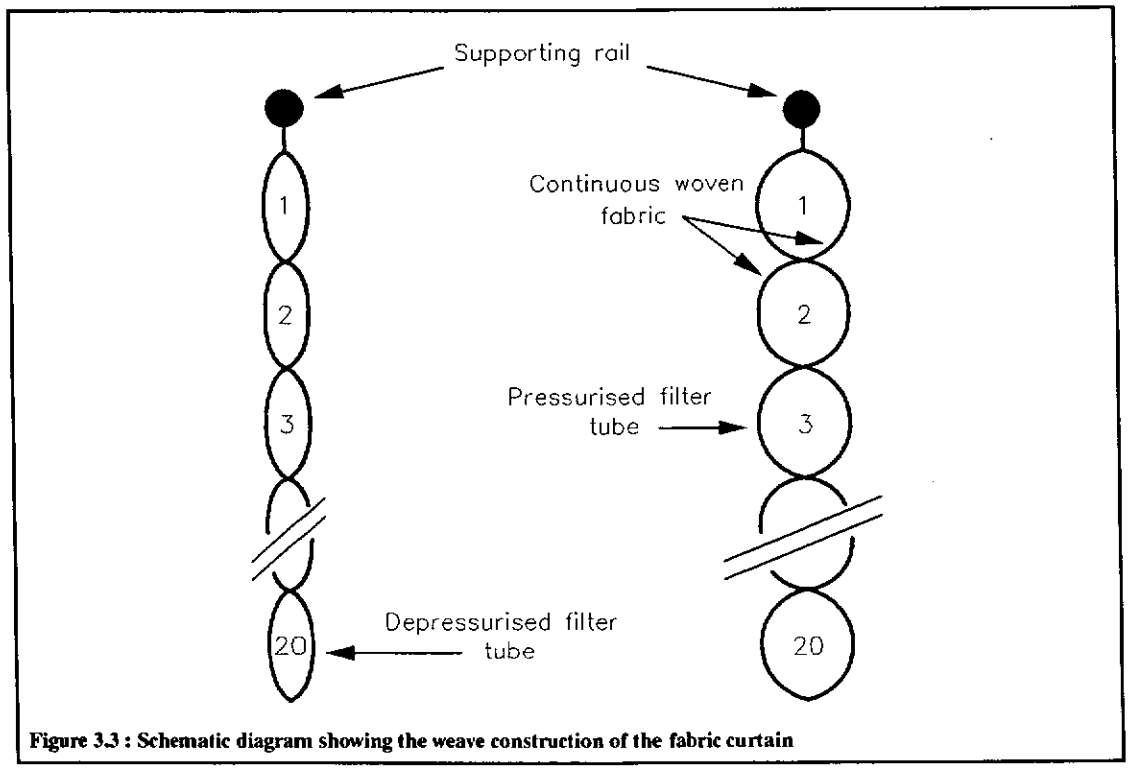

Figure 3.3 : Schematic diagram showing the weave construction of the fabric curtain

The twill weave gives the fabric intermediate properties relative to two other common methods of weaving namely plain and satin. This is illustrated in Table 3.2.

Maximum Filtrate Clarity	Minimum Resistance to Flow	Minimum Moisture in Cake	Easiest Cake Discharge	Maximum Cloth Life	Least Tendency to Blind
Plain	Satin	Satin	Satin	*Twill*	Satin
Twill	*Twill*	*Twill*	*Twill*	Plain	*Twill*
Satin	Plain	Plain	Plain	Satin	Plain

Table 3.2[1] : Effect of weave pattern on cloth performance in decreasing order of preference

The fabric has a warp of 280/48 (decitex) and a weft of 560/96 (decitex).

3.2.2 Experimental Fabric

Experiments for this study were conducted on single tubes cut from a tube curtain. When a single tube was pressurised, extensive *pinholing* occurred along the length of the tube seams. *Pinholing* occurs when the seams move apart under pressure causing the suspension to spray through the enlarged pores. The holes formed along the length of the seam are not easily plugged by the suspension, since they are orders of magnitude greater than the mean particle size. The *pinholing* does not occur in the uncut tube curtain, due the interleaving of the cloth where each tube is supported by two adjacent tubes which seal the seam.

Rencken [1992] and Pillay [1992a] also experienced *pinholing* along the seams of single tubes. They used a commercial sealant, SHOEPATCH, to seal the seams of the single tubes and hence simulate what might occur in a pressurised tube curtain.

The sealant was not perfect, since it had a comparatively short life-span and its application onto the fabric was difficult. It was important to find a sealant that could easily penetrate the fabric and once set, also be flexible. The slurry concentrations used in Pillay and Rencken's studies were 100 times that used in this study, with the result that pinholes arising through poor application of the sealant were more easily plugged by the suspension. At low concentrations (< 1 000 mg/ℓ), effective sealing of the seams is very important.

Various commercial sealants were tested for this application and it was found that optimal results were achieved with an acetone based sealant VAW 595 manufactured by GENKEM.

1 This table was reproduced from Clark [1990]

3.2.3 Construction of the Experimental Single Tubes

Sealing the Tube Seams

A single tube of the required length was cut from a tube curtain. The sealant was drawn into a syringe and allowed to stand inverted till all the air bubbles has escaped. If air bubbles were allowed to set on the fabric, weak spots would form and *pinholing* might occur, contaminating the permeate. The sealant was then applied in the form of a continuous bead along the length of the seam. It took approximately 1 h to penetrate the fabric and dry. It was applied along the cross-over seams on both sides of the tube and along the insides of what would have been the adjacent tubes. Three coats of sealant were applied. The areas of application are illustrated in Fig. 3.4.

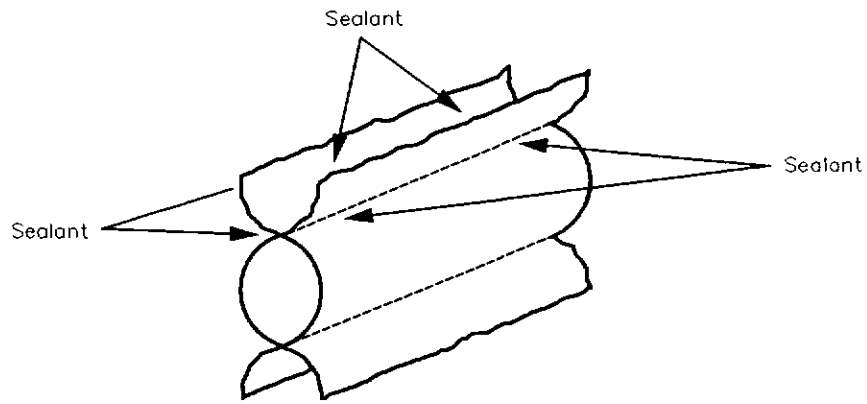

Figure 3.4 : Diagram showing where sealant was applied on a single fabric tube. The bottom cross-over seam of the tube was similarly treated.

Once all three coats of sealant had been applied, acetone was painted over the sealed seams to dissolve any ridges that might have formed and to spread any excess sealant uniformly.

Tube Connections

The ends of the fabric tubes were connected to 25 mm PVC nozzles. The tube was wired onto the nozzles and a polyester resin was applied over the fabric. A schematic of the tube construction is shown in Fig. 3.5.

It was found that excessive weeping also occurred on the fabric area immediately adjacent to the nozzles. This was due to the sudden change in rigidity between the PVC and the fabric. The 20 mm of fabric adjacent to each of the nozzles was also sealed in the same manner as the seams. This minimised contamination of the permeate.

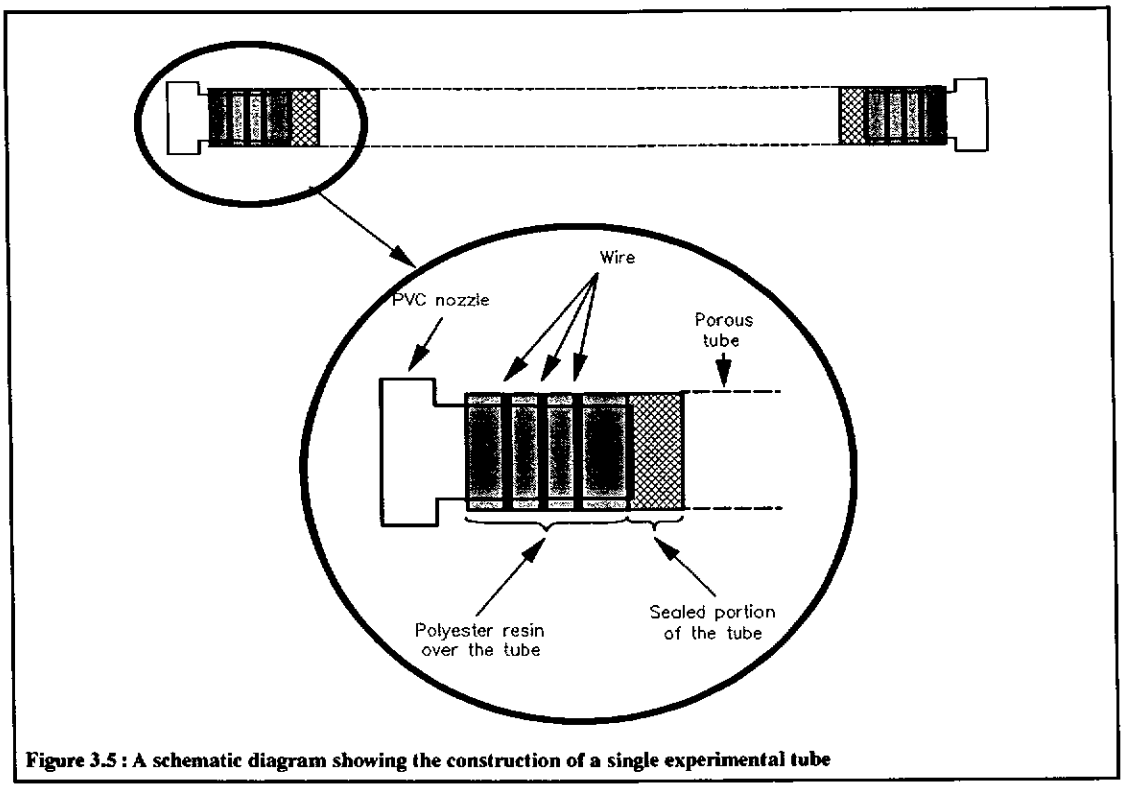

Figure 3.5 : A schematic diagram showing the construction of a single experimental tube

3.3 DYNAMIC MEMBRANES

The EXXFLOW Cross-flow Microfilter differs from many other cross-flow microfiltration systems in that it does not have a preformed or manufactured membrane to perform the separation of suspended solids from the carrier liquid. The EXXFLOW system utilises a dynamic membrane which is formed during the initial flux period of flux decline when the suspended solids are deposited on the fabric support [Pillay, 1992a]. The woven fabric tubes act only as the membrane support structure.

Once the dynamic membrane is in place on the fabric, particles in suspension which have diameters smaller than the fabric pore size are rejected at the membrane surface. These particles are either transported into the bulk suspension or trapped in the membrane structure. A clear liquid then permeates through the wall.

The use of dynamic membranes has been widely reported [Bhave, 1991; Townsend, 1991; Murkes & Carlsson, 1988], and is not unique to the EXXFLOW system. Much of the initial work on these dynamic membranes revolved around hydrous zirconium (IV) oxide and the hydrous zirconium (IV) oxide / polyacrylic acid composite membranes. In these studies the dynamic membranes were used to alter the surface properties of the manufactured membrane or porous substrate, giving the microporous structure rejection characteristics similar to those usually expected of ultrafiltration or nanofiltration membranes. Work has also been conducted on the use of fumed silica [Townsend, 1991] to alter the pore size of the fabric porous support.

The advantages of using dynamic membranes to alter the rejection capabilities of preformed membranes are outlined by Murkes & Carlsson [1988] :-

- *The membranes become tighter, the rejection of the macromolecules and particles becomes better than that of 'naked' supporting membranes.*
- *The relatively open membrane rejects much finer particles / molecules than pore openings themselves would allow.*
- *The flux is stabilized on a relatively satisfactory level and remains almost constant with a very slow decline as the process goes on.*
- *An adequate secondary membrane protects the support against plugging by particles and contributes therefore to a higher and more stable flux.*

In the EXXFLOW system, situations might arise where the suspended solids in the feed forms an inadequate dynamic membrane. Under these circumstances, a dynamic membrane can be artificially laid down by precoating the fabric tubes with another suspension such as limestone or fumed silica prior to the introduction of the feed. This is usually carried out by running the EXXFLOW system in cross-flow mode first with the precoating suspension and then switching to the feed [Pillay, 1992b; Townsend, 1991]. In some cases the precoating material is added to the feed tank to enhance the membrane-forming properties of the feed suspension.

The use of one type of artificial dynamic membrane under one set of precoating conditions was investigated in this dissertation. The aim was not to optimise the use of dynamic membranes, though clearly in any future work on a real suspension various precoats as well as various operating conditions should be investigated.

CHAPTER

FOUR

Experimental Work

4.1 INTRODUCTION

The aim of the experimental work was to obtain flux and permeate quality data for the CFMF and the DEMF using a low suspended solids water (<1 000 mg/ℓ). A suspension of equal mass proportions of bentonite and kaolin made up in tap water, was selected (Sec. 3.1.2).

The average flux in the CFMF tube has been shown (Sec. 2.3.2) to be a function of five variables :

$$J = f_1(c, p, v, t_c, l) \qquad (2.19)$$

Flux data was thus obtained over a range of concentrations, pressures and velocities[1] while the flux profile as a function of time was also monitored. The experiments were only conducted on a single length of tube, but for any design analysis, the data collected for a short tube could be integrated for any desired length.

An aspect that was considered was the use of artificial dynamic membranes (precoats) to enhance the performance of the filters. Experiments were conducted on the DEMF with and without the use of precoats at one set of precoating conditions. As stated in Sec. 3.3, the aim was not to optimise the type of precoat, nor to optimise the conditions, but to investigate whether the use of precoats makes a significant difference to the flux and permeate quality.

Permeate quality was also monitored, since it would determine the transition between the dead-time and the production time in the CFMF cycle (Sec 2.3.1). There are various means of characterizing water quality, which might include turbidity, bacterial plate counts and concentration of heavy metals. In this study turbidity was chosen as an appropriate measure of the permeate quality.

1 As stated previously, the DEMF is considered a limiting case of the CFMF as the cross-flow velocity approaches zero. Hence in the DEMF, velocity is not a manipulable variable.

4.2 TURBIDITY AS A MEASURE OF WATER QUALITY

Turbidity is an expression of the optical properties of a sample that causes light rays to be scattered and absorbed rather than transmitted in straight lines through the sample [ASTM D 1889-88A]. Measurement of the turbidity is accomplished by passing a strong beam of light through the sample. Suspended matter reflects a portion of the light beam (proportional to the turbidity present), and the reflected light is received by a photoelectric detector. The light energy is then converted to an electrical signal and displayed on a meter.

Turbidity is caused by the presence of suspended organic and inorganic material in water. The presence of turbidity can also have a significant effect on the microbiological quality of drinking water. Nutrients, bacteria and viruses readily absorb onto the surfaces of suspended matter [World Health Organisation, 1984] which then protect the micro-organisms from the effects of disinfection.

The adequacy of treatment of a raw water source cannot be assessed continuously in an absolute sense since there are no available on-line techniques sensitive enough to ensure the absence of viruses in the treated water. The World Health Organisation [WHO, 1984], does however consider a contaminated water source adequately treated for potable purposes if the following conditions are met :

- *a turbidity of 1 NTU or less is achieved (prior to disinfection)*
- *disinfection of the water with at least 0,5 mg/ℓ of free residual chlorine after a contact period of at least 30 min at a pH below 8,0.*

There is a trend in the South African water treatment field [Viljoen, 1992] to produce water with a turbidity of less than 0,5 NTU and it was decided to adopt this turbidity level as an indication of acceptable permeate quality in this study. Disinfection of the water would clearly also have to take place in any commercial operation, but was not the subject of this investigation. It should be noted that the 0,5 NTU limit adopted in this study is below the 1 NTU recommended limit put forward by the South African Bureau of Standards for supply of domestic water [SABS 241-1984].

The measurement of turbidity was done in accordance with the ASTM Standard Test Method for Turbidity of Water [ASTM D 1889-88A]. A HACH 2100A turbidity meter was available for use in this study. The meter was calibrated against HACH secondary turbidity standards which provided a quick method of re-calibrating the instrument for measurement in different ranges. The secondary standards were initially calibrated against a primary formazin standard, but no difference between the two could be detected and hence it was decided to use the secondary standards as the calibration reference.

A series of standard clay suspensions were also made up over the concentration range of 40 to 160 mg/ℓ and the turbidities measured. A standard concentration versus turbidity calibration was constructed (**Appendix C**). The calibration was used to determine the concentration in the feed tank.

4.3 SUSPENSION PREPARATION

The selection of the experimental suspension was outlined in Sec. 3.1. A tap water suspension of equal mass proportions of commercial bentonite and kaolin was selected for this study.

The kaolin dispersed easily in water, but the bentonite, which is primarily made up of montmorillonite is a swelling clay which takes up inter-layer water. The bentonite is thus very difficult to disperse.

Fordham and Ladva [1989] conducted cross-flow investigations on bentonite muds. In order to obtain reproducible mud rheology, they used a combination of high shear mixing, heat and overnight hydration in order to disperse the bentonite in water. They operated at concentrations of 6,8 g/ℓ which was two orders of magnitude above the highest concentration used in this study. It was found that the rigourous procedure used by Fordham and Ladva was unnecessary when operating at low concentrations.

It was found that reproducible results were obtained if the bentonite and kaolin solids (between 15 and 240 g) were added to 1,5 ℓ of water and mixed for a period of 12 h using a laboratory stirrer. The viscous suspension was then introduced into the feed tank and tap water was added in order to make up the desired feed concentration. The feed suspension was then stirred for about 2 h while heating to 30 °C, the operating temperature of all the experiments. The above feed suspension preparation procedure was used for all experiments.

4.4 THE CROSS-FLOW MICROFILTRATION EXPERIMENTAL SYSTEM

4.4.1 Apparatus

A schematic diagram of the CFMF system is shown in Fig 4.1.

The apparatus was equipped with a 400 ℓ feed tank fitted with a stirrer The tank was well mixed and no deposition of solids was observed.

Suspension from the feed tank was pumped into the CFMF tube by two HYDRACELL D25 triplex positive displacement pumps driven by a single 7,5 kW ac motor. The phase of the pump diaphragms were offset by 60 ° from each other and in conjunction with the downstream accumulator, A1, a smooth delivery of pumped fluid was ensured. The speed of the motor and hence the pumping rate was controlled by an INVERTRON GPI frequency convertor. The frequency convertor was fitted with a potentiometer in order to set the pumping rate accurately and repeatably.

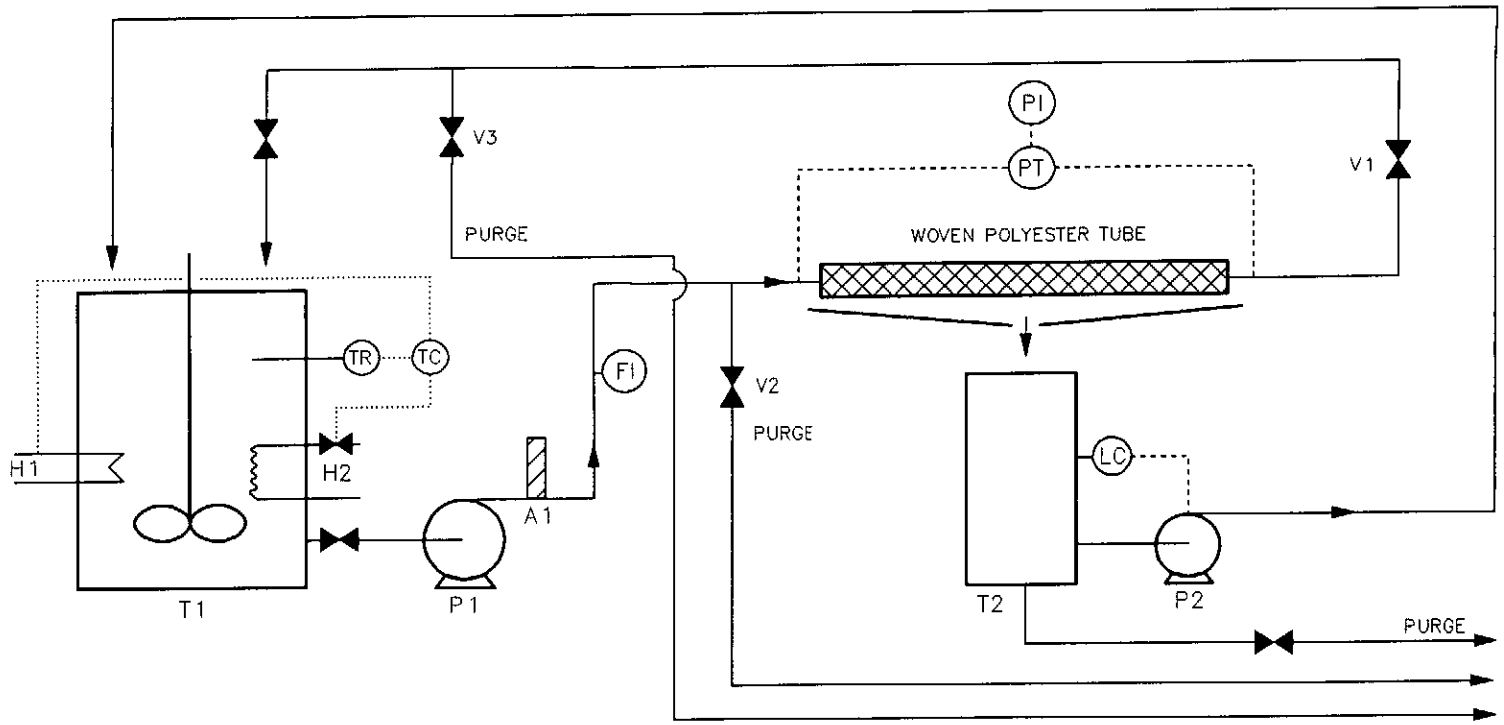

EQUIPMENT LABELS

Label	Description
T1	Feed tank (400 l)
T2	Permeate collection tank
P1	Variable speed pump
P2	Centrifugal pump
V1	Back–pressure diaphragm valve
V2, V3	Purge ball valves
A1	Accumulator
H1	Heating element
H2	Cooling coil

INSTRUMENTATION LABELS

Label	Description
LC	Level controller
FI	Magnetic induction flow meter
PT	Pressure transducer
PI	Digital pressure indicator
TC	Temperature controller
TR	Thermocouple

Figure 4.1 : A schematic diagram of the CFMF apparatus

In order to prevent temperature fluctuations in the system due to the stirrer and the pumps, the feed tank was fitted with a cooling coil and a 3 kW heater. The cooling coil was fed with cooling water from an air draught cooler operating at ±21 °C. The flow through the coil was controlled by a solenoid valve which together with the heater was connected into a Eurotherm controller which maintained the feed tank at constant temperature.

The pressure in the tube was set using a Saunders diaphragm valve, (V1), located just downstream from the tube. The retentate stream from the tube was returned to the feed tank[2].

The permeate from the CFMF tube drained down the permeate gutter into the permeate tank. The permeate was returned to the feed tank by a centrifugal pump controlled by level probes in the permeate tank. The volume in the permeate tank was kept below 10 ℓ in order to minimise fluctuations of the feed tank concentration.

The permeate gutter and feed tank were both covered with plastic sheeting in order to reduce evaporation and contamination of the permeate. The tank and all the pipework was made from either 316 stainless steel or polypropylene (POLYCOP) so as to prevent any contamination due to rust. The tap water inlet to the feed tank was fitted with a 50 μm cartridge filter so as to remove any rust particles.

The system was operated in a closed recycle mode so as to keep the feed concentration constant. The pressure, flowrate and concentration could all be varied independently.

4.4.2 Instrumentation

Flowrate

The flowrate into the CFMF tube determines the inlet velocity. The flowrate was set by the potentiometer connected to the variable speed motor drive. The flowrate was measured using a 25 mm KROHNE magnetic induction flowmeter.

Pressure

Pressure tappings were placed at the entrance to and exit of the CFMF tube. These tappings were connected to a WIKA pressure transducer and digital display which displayed the pressure to the nearest 1 kPa. Readings at the entrance and exit could be taken independently via switching valves.

Solids Concentration

The concentration of the feed was determined by turbidity measurement. The concentration vs turbidity curve appears in **Appendix C**. For concentrations >160 mg/ℓ, the concentration was determined by serial dilution, using distilled water filtered through a 0,2 μm membrane filter as the diluent. This was in accordance with the ASTM standards [ASTM D 1889-88A] which considers this diluent to have no background turbidity

2 While the tube was being precoated, the reject was be returned to the precoating tank.

Temperature

The feed tank was maintained at 30 °C ± 2 °C for all experiments and this was indicated on the temperature controller. The temperature was checked regularly using a mercury thermometer.

4.4.3 Experimental Procedure (Cross-flow Microfiltration)

The suspension in the feed tank was prepared as outlined in Sec. 4.3.

The potentiometer was set to the required flowrate and valves V2 and V3 were opened. The system was started and residual rinse water from the previous experiment was purged to prevent feed contamination or dilution. The valve V2 was then closed and the suspension flowed into the CFMF tube; once the residual water was purged from the remainder of lines, the valve V3 was closed and the tube pressurised.

The system was rapidly brought up to pressure by adjusting the Saunders back-pressure valve, V1. The flow did not alter significantly and minor fluctuations were eliminated by adjustments to the potentiometer setting. The desired operating pressure and flowrate were obtained within 30 s of start-up.

Since both the reject and permeate were returned to the feed-tank, the system was operated at constant feed concentration.

4.5 THE DEAD-END MICROFILTRATION EXPERIMENTAL SYSTEM

It should be remembered that in the DEMF, the velocity approaches zero and is not a manipulable variable. In the CFMF, the pumping rate determined the cross-flow velocity and this was controlled via the speed of the motor. In the DEMF, the pumping rate and pressure cannot be kept constant simultaneously, since at constant pressure the pumping rate declines with time as solids build up in the tube. As in most dead-ended filtration systems, the controlled variables in the DEMF were the pressure and feed concentration.

4.5.1 Apparatus

A schematic diagram of the DEMF apparatus is shown in Fig. 4.2.

The DEMF apparatus was equipped with a feed tank and a precoating tank, both of 200 ℓ volume. The feed tank was kept thoroughly mixed with a stirrer while the precoating material was mixed with a drum pump.

The feed and precoating suspensions were pumped by a MONO CM20 pump, each driven by a 2,1 kW dc motor and gearbox. The speed of the motor was controlled by a variable speed dc drive which was connected to a digital proportional-integral-derivative (PID) controller. The PID controller took its input signal from a WIKA pressure transducer located immediately downstream of the pump and varied the speed of the motor to control the pressure at the set-point.

The system was fitted with a back-pressure needle valve, V1. An accumulator, A1 downstream of the pump ensured a smooth delivery of fluid.

If the suspension was pumped directly into the DEMF tube, the motor was not able to turn down sufficiently for a low flow condition. This would have led to large fluctuations in pressure as the PID controller attempted to control around the set-point. This would have occured during the course of a constant pressure run when the flow had declined due to the increased resistance in the tube. A by-pass line was thus used to keep a continuous circulation of suspension, and allowed the PID controller to maintain the system at a constant pressure.

Temperature rises in the system would have occured as a result of the energy imparted due to the stirrer and the pump. In order to keep the temperature of the feed constant, the feed tank was fitted with a cooling coil and a 2,5 kW heating element. Cooling water was available from an outside air-draught cooler which supplied cooling water at ±21 °C. The flow of cooling water through the coil was regulated by a solenoid valve which was controlled by a proportional EUROTHERM controller. The heating element was controlled by another proportional EUROTHERM controller. The two set-points were offset to give a dead-band of 4 °C.

The permeate from the DEMF tube was collected in a permeate tank and purged to drain. The feed tank and gutter were both covered with plastic in order to minimise heat losses and reduce evaporation.

All pipework was made from 316 stainless steel or flexible polypropylene tubing (POLYCOP) in order to prevent contamination due to corrosion. The tap water inlet to the system was fitted with a cartridge filter in order to prevent any rust particles or solids from entering the system.

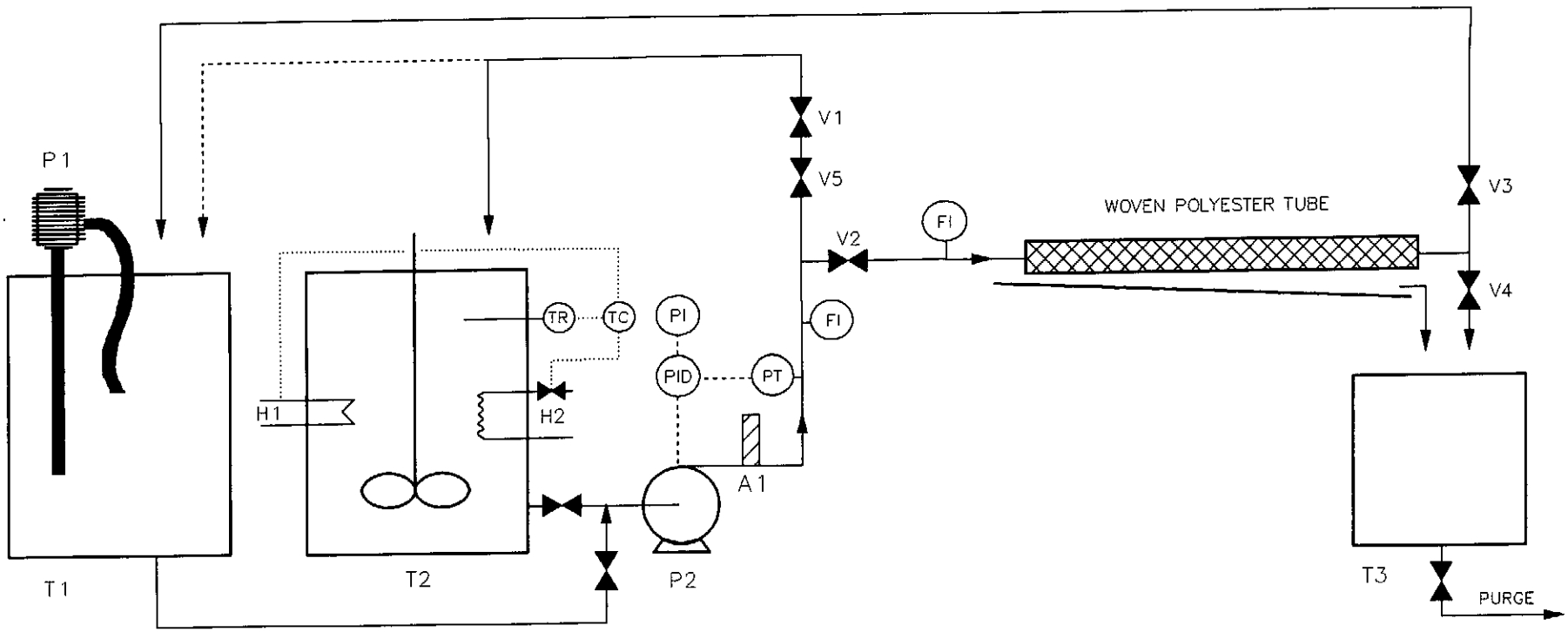

EQUIPMENT LABELS

Label	Description
T1	Precoating tank (200 l)
T2	Feed tank (200 l)
T3	Permeate collection tank
P1	Drum pump
P2	Mono pump
V1	Needle valve
V2 .. V5	Ball valves
A1	Accumulator
H1	Heating element
H2	Cooling coil

INSTRUMENTATION LABELS

Label	Description
PID	Proportional Integral Derivati
FI	Magnetic Induction Flow Meter
PT	Pressure Transducer
PI	Digital Pressure Indicator
TC	Temperature controller
TR	ıocouple

Figure 4.2 : A schematic diagram of the DEMF apparatus

4.5.2 Instrumentation

Flowrate

The pump delivery flowrate and the flowrate into the DEMF tube were both measured using KROHNE magnetic induction flowmeters.

Pressure

The operating pressure of the system was measured with a WIKA pressure transducer located downstream of the pump. The transducer was fitted with a digital display capable of reading to the nearest 1 kPa.

Solids Concentration

The concentration of the feed was determined by turbidity measurement. The concentration vs turbidity curve appears in **Appendix C**. For concentrations >160 mg/ℓ, the concentration was determined by serial dilution, using distilled water filtered through a 0,2 μm membrane filter as the diluent. This was in accordance with the ASTM standards [ASTM D 1889-88A] which considers this diluent to have no background turbidity

Temperature

The feed tank was maintained at 30 °C ± 2 °C for all experiments and this was indicated on the temperature controller. The temperature was checked using a mercury thermometer.

4.5.3 Experimental Procedure (Dead-end Microfiltration)

The start-up procedure for experiments with and without the use of a precoat was as follows:

Start-up Procedure without a Precoat

The suspension in the feed tank was prepared as outlined in Sec. 4.3.

The desired operating pressure was entered into the digital PID controller. Valve V2 was initially closed. The system was started up and any residual rinse water from the previous experiment was purged via the flexible POLYCOP by-pass line. The valve V1 was then adjusted till the pressure was controlled at the chosen set-point and a delivery flowrate of 7,0 ℓ/min. The delivery flowrate was always initially set to this value so that when V2 was opened, the tube would always experience the same inlet conditions.

Once the system had stabilised around the set-point, V2 was opened with valves V3 and V4 closed. The by-pass line which contained suspension at the feed concentration, was returned to the feed tank. The system was operated at constant feed concentration.

Start-up Procedure with a Precoat

It was stated in Sec. 3.3, that the aim of this work was not to optimise the use of artificial membranes or precoats. It was however found, as will be shown in **Chapter 5**, that the use of precoats had a significant impact on the operation of the DEMF and were very useful in overcoming certain operational difficulties.

Experiments were conducted using only one type of precoat and on one set of precoating conditions. No attempt was made to optimise either the type of precoat or the precoating conditions.

It was decided to lay down the precoat in a cross-flow mode prior to switching over to the feed suspension in the dead-end mode. The application of the precoat in the form of a body-feed was not employed since it would essentially alter the nature and concentration of the feed suspension and this might lead to erroneous conclusions.

A suspension of pulverised limestone ($d_{50} = 5\,\mu m$), was used as the precoating suspension. Pillay (1992b) used a limestone precoat on a wastewater effluent in order to enhance the flux and rejection and very positive results were obtained in that study. The precoat for this investigation was laid down at 0,5 m/s and 100 kPa for a period of 5 min.

The limestone suspension was made up in the precoating tank to a concentration of 300 mg/ℓ. The operating pressure of the actual experiment (200 to 400 kPa) was entered as the PID controller setpoint. The system was then started up with valve V2 closed, and the limestone suspension was circulated back into the precoating tank via the flexible by-pass line. The valve V1 was then adjusted so as to set the delivery flow to 7,0 ℓ/min as was done in the normal start-up procedure. Once the system was stabilised, V2 was opened and V5 was then closed. The limestone suspension flowed into the DEMF tube and valve V3 was then used to control the precoating pressure at 100 kPa (this was below the normal operating pressure). During the precoating cycle, which operated in cross-flow mode, the cross-flow velocity and pressure were kept constant.

After the precoating cycle, the flow to the pump suction was switched from the precoating to the feed suspension. Valve V5 was then opened, valve V3 closed and the tube was once again operated in the dead-end mode. The PID controller would then bring the system up to operating pressure and control the system as normal. The return line was purged to drain for a short while to prevent any residual precoating material from entering the feed tank.

4.6 MEASUREMENT TECHNIQUES (CROSS-FLOW MICROFILTRATION AND DEAD-END MICROFILTRATION

Permeate Flux

The majority of flux readings were collected in the first hour of operation since the largest flux decline occurred in the first 45 min of operation after which the flux levelled out.

A beaker was tared on a Mettler electronic balance, accurate to 1g. At least 100 g of permeate was collected for each reading so as to minimise the uncertainty associated with the measuring technique.

Turbidity

A turbidity reading was taken after every flux measurement in accordance with the procedure outlined in Sec. 4.2.

4.7 DATA PROCESSING AND ERROR ANALYSIS (CROSS-FLOW MICROFILTRATION AND DEAD-END MICROFILTRATION)

The error associated with the measurement of key variables will be outlined as well as errors associated with the display of graphical data. This section combines the analysis for the DEMF and the CFMF.

4.7.1 Calculation of the Permeate Flux and the Superficial Inlet Velocity

The density of water was taken to be equal 1 000 g/ℓ.

$$\text{Permeate Flux } (\ell/m^2h) = \frac{Permeate\ Flowrate}{Filtration\ Area} \times \frac{3\ 600}{1}$$

$$= \frac{V}{t} \times \frac{1}{2\pi r l} \times \frac{3\ 600}{1}$$

$$= \frac{V}{t} \times \frac{1}{0,0252\pi l} \times \frac{3\ 600}{1}$$

Superficial Inlet Velocity (m/s)

$$= \frac{Feed\ Flowrate}{Flow\ Area} \times \frac{1}{3\ 600} \times \frac{1}{1\ 000}$$

$$= \frac{Q_f}{\pi r^2} \times \frac{1}{3\ 600\ 000}$$

$$= \frac{Q}{\pi \cdot (0,0126)^2} \times \frac{1}{3\ 600\ 000}$$

$$= \frac{Q}{1795,5}$$

4.7.2 Uncertainties in Primary Measurements

Table 4.1 lists the various measurements that were taken during the course of the experimental program, the range of the values and estimated maximum and minimum errors associated with each variable.

Variable	Value		Uncertainty	%Uncertainty	
	Max	Min		Max	Min
Equipment Variables					
Tube radius (m)	0,0126	-	0,00025[3]	1,98	-
Tube length (m)	0,926	0,741	0,001	0,13	0,11
Measured Variables					
Mass of permeate collected (g)	0,790	0,097	0,001	1	0,1
Time to collect the permeate (s)	600	60	0,5	0,8	0,1
Turbidity (feed) - range 1 (NTU)	90	40	1	2,5	1,1
Turbidity (permeate) - range 1 (NTU)	40	10			
Turbidity (permeate) - range 2 (NTU)	10	1			
Turbidity (permeate) - range 3 (NTU)	1	0,1			
Operating Variables					
Flowrate (ℓ/h)	4 100	2 300	50	2,2	1,2
Pressure (kPa)	400	100	1	1	0,3

Table 4.1 : The range of variables and uncertainties associated with each are tabulated

3 Pillay, [1992a]

4.7.3 Uncertainties in Calculated Parameters

The percentage uncertainty associated with each of the calculations in Sec. 4.7.2 is given by the largest percentage uncertainty among the independent variables (given by Table 4.1). Thus the percentage uncertainty associated with the permeate flux and the superficial inlet velocity is given by :

Permeate Flux :

Variable	Uncertainty
Permeate flowrate	1 %
Time	0,8 %
Radius	2 %
Length	0,1 %
Max. uncertainty	2%

Superficial Inlet Velocity :

Variable	Uncertainty
Feed flowrate	2,2 %
Radius[4]	2 × 2%
Max. uncertainty	4%

Feed Concentration

The feed concentration was calculated by measuring the turbidity of the feed and reading the concentration off a standard turbidity - concentration curve (**Appendix C**). For high concentrations (>160 mg/ℓ), this was done using serial dilution as outlined in Sec. 4.2.

The maximum error associated with the measurement of the feed turbidity was 2,5%. This translates to a maximum concentration error of 2,5%.

4.7.4 Processing of Experimental Results

A model for the flux-time curve was developed for the DEMF in Sec. 2.1.1. The model equation took on the form :

$$\frac{dV_a}{dt} = \frac{1}{2b\sqrt{t/b}} \qquad (2.9)$$

4 The uncertainty is doubled since the radius was raised to the power of 2 in the calculation of the velocity (See Sec 4.7.1)

Various empirical modifications of Eqn. 2.9 were tested against the data and it was found that for the DEMF, the following form gave consistent and reliable fits :

$$\frac{dV_a}{dt} = \frac{X}{\sqrt{t+Z}} + Y \tag{4.1}$$

where X , Y and Z are constants.

It was felt that the basis for developing Eqn. 4.1 might have some similarities with the CFMF. Eqn. 4.1 was extended for use with the CFMF by adding an additional term to the equation. There was no theoretical basis for adding the additional parameter, but the new equation was found to give excellent correlation with the actual experimental data points. The general form of the equation was as follows :

$$\frac{dV_a}{dt} = \frac{A}{\sqrt{t+C}} + B + \frac{D}{t} \tag{4.2}$$

where A , B , C and D are constants.

The actual experimental results appear in Appendix D. A computer program was written which took the raw data and regressed against the constants for the DEMF and CFMF in Eqns. 4.1 and 4.2 respectively. The constants obtained are also listed in Appendix D. Typical experimental fits obtained for the DEMF (Run D19) and the CFMF (Run 17) are shown in Figs. 4.3 and 4.4. Similar fits were obtained with all the experiments.

Note on the experimental data

The regressed function obtained for each experiment was used to generate the flux-time curves which have subsequently been plotted through the experimental points.

The experiments were conducted over differing time periods. In order to standardize the graphs, all flux-time curves (unless otherwise indicated) have been plotted for a 24 h period (or 1440 min). Experiments conducted for a shorter time period have been extrapolated to 24 h and this would be apparent from the actual data points which are also plotted. Experiments of a longer duration have only been plotted up to 24 h, though the regressed parameters were obtained by using the full experimental data set.

All the DEMF experimental run numbers have been prefixed with a *D* (eg. Run D17) while all CFMF experiments have no prefix (eg. Run 17).

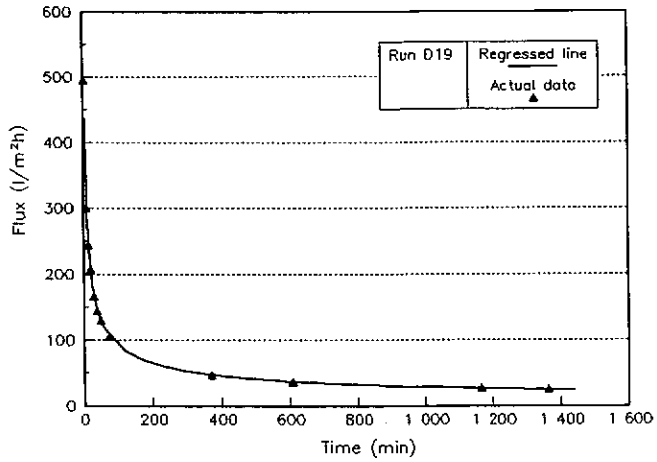

Figure 4.3 : Graph showing a typical regressed experimental curve (Run D19) together with experimental data for the DEMF

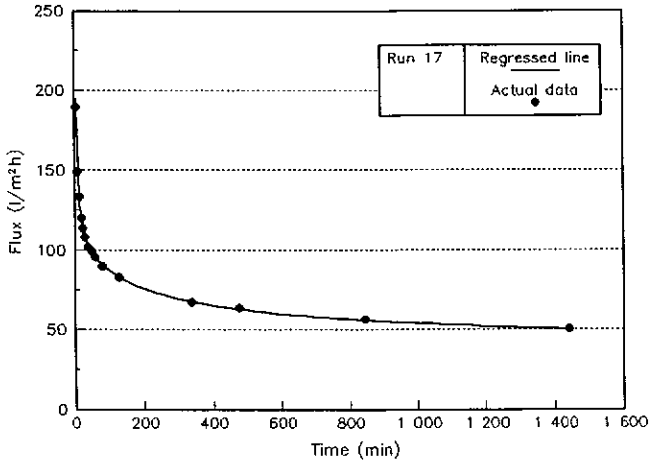

Figure 4.4 : Graph showing a typical regressed experimental curve (Run 17) together with experimental data for the CFMF

4.7.5 Errors Associated with the Flux - Time Curves

There are two sources of errors inherent in the flux-time curve reported in **Chapter 5**, namely :

- Uncertainty in the flux value, ± 2% (See Sec. 4.7.3)
- Uncertainty in the time at which the flux is plotted. The uncertainty associated with the time at which the flux is plotted is given by $t \pm t_{perm} / 2$ where t_{perm} is the time taken to measure a quantity of permeate and t is the time at which the flux has been plotted and the time at which the measuring of the permeate began.

A typical flux-time curve for the CFMF, with an uncertainty envelope calculated from both the flux and time uncertainties, is shown in Fig. 4.5. The uncertainties are clearly insignificant and have not been included in subsequent flux-time curves.

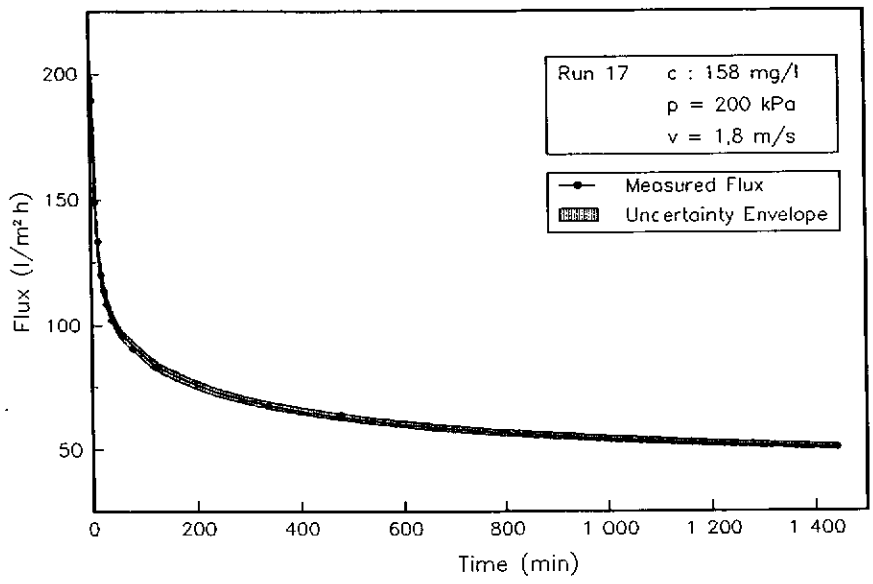

Figure 4.5 : A graph showing the uncertainty associated with a typical CFMF flux-time curve

4.7.6 Repeatability

Several experiments were conducted at similar operating conditions in order to establish the repeatability of the experiments. Figs. 4.6 and 4.7 show separate experiments for the CFMF and the DEMF respectively, conducted under similar conditions for each system.

When testing the sensitivity of the flux to various operational parameters (such as pressure) it is important to establish a threshold below which an experimental deviation cannot be distinguished from experimental error. If the dependence of flux on the operating parameters (Eqn. 2.19) were known, this threshold could be determined from the uncertainties in the measured values.

Since this was not the case, the threshold was estimated from replicated experimental measurements summarised in Fig. 4.6 and 4.7 by taking the sample standard deviation of the flux measurements made at each elapsed time, and expressing it as a percentage of the mean flux measurement at that time. A figure of approximately 6% was found to represent all the data of Figs. 4.6 and 4.7.

Assuming that the distribution of values is normal, then roughly 60 % of the experimental values are expected to fall within one standard deviation of the mean. In order to conclude that a variation in any one of the control variables has a real effect on the flux, the flux value would have to lie substantially outside the error band.

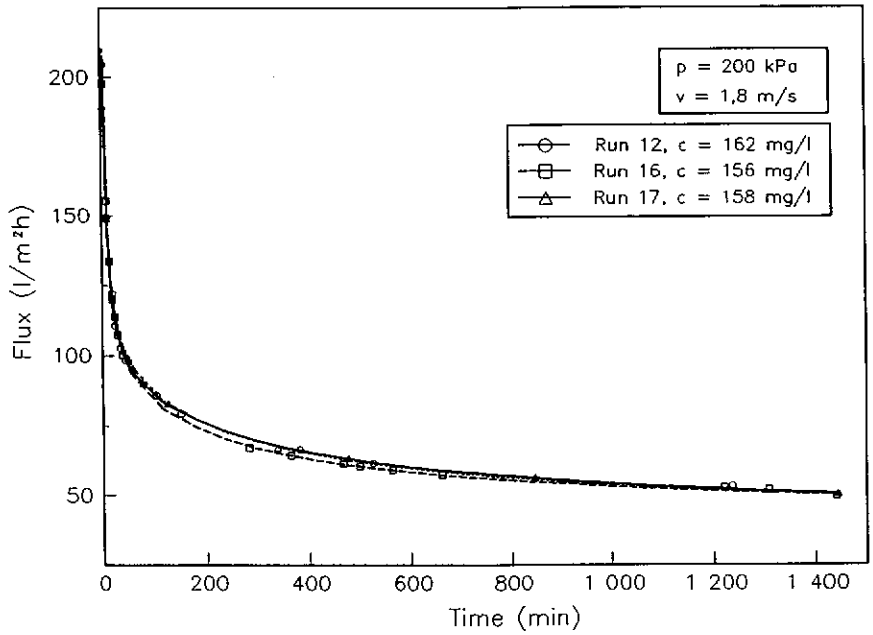

Figure 4.6 : A graph showing flux-time curves for the CFMF for different experiments conducted under similar operating conditions in order to establish the repeatability of the experiments. The regressed parameters were used to plot the curves through the actual experimental points

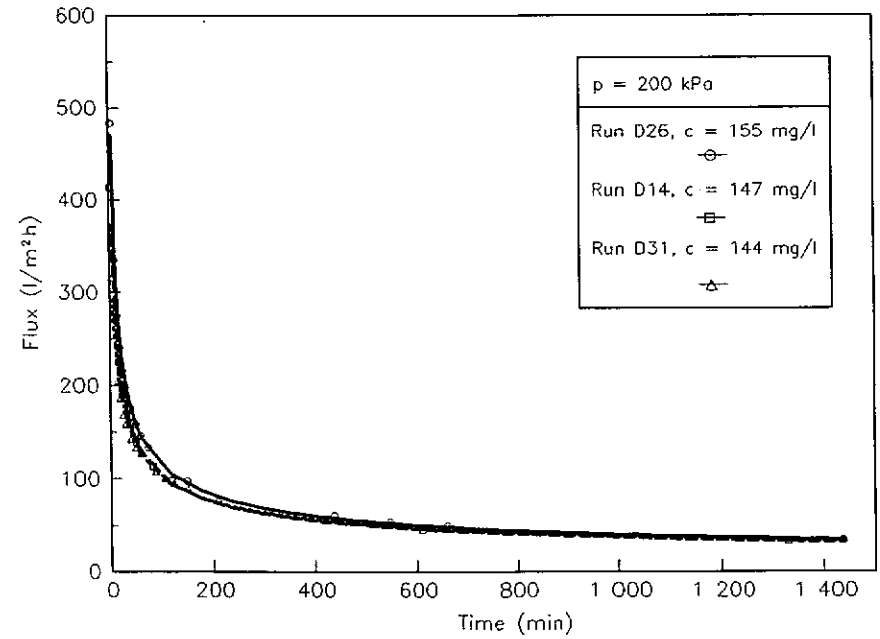

Figure 4.7 : A graph showing flux-time curves for the DEMF for different experiments conducted under similar operating conditions in order to establish the repeatability of the experiments. The regressed parameters were used to plot the curves through the actual experimental points

CHAPTER

FIVE

Results and Discussion

It would be beneficial to restate the aims of the project :

(i) To obtain flux and permeate quality data for the CFMF and the DEMF, using a low suspended solids water (<1 000 mg/ℓ)

(ii) To compare the performance of the two processes and to develop criteria for their selection

5.1 CROSS-FLOW MICROFILTRATION EXPERIMENTAL WORK

5.1.1 Experimental Methodology - Cross-flow Microfiltration

Sensitivity of the experimental system to pressure

It was outlined in Sec. 4.4.1 that the three variables which could be controlled in the system are the pressure, flowrate (and therefore the velocity) and the feed concentration.

Many CFMF systems display a relative insensitivity to pressure. In order to reduce the number of experimental variables, the sensitivity of this experimental system to pressure was tested. Experiments were conducted at two concentrations (approximately 75 mg/ℓ and 300 mg/ℓ) and two outlet pressures (200 and 300 kPa). The results for Runs 9 and 25 are displayed in Fig. 5.1 while the results for Runs 10 and 11 are shown in Fig. 5.2.

From Fig. 5.1 and Fig. 5.2 it is clear that the cross-flow system was relatively insensitive to pressure and that the flux variation was only marginally wider than the error band that could be attributed to an error in repeatability. This error band has been established to be approximately ± 6% (See Sec 4.7.6).

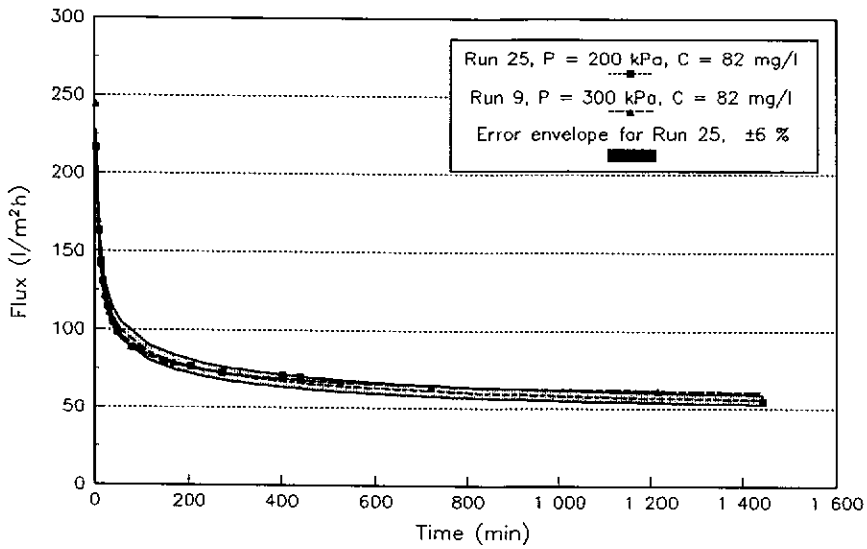

Figure 5.1 : A graph showing flux-time curves for the CFMF for experiments conducted at two pressures (200 and 300 kPa) and a concentration of approximately 75 mg/ℓ with a cross-flow velocity of 1,8 m/s, in order to establish the pressure sensitivity of the system. The error envelope of ± 6 % corresponding to Run 25 is shown.

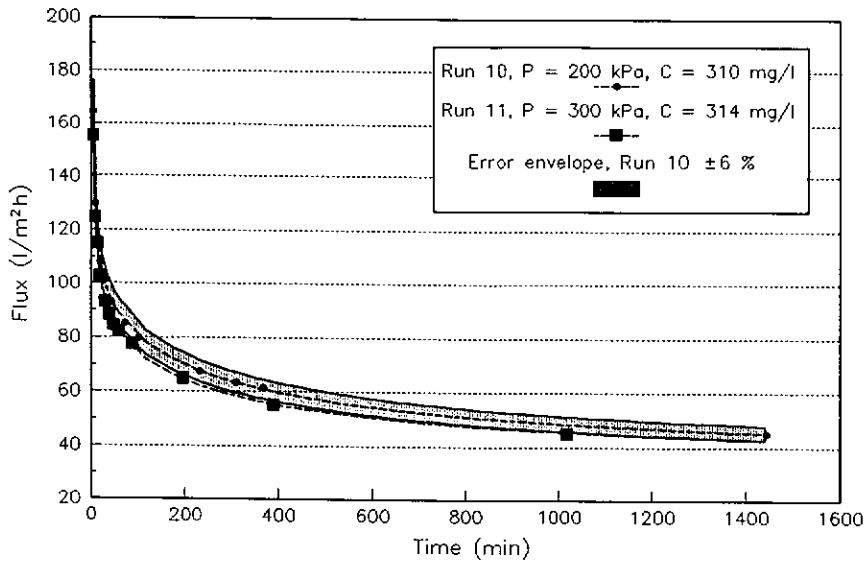

Figure 5.2 : A graph showing flux-time curves for the CFMF for experiments conducted at two pressures (200 and 300 kPa) and a concentration of approximately 300 mg/ℓ with a cross-flow velocity of 1,8 m/s, in order to establish the pressure sensitivity of the system. The error envelope of ± 6 % corresponding to Run 10 is shown.

The insensitivity of some suspensions to pressure has been widely reported in ultrafiltration and to a lesser extent in microfiltration. Some researchers have reported an insensitivity to pressure [Tarleton & Wakeman, 1991; Hoogland, Fane & Fell, 1988;

Fordham & Ladva, 1989], while others found the flux to pass through a maximum [Saw *et al.*, 1985] or minimum [Baker *et al.*, 1985] as the trans-membrane pressure was increased. Some researchers found a dependence at very low pressures but when the pressure exceeded a particular value, the flux reached a plateau and became relatively insensitive to pressure [Henry, 1972]. The insensitivity of flux to increases in pressure has been widely reported in ultrafiltration and has been explained by the solute polarization mechanism [Blatt *et al.*, 1970]. The phenomenon arises where potential improvements gained by raising the pressure are offset by an increase in the flow resistance of the fouling layer.

Experimental Matrix

Based on the observed insensitivity of this experimental system to variations in pressure, it was decided to eliminate pressure as a variable and all subsequent experiments were conducted at 200 kPa.

The remaining two manipulable variables were velocity and concentration. A concentration range from 75 mg/ℓ to 600 mg/ℓ was spanned and it was felt that if no firm conclusions could be drawn at the extremes of the concentration range then further experiments would be undertaken. Five concentrations were chosen at approximately 75; 150; 300; 450 and 600 mg/ℓ. Since the solids content was fairly small, it was difficult to control the feed concentration accurately and hence (Sec. 4.2) the turbidity of the feed suspension was measured and the feed concentration was thus determined from a calibration chart (Appendix C).

Economic velocities for CFMF are generally considered to lie between 1 and 3 m/s. Three velocities were chosen namely 1,3; 1,8 and 2,3 m/s.

A 5 by 3 experimental matrix (Fig. 5.3) was used. The experiments were performed in a random order and the point (1,8 m/s ; 150 mg/ℓ) was used as the reference point. The entire matrix was not completed as it was felt that sufficient trends were obtained from the pattern of experiments that were chosen. The reference point was repeated after every few experiments or whenever a major change was implemented in the system such as replacing a fabric tube.

	1,3 m/s	1,8 m/s	2,3 m/s
75 – 82 mg/ℓ	22	8, 9, 25	30
158 – 167 mg/ℓ	20	12, 15, 16, 17	13, 21
304 – 314 mg/ℓ		10, 11, 26	
448 mg/ℓ		27	
582 – 617 mg/ℓ	19, 28	23, 24	14, 29

Figure 5.3 : A matrix showing the experimental design for the CFMF experiments. Experiments were conducted at five approximate concentrations (75; 150; 300; 450 and 600 mg/ℓ) and three superficial inlet velocities (1,3; 1,8 and 2,3 m/s). The concentration range at each approximate concentration is shown on the matrix. The experiment numbers are shown on the matrix and coincide with the order in which the experiments were performed.

5.1.2 Experimental Results - Cross-flow Microfiltration

Effect of velocity on flux

The inlet velocity of the suspension was varied over the five feed concentrations and the pressure maintained at 200 kPa. It was found that increasing the velocity at approximately 75 mg/ℓ did not increase the flux significantly whereas at approximately 600 mg/ℓ, the effect on flux was very noticeable. The effect of velocity at different concentrations is shown in Figs. 5.4, 5.5 and 5.6.

A significant feature of Fig. 5.4 and 5.5 is an apparent *cross-over* after the period of initial decline. The lower velocity has a higher flux until the *cross-over* point, after which the higher velocity maintains a higher flux. The *cross-over* point is shown on both figures. It should be noted that as the concentration increases so the *cross-over* point moves closer to the start of the experiment. At approximately 600 mg/ℓ, the *cross-over* occurs within the first few minutes and is not graphically distinguishable.

There is general agreement in the literature that the steady state flux increases with an increase in the superficial inlet velocity. However, to the knowledge of the author, there have been no other references in the literature which report the *cross-over* observed in this study. This is largely due to the fact that the majority of the researchers report steady state flux values as opposed to flux profiles. In this study the profile of the flux-time curve was of interest as it gives insight into the operation of the filter over a production cycle.

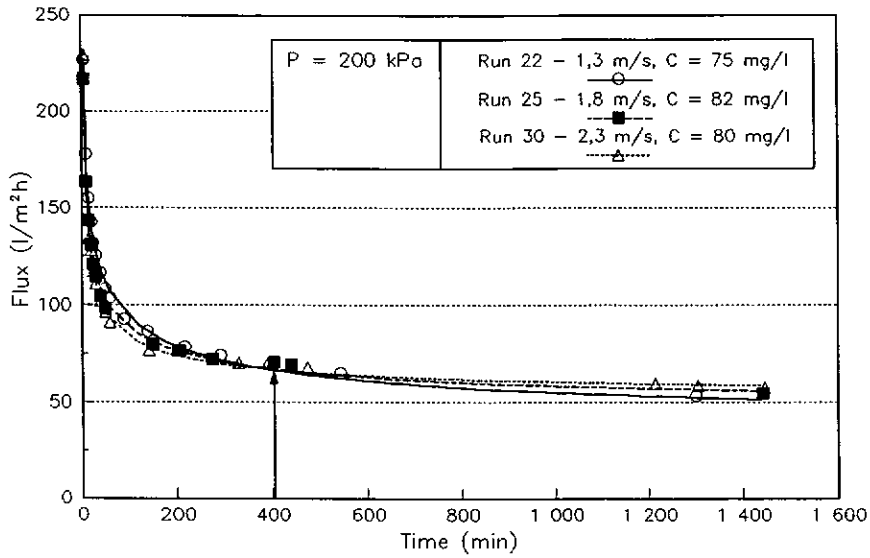

Figure 5.4 : Figure showing the effect of the variation of velocity at a feed concentration of approximately 75 mg/ℓ and a pressure of 200 kPa

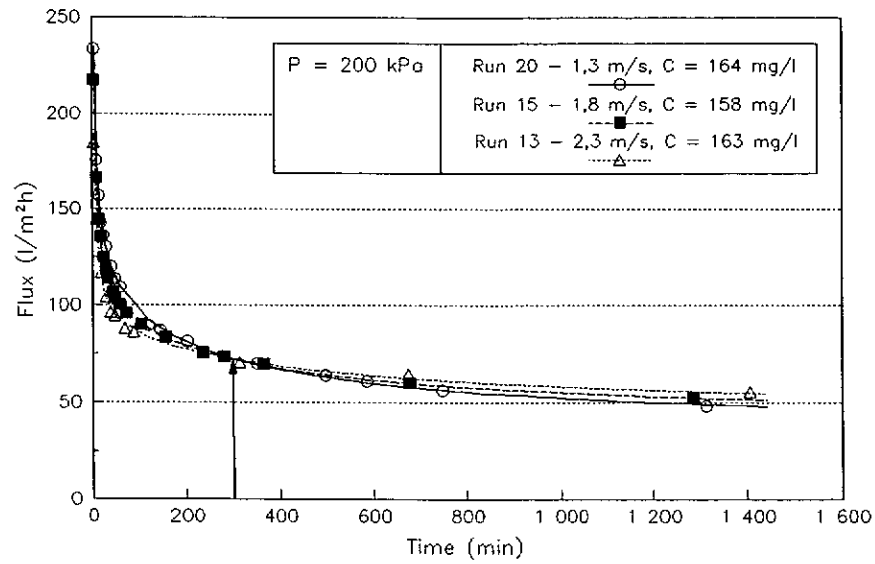

Figure 5.5 : Figure showing the effect of the variation of velocity at a feed concentration of approximately 150 mg/ℓ and a pressure of 200 kPa

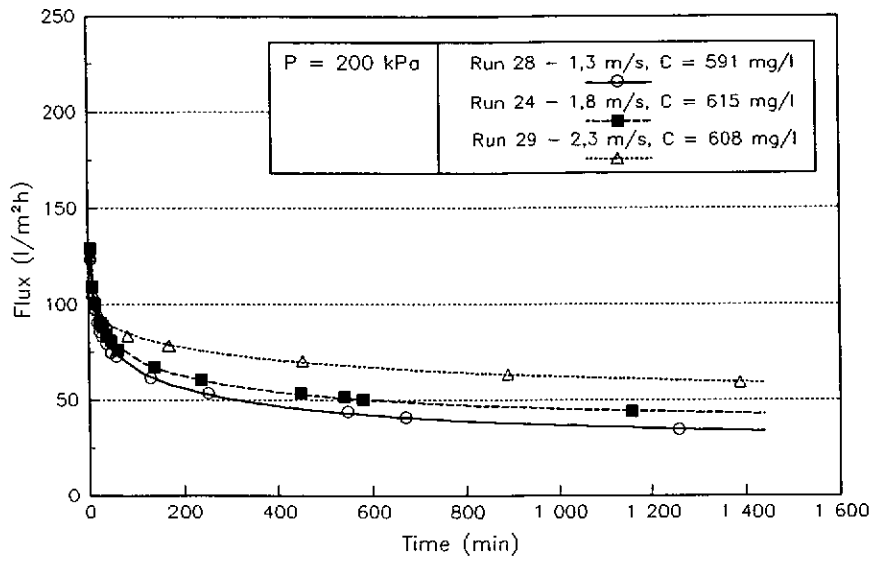

Figure 5.6 : Figure showing the effect of the variation of velocity at a feed concentration of approximately 600 mg/ℓ and a pressure of 200 kPa

Effect of concentration on flux

The inlet velocity and the pressure were held constant at 1,8 m/s and 200 kPa while the concentration was varied. Fig. 5.7 shows the effect of concentration on the permeate flux. It can be seen that the permeate flux showed only a minor dependence on concentration when the system was operated in the CFMF mode. It is worth noting that at the high concentration range (approximately 600 mg/ℓ), the steady state flux appeared to be established at a much faster rate. This trend was confirmed with repeatable experiments. Tarleton and Wakeman (1991) report a similar trend on calcite suspensions and found that this was exaggerated at smaller particle sizes. They suggest that for different feed concentrations, the fouling mechanisms are significantly dissimilar.

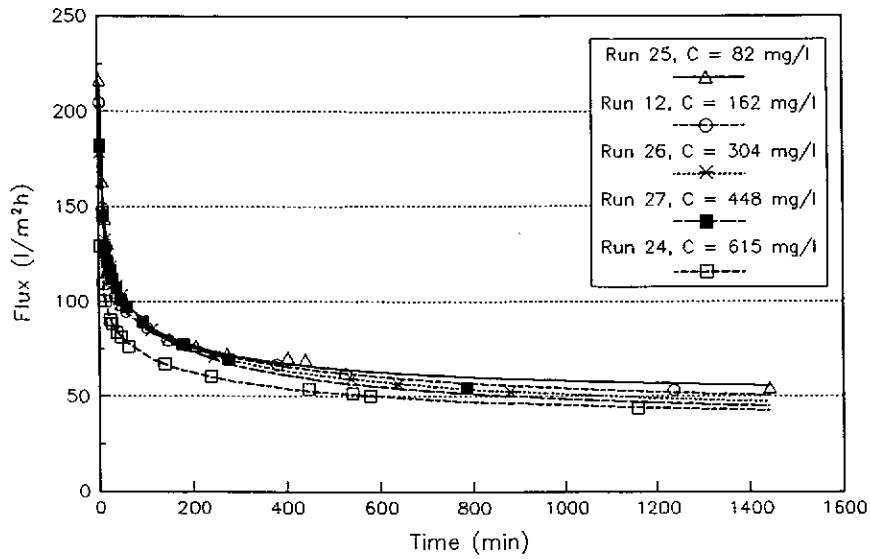

Figure 5.7 : Figure showing the effect of the variation of concentration while the feed velocity was maintained at 1,8 m/s and the pressure at 200 kPa

Permeate quality

The permeate quality or turbidity was monitored in all the CFMF experiments. It was found that in all experiments, a permeate turbidity of below 0,5 NTU was achieved within 10 to 15 min of start-up. No trends could be established with respect to changes in concentration, velocity or pressure. A typical turbidity profile (Run 15) is shown in Fig. 5.8.

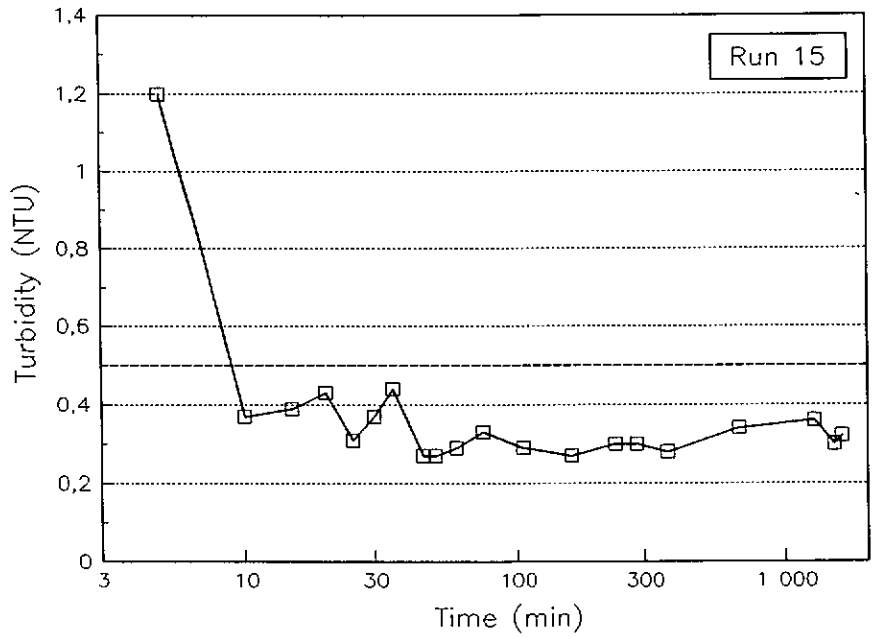

Figure 5.8 : A typical permeate turbidity profile. Note that the x-axis is plotted on a logarithmic scale.

Precoats

It will be shown in the next section that the main motivation for using precoats in the DEMF was to enhance the permeate quality. The quality of the permeate in the CFMF was found to meet the criteria laid down in Sec. 4.2. and hence there was little motivation to use a precoating material in the CFMF. The use of precoating materials on the CFMF is also being investigated at Natal University and hence did not form part of the scope of this dissertation.

It will be shown in Sec. 5.2.2. that the use of precoats in the DEMF gave significant flux enhancements in addition to enhancing the permeate quality. Pillay (1992b) found that the use of precoats in the CFMF gave significant flux enhancements on a feed suspension of activated sludge and hence it might be possible that under certain precoating conditions, using the feed suspension identified in this study, the CFMF might also display flux enhancements. However, as outlined in Sec. 3.3. the aim of this dissertation was not to optimise the use of precoats and this should rather form the basis of future work. All experiments in this study have thus been performed using unprecoated CFMF.

5.2 DEAD-END MICROFILTRATION EXPERIMENTAL WORK

5.2.1 Experimental Methodology - Dead-end Microfiltration

It was outlined in Sec. 4.5 that the two variables which could be manipulated in the DEMF system are the pressure and the feed concentration.

The body of literature available relating to the TFP (or DEMF - see Sec. 2.1.1) is small in comparison to the CFMF and relates mainly to the work performed by Rencken and associated researchers.

Rencken (1992) used a waterworks sludge which was compressible in nature. As would be expected for a compressible cake, the effect of filtration pressure on dead-ended permeate flux was not very great. It was decided to test the sensitivity of the system in this study to variations in pressure with a view to eliminating pressure as a variable as was done in the CFMF system.

5.2.2 Experimental Results - Dead-end Microfiltration

Effect of pressure

The pressure was varied over two concentration ranges to determine the sensitivity to pressure. The results are shown in Fig. 5.9 and Fig. 5.10 together with the error bands, namely ± 6% (See Sec. 4.7.6). Only one such band has been plotted in each case, but clearly these bands overlap. In Figs. 5.9 and 5.10 the error bands for Run D5 (300 kPa) and Run D10 (300 kPa) have been plotted respectively. The system appears to become less insensitive with respect to pressure as the pressure increases, however this is at the expense of permeate quality. It was decided that all the DEMF experiments would be performed at 200 kPa which would also give a basis for comparison with the CFMF.

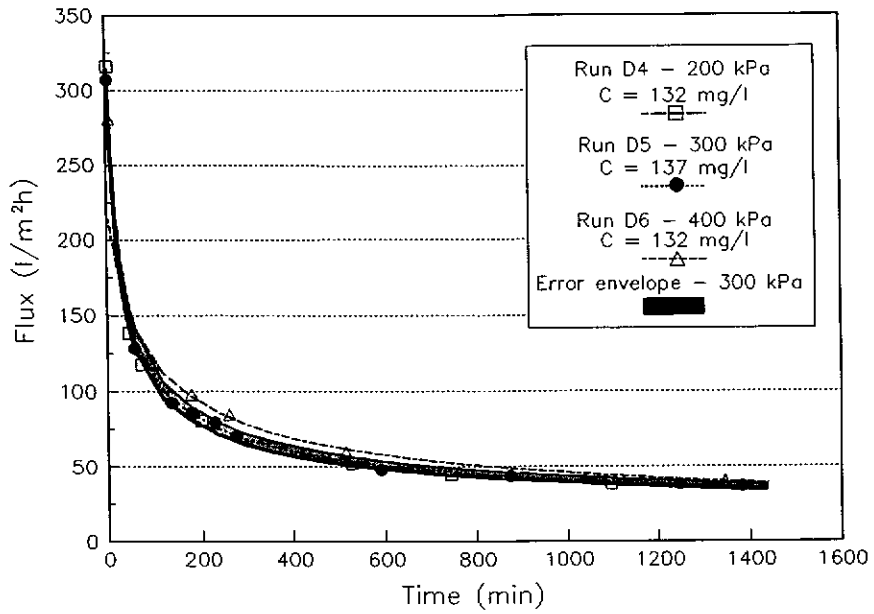

Figure 5.9 : A graph showing the variation of pressure at a feed concentration of approximately 135 mg/L

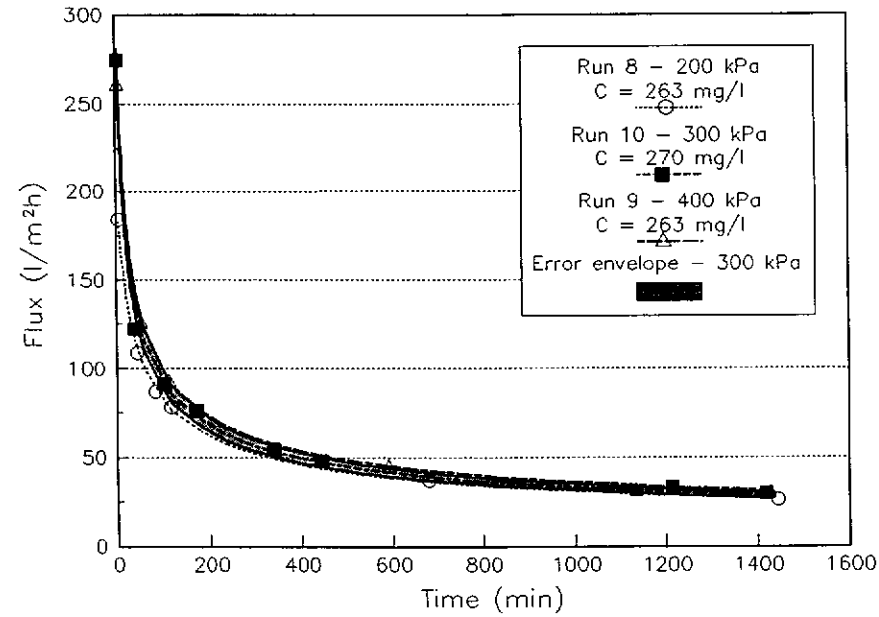

Figure 5.10 : A graph showing the variation of pressure at a feed concentration of approximately 270 mg/l.

DEMF permeate quality

Early experiments indicated that a very poor permeate quality was obtained from the DEMF. It was found that the dead time (time taken from the start of the run before an acceptable permeate quality was obtained) varied considerably and no trends could be established with regard to either concentration or pressure. The poor permeate quality was due largely to isolated areas of pinholing (see Sec. 3.2.2). The pinholing is mainly affected by particle orientation at the fabric surface. Variation of the experimental parameters had little or no impact on the turbidity profiles. Fig. 5.11 shows typical turbidity profiles found in the unprecoated DEMF experiments. It was found that there was very poor repeatability with respect to the turbidity profiles and the dead time could vary from 5 to 300 min.

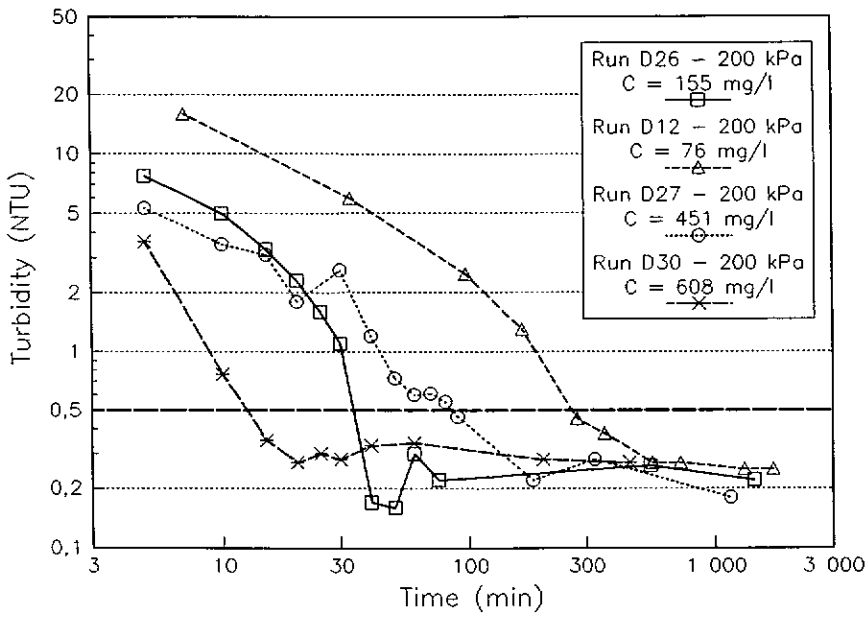

Figure 5.11 : A graph showing the variation of turbidity profiles. The level of acceptable turbidity is indicated on the graph at 0,5 NTU. Note that both axis are on a logarithmic scale

Effect of Precoats on the Dead-end Microfilter

The poor and unpredictable nature of the DEMF permeate turbidity was considered to be a major obstacle in the initial phase of the research. It was outlined in Sec. 3.3 that instances arise where the suspended matter in the feed does not form an adequate membrane and hence a dynamic membrane needs to be artificially laid down prior to switching to the feed suspension. Various precoating methods were initially tested, but it was found that precoating in the cross-flow mode (Sec. 4.5.3) with a 300 mg/ℓ suspension of KULU 5 limestone before switching to the dead mode, gave a consistent high quality permeate. As was stated in Sec. 3.3. no attempt was made to optimise the precoating material or the precoating conditions as that was beyond the scope of this project. It

was found that using the precoating method outlined in Sec. 4.5.3, a turbidity of below 0,5 NTU was consistently established within 5 min of the introduction of the feed suspension into the tube. This gave the DEMF and CFMF comparable permeate qualities. Typical turbidity profiles have been plotted in Fig. 5.12.

The high quality permeate that was obtained via this method was found to be only possible at an operating pressure of 200 kPa. If after precoating, the suspension was introduced at a higher pressure, say 300 or even 400 kPa, extensive pinholing occurred along the seams. Several techniques were used to try and seal the seams as outlined in Sec. 3.2.3 but the method that was finally used was found to be suitable only for low pressures, namely 200 kPa. It would appear that as the pressure is increased, the seams move apart with the result that even the precoating layer is forced through thus resulting in poor permeate quality. This might be overcome using a precoating material with a different particle size distribution or morphology, but as was mentioned, only one precoating material was used and no attempt was made to optimise the precoating technique. Using the commercial full scale curtain might also prevent pinholing at the seams since the seams become self sealing as outlined in Sec. 3.2.2. The pressure of 200 kPa was thus used for all experiments.

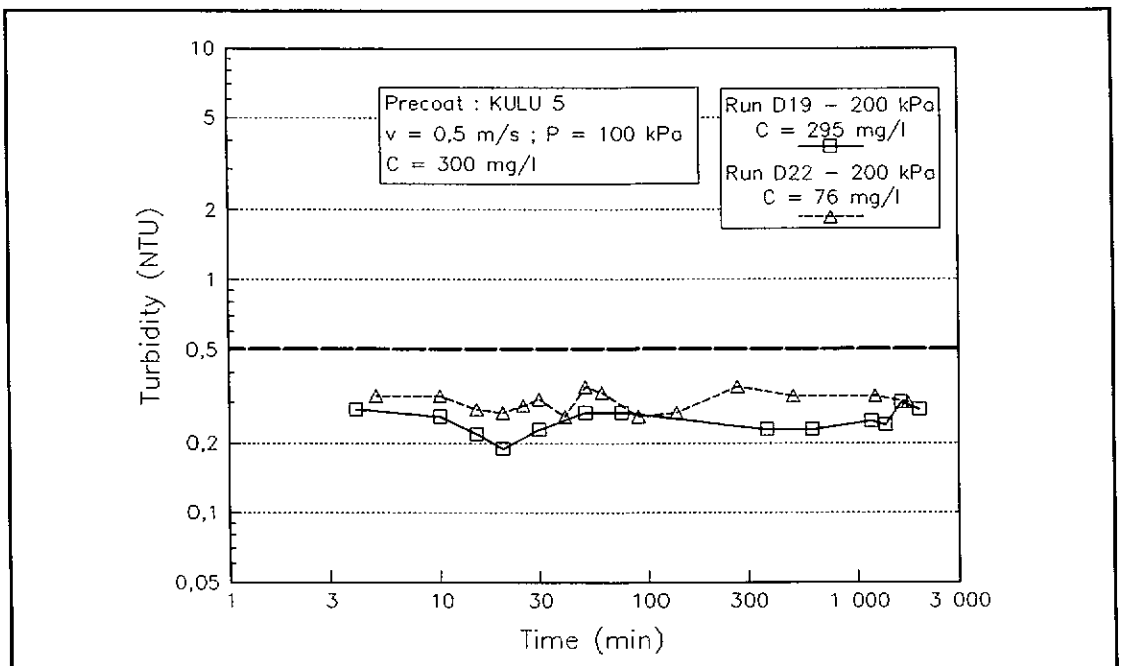

Figure 5.12 : A graph showing the variation of turbidity profiles for a precoated DEMF experiment. Both axis are plotted on a logarithmic scale. The level of acceptable turbidity is indicated on the graph at 0,5 NTU.

Effect of concentration

The concentration was varied between approximately 75 and 600 mg/ℓ at a fixed pressure of 200 kPa. The DEMF tube was first precoated with a limestone suspension as outlined in Sec. 4.5.3 before switching to the dead end mode of operation. The concentrations were randomly varied and the experimental point of approximately 150 mg/ℓ was used as the reference experiment against which any changes in the system were measured and repeatability tested. A matrix of the experimental design is shown in Fig. 5.13.

	12, 28	22, 25
	1, 2, 3, 4, 5, 6, 7	
	14, 26, 31	16, 17, 20
	8, 9, 10, 13, 29	18, 19, 24
	27	23
	15, 30	21

Figure 5.13 : **A matrix showing the experimental design for the precoated and unprecoated DEMF experiments. The concentration range at each approximate concentration is shown on the matrix. The experiment numbers are shown on the matrix, and coincide with the order in which the experiments were performed.**

Fig. 5.14 shows permeate flux profiles with changes in the feed concentration for a precoated DEMF experiment. As would be expected, the permeate flux profiles showed a dependence on the feed concentration, with an increase in concentration showing a decrease in flux. Fig. 5.15 shows flux profiles of precoated and unprecoated experiments. The permeate quality of the unprecoated experiments was poor as discussed in the previous section, but what was also apparent was the significant initial flux enhancement that precoating gave the DEMF. This flux enhancement was most significant in the lower concentration ranges, but as the concentration increased, the precoating was seen to retard the flux after the initial enhancement.

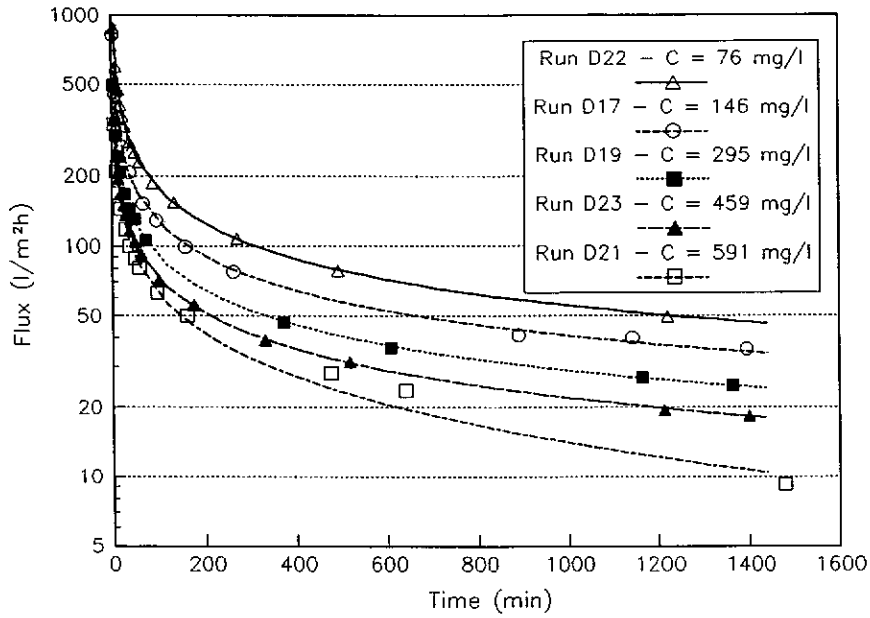

Figure 5.14 : **A graph showing flux profiles for variations in concentration for a precoated DEMF experiment. The Y-axis is plotted on a logarithmic scale. All experiments used the same precoating conditions and operated at a pressure of 200 kPa.**

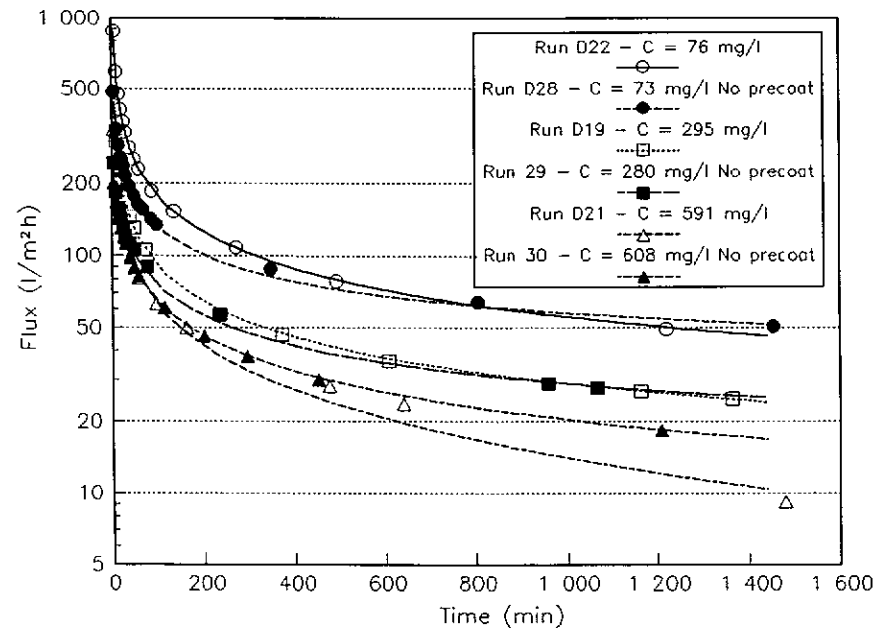

Figure 5.15 : **A graph showing flux profiles for variations in concentration for both precoated and unprecoated DEMF experiments. The Y-axis is plotted on a logarithmic scale. All experiments operated at a pressure of 200 kPa.**

The previous sections have outlined the significant process trends of the CFMF and the DEMF for a low suspended solids water. The two processes will now be compared and process choices and trends outlined.

5.3 COMPARISON BETWEEN THE CROSS-FLOW MICROFILTER AND THE DEAD-END MICROFILTER

It has been established that with a precoat the DEMF is able to give a permeate of the same quality as the CFMF. In both processes a permeate quality meeting the 0,5 NTU limit, was established within the first 10 min of operation. The dead-time, t_d for the two processes was thus the same.

The other variable which needs to be compared is the permeate flux. The flux profile will have an influence on the choice of cycle time and therefore on the mode of operation. A comparison is made in Figs. 5.16 to 5.20 where the flux profile for both precoated and unprecoated DEMF is plotted alongside the profile for unprecoated CFMF. From the graphs it is clear that the precoated DEMF, besides giving enhanced permeate quality over unprecoated DEMF, also gives a higher flux than unprecoated CFMF. This is particularly true in the lower concentration ranges.

From Fig. 5.16 it is seen that the precoated DEMF has a higher flux than the unprecoated CFMF up to approximately 400 min, whereafter the flux profiles cross and the unprecoated CFMF has a higher flux. As the concentration of the feed suspension is increased, the *cross-over* point moves closer to the start of the run.

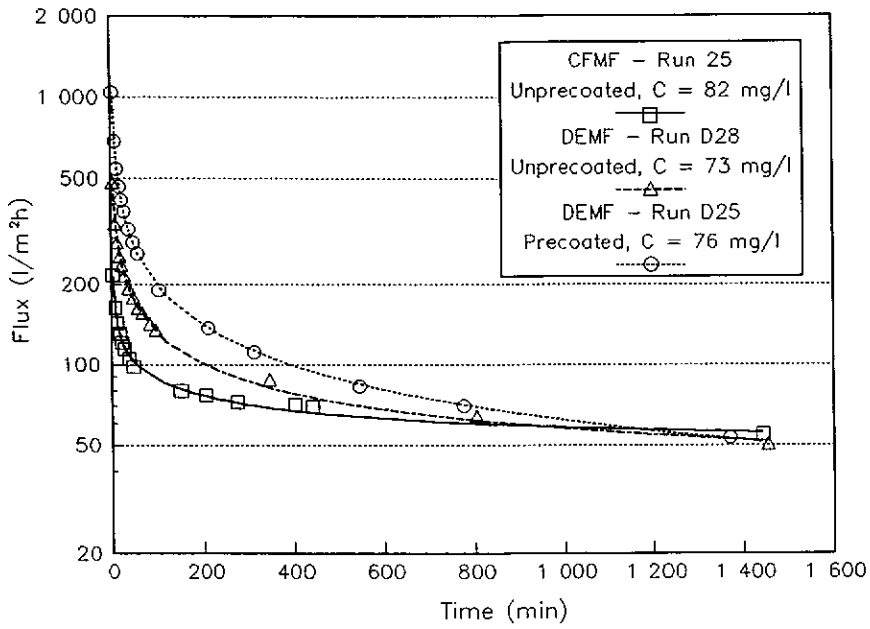

Figure 5.16 : **A graph showing a comparison between the flux profiles of unprecoated CFMF and both precoated and unprecoated DEMF. The experiments were undertaken at a feed concentration of approximately 75 mg/l and all experiments operated at a pressure of 200 kPa.**

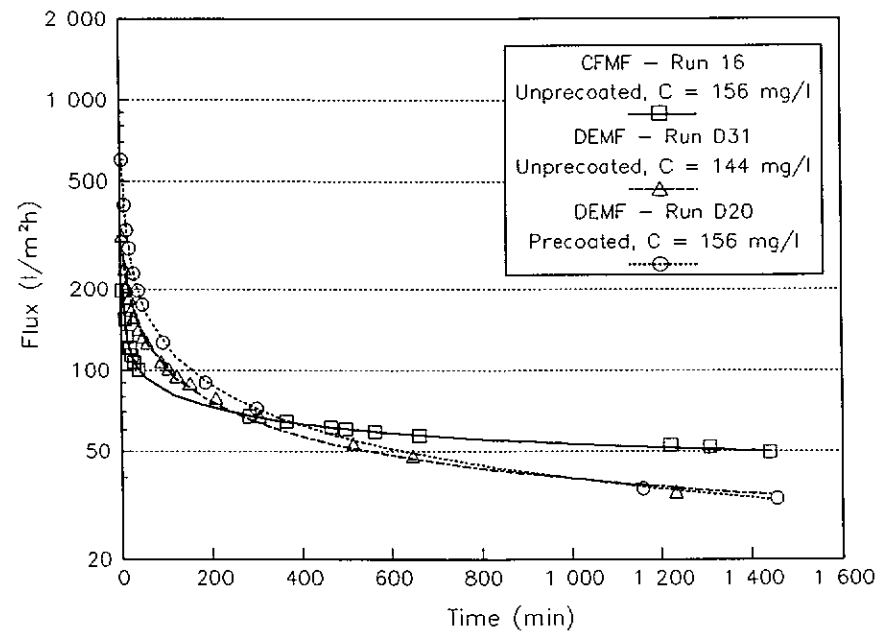

Figure 5.17 : **A graph showing a comparison between the flux profiles of unprecoated CFMF and both precoated and unprecoated DEMF. The experiments were at a feed concentration of approximately 150 mg/l and all experiments operated at a pressure of 200 kPa.**

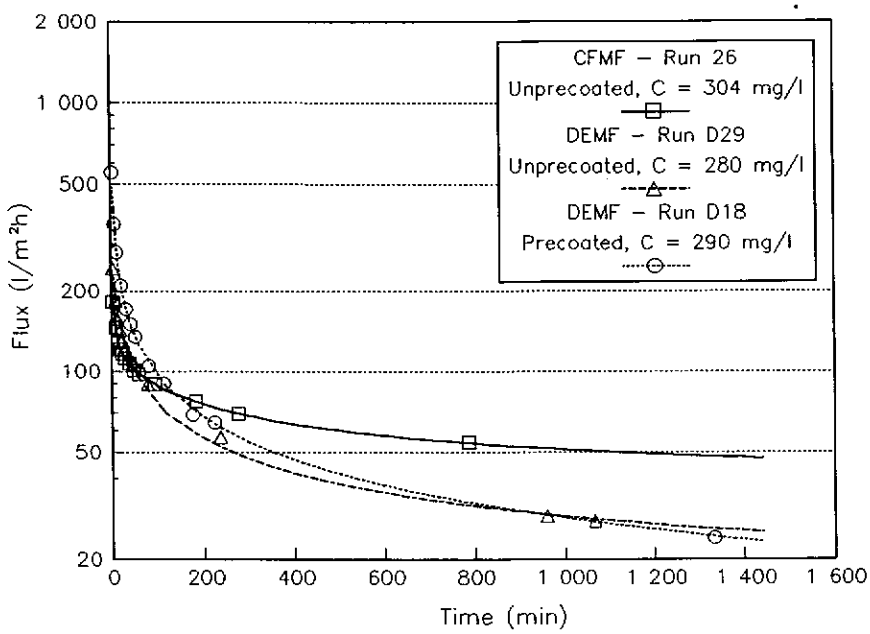

Figure 5.18 : **A graph showing a comparison between the flux profiles of unprecoated CFMF and both precoated and unprecoated DEMF. The experiments were at a feed concentration of approximately 300 mg/l and all experiments operated at a pressure of 200 kPa.**

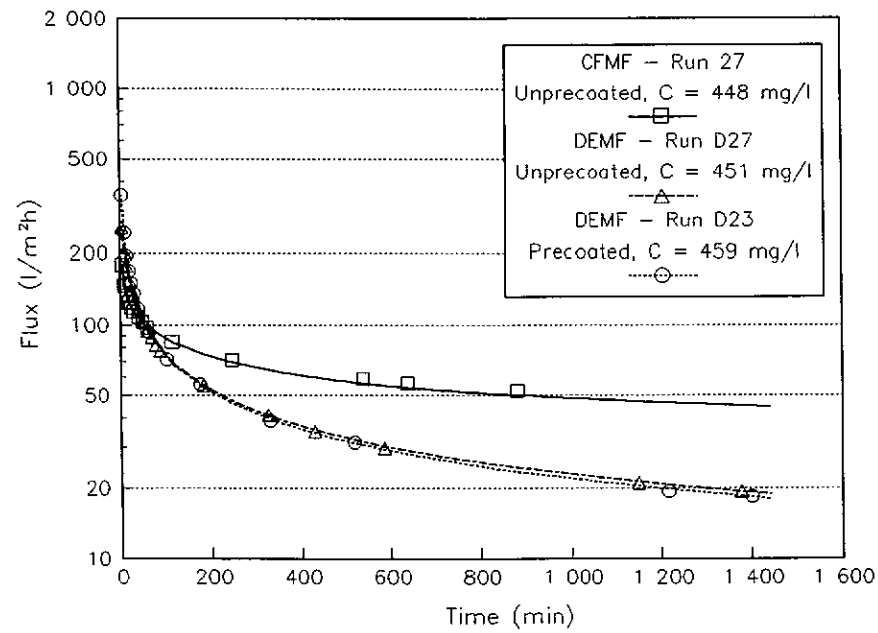

Figure 5.19 : **A graph showing a comparison between the flux profiles of unprecoated CFMF and both precoated and unprecoated DEMF. The experiments were at a feed concentration of approximately 450 mg/l and all experiments operated at a pressure of 200 kPa.**

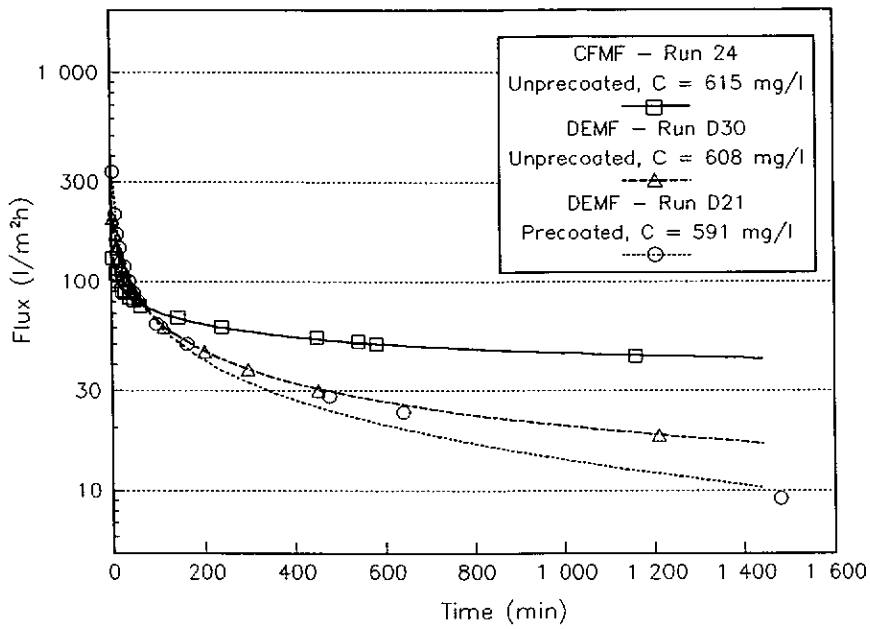

Figure 5.20 : A graph showing a comparison between the flux profiles of unprecoated CFMF and both precoated and unprecoated DEMF. The experiments were at a feed concentration of approximately 600 mg/l and all experiments operated at a pressure of 200 kPa.

This observation of the *cross-over* point is in agreement with the velocity trends that were noted with the CFMF (Sec. 5.1.2). It was found that in the CFMF a lower cross-flow velocity would give a higher flux up to a particular *cross-over* point and that this cross-over point moves closer to the origin as the concentration increases. Since DEMF is an extreme operating condition of the CFMF, namely where the cross-flow velocity approaches zero, the trend that was established with CFMF velocity profiles is confirmed when the CFMF and the DEMF are compared. The physical mechanism of the *cross-over* point has not been established nor explained, but what should be noted is the trend, that as the feed concentration decreases, operation in the DEMF mode is favoured.

The observations made in this study have not been widely reported by other researchers. Similar findings have however been reported by Kim *et al.* (1991). In that study, ultrafiltration and microfiltration of a dilute suspension (2,7 mg/ℓ) of fine silver particles was studied for a range of membranes in a batch cell with and without stirring. The stirring and non-stirring conditions can be equated to the cross-flow and dead-end conditions. The study found that the unstirred conditions gave greater fluxes than the stirred. The *cross-over* point that was discussed earlier, was not observed in this study and this could be due to the fact that the experimental runs were comparatively short, namely 30 to 40 min.

The point is made by the authors that *the most interesting feature of these results is that the unstirred UF had the greater filtration rate than the stirred, which contradicts observations made with other colloidal particles at higher concentration.* The authors attribute the difference in flux to the formation of larger aggregates in the unstirred condition which may be related to the greater level of concentration polarization in the absence of stirring. A similar mechanism might be active in the experiments reported earlier in this chapter.

5.4 DISCUSSION

The experimental work in this study was performed on a low suspended solids feed consisting of equal mass proportions of commercial bentonite and kaolin. The suspension was chosen as having properties similar to some Natal natural waters though the intention was not to model these waters. The experimentation has established the trend that as the feed concentration is decreased, operation in a precoated DEMF mode initially gives a higher permeate flux than operation in the CFMF mode. For the remainder of the chapter DEMF will refer to operation with a precoat and CFMF will refer to operation without a precoat.

It was also established that there exists an experimental point, the *cross-over* point, where the flux curves of the DEMF and CFMF cross for any given concentration. As the concentration decreases, the *cross-over* point moves away from the origin, favouring operation in the DEMF mode.

The *cross-over* point was also observed in the constant velocity experiments of the CFMF. In these experiments, the cross-flow velocity was varied, while other parameters were held constant. It was found that the flux curves crossed at a particular point. Initially the lower velocity gave a higher flux up to the *cross-over* point, whereafter the higher velocity maintained a higher flux. The *cross-over* point was also found to vary with concentration. The fact that the *cross-over* point was observed in both the CFMF constant velocity experiments and in the CFMF/DEMF comparative experiments, is more that just co-incidence. It should be recalled that the DEMF should be viewed as an extreme operating condition of the CFMF as the cross-flow velocity approaches zero. The cross-over points for the CFMF/DEMF and CFMF velocity experiments have been plotted in Fig. 5.21.

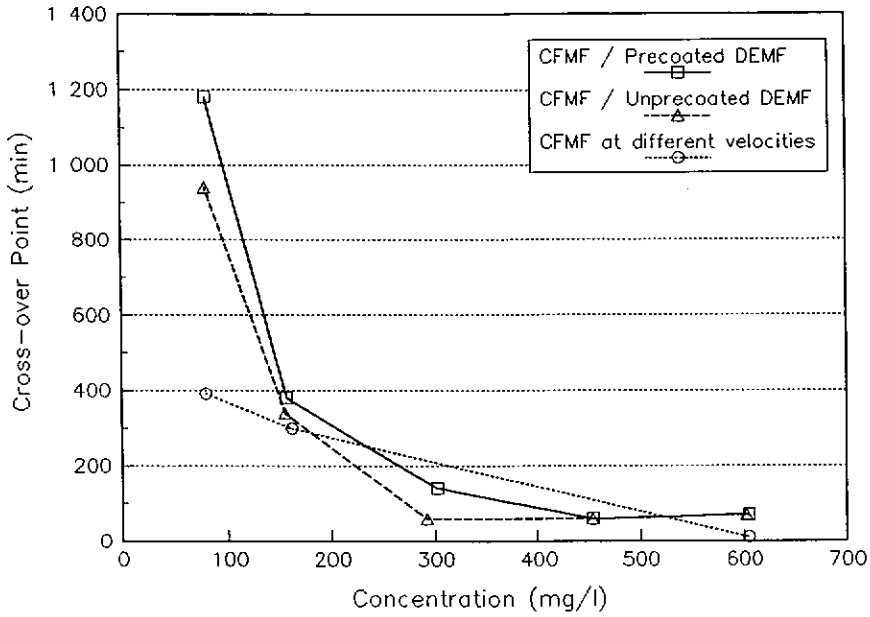

Figure 5.21 : A graph showing the variation of the cross-over point with concentration. Three conditions have been plotted, namely the cross-over between CFMF and precoated DEMF, CFMF and unprecoated DEMF and the CFMF constant velocity experiments.

It should be noted that existence of a *cross-over* point is an experimental observation which holds particular significance to the later discussion. No mechanistic or theoretical explanation could be found for the observation and this should be the subject of future work.

The *cross-over* point should not be confused with the cycle time of the run although the two would be related. If the cycle time were less than the time to the *cross-over* point, clearly the DEMF would produce more permeate than the CFMF over the same period time. However, as the cycle time increases beyond the *cross-over*, so the DEMF permeate production is offset by the higher CFMF fluxes, until a point is reached, beyond which operation in the CFMF mode becomes favoured. The choice of cycle time is an economic choice based on power and required permeate production rates.

The general point that should be noted from Fig. 5.21 is that as the concentration decreases, operation in the dead-end mode is favoured for a longer period of time. Fig. 5.21 does not quantify the advantage that is given in terms of flux and this is the subject of the next section.

5.4.1 Criteria for the Selection of the Operating Mode of the Cross-flow Microfilter

The second aim in this study was to develop criteria for the selection of the operating mode of the CFMF. Three operational configurations of the CFMF were outlined in Sec. 2.3.2 and have been reproduced in Fig. 5.22. Selecting the most economically favourable configuration requires the optimum power and area cost associated with each configuration to be determined. To perform such an evaluation would require the knowledge of the physical relationships governing the system in question. In this study experiments were conducted at constant concentrations, but this has not been extended to a point where the function f_t (Eqn. 2.19) can be evaluated over the full range of operating parameters that would be required for a complete economic choice of the operating mode of the CFMF.

Another complicating factor is the fact that to date, operation in the DEMF mode has not been attempted for full scale rigs. The only full-scale operational experience has been in the CFMF and the TFP modes. Any attempt to model the DEMF using TFP operational parameters would be problematic since the focus of the operation is not on the recovery of a cake but on the production of a high quality permeate. It has already been shown that the filter would have to be precoated and this would have to be considered in both the design and operation of the DEMF.

In was shown in Sec. 2.3.2, that the selection of the most *economically* favourable mode is dependent on several given design parameters. In order to evaluate the mode of operation of the CFMF for a given application an economic analysis as outlined in Sec. 2.3.2 would have to be undertaken.

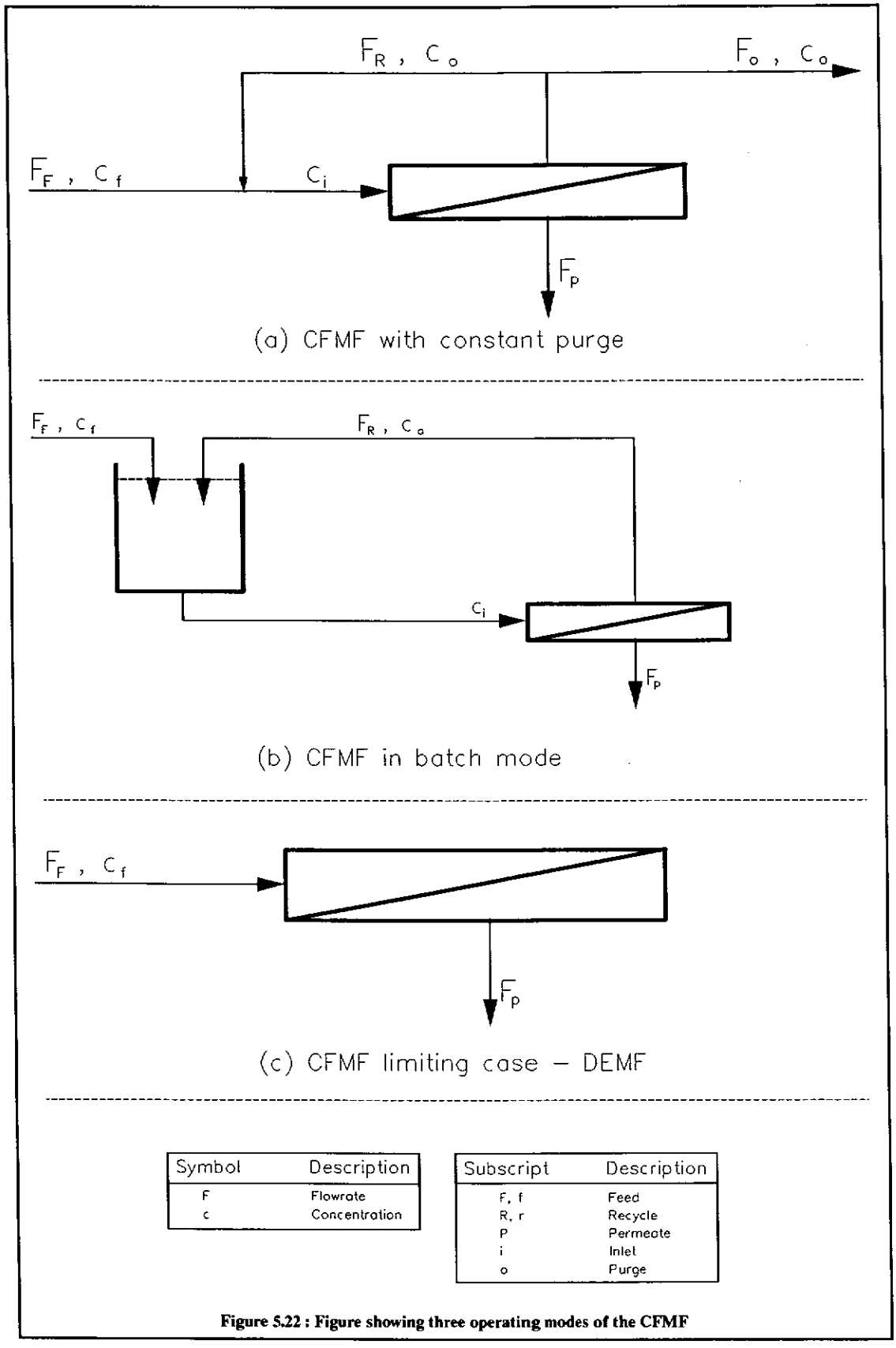

Symbol	Description
F	Flowrate
c	Concentration

Subscript	Description
F, f	Feed
R, r	Recycle
P	Permeate
i	Inlet
o	Purge

Figure 5.22 : Figure showing three operating modes of the CFMF

In each of the three configurations, the feed concentration to the system, c_f and the required production permeate rate, F_p are fixed external design parameters. The variables that are free to be optimised are listed in Table 5.1.

Configuration	Variables to be optimised
CFMF with continuous purge	F_R , F_o , t_c , l
CFMF in batch mode	F_R , V_t , t_c , l
CFMF limiting case - DEMF	t_c , l

Table 5.1 : The variables which are free to be optimised for the three CFMF configurations

The commercial versions of this experimental filter, operate in a number of different curtain configurations, which include different numbers of tube passes, different tube diameters as well as the modes shown in Fig. 5.22. To develop a universal model which caters for all possible modes of operation and configurations has not been achieved. Without a comprehensive model which encompasses the above parameters it is not possible to derive the exact point at which one filtration mode becomes more economically favourable. It is possible however, to illustrate the trends and hence develop criteria by which a selection might be made.

The selection of the mode of operation, namely CFMF or DEMF, would be done on the basis of minimum power consumption and area cost. It is clear that since operation in the DEMF mode does not require the high cross-flow velocities of the CFMF, that its associated pumping power will be less. Furthermore, the experimental trends have illustrated that at low concentrations, the fluxes derived from operation in a precoated DEMF mode are initially higher than operation in the unprecoated CFMF mode, thus giving a lower area cost for a required permeate production rate, F_P . Thus at low concentrations and low cycle times DEMF is more favourable. What needs to be determined then is at what point, as the operational cycle time, t_c and inlet concentration, c_f are increased, does operation in the CFMF mode become more favourable.

A simple criterion will now be developed which will allow certain boundaries to be established from the experimental data. For the purposes of simplicity, the operational configurations (a) and (b) shown in Fig. 5.22 will be grouped together as CFMF as opposed to the limiting case which will be referred to as the DEMF. It is clear that in the case of the CFMF, the inlet feed concentration, c_f is initially the same as the tube inlet concentration, c_i , but as the cycle progresses, c_i will progressively increase and hence the average flux obtained would be less than if no recycle were present and c_i was the same as c_f for the duration of the run. With the operation in the DEMF mode, c_i remains the same as c_f for the duration of the run. The constant concentration experimental runs of the DEMF are thus a fair approximation of the operation in practise. The constant concentration runs of the CFMF on the otherhand would represent a

theoretical best performance curve. Therefore, if one were to compare the performance of the CFMF and the DEMF on the basis of the constant concentration experimental runs and obtain the point where CFMF becomes more favourable, then this would represent a minimum point both in terms of cycle time and concentration. In other words, in practise one could run at even longer cycle times in the DEMF mode and even higher concentrations before it became less favourable than the CFMF.

The other assumption that has been made in this simplified model is one of constant pressure and velocity. In the experimental system used in this study, the experimental tubes were short (< 1 m) and therefore the pressure and velocity remained virtually constant over the length of the tube. In real systems where the tube lengths are approximately 12 m in length, together with multiple tube passes, this assumption is not valid. Under those circumstances a model would have to be developed using the short tube experimental results and integrated into a broader system to account for tube profiles [Rencken, 1992; Pillay, 1992b]. This would however apply to both systems, and for the purposes of this model, this effect has been ignored and it has been assumed that the short tube results would apply on the larger systems.

To obtain the exact point where one system becomes more favourable than the other, one would not only require the model outlined earlier, but also a quantification of the area and the power in terms of monetary units. In order to quantify the flux advantage given by the DEMF mode using this simple model, cumulative volumetric-time plots of both the CFMF and the DEMF can be drawn. The cumulative volume is obtained as follows :

$$\int_{t_0}^{t} J\,dt \tag{5.3}$$

The plots of cumulative volume for both the CFMF and the DEMF are shown in Figs. 5.23, 5.24, 5.25, 5.26 and 5.27. The curves were plotted by integrating the flux function using the regressed parameters obtained as outlined in Sec. 5.1. In the case of the concentration of approximately 75 mg/ℓ, the curve has been extrapolated beyond what was experimentally determined in that particular run. The cross-over points are also realistic in the sense that they have been tested to see whether the tube would choke at that point and it was found that the cake thickness was realistic and fractional in comparison to the tube diameter.

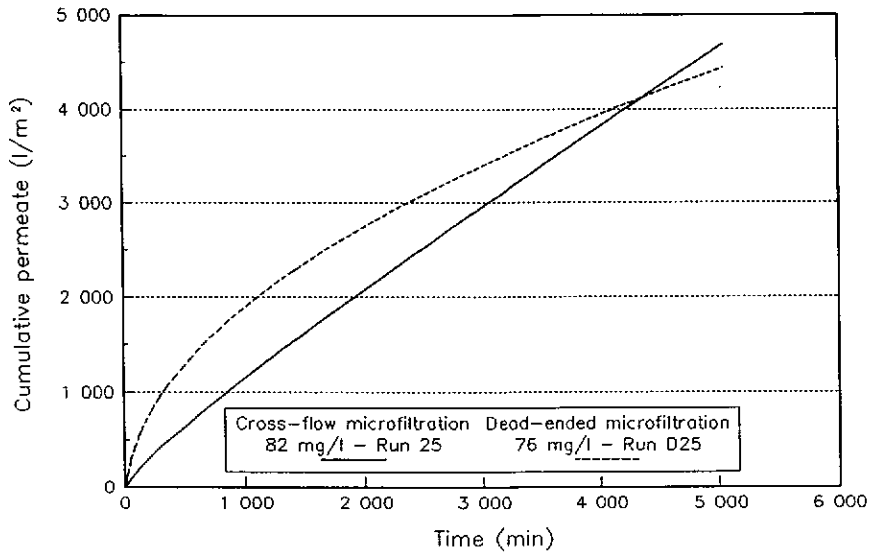

Figure 5.23 : Graph showing the cumulative volume of permeate produced vs time for the DEMF and the CFMF. The two runs were performed at similar concentrations (approximately 75 mg/ℓ). Both runs were performed at 200 kPa. Note the x-axis scale on this plot is greater than the next four figures.

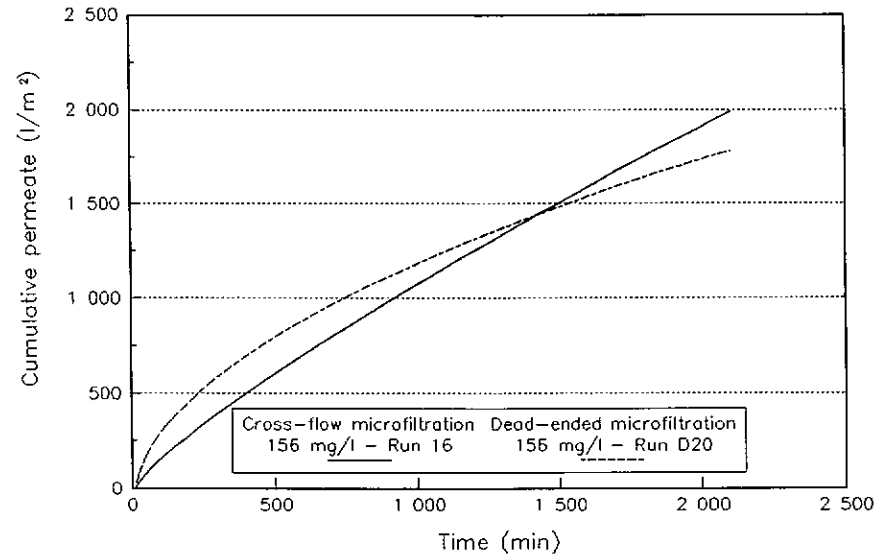

Figure 5.24 : Graph showing the cumulative volume of permeate produced vs time for the DEMF and the CFMF. The two runs were performed at similar concentrations (approximately 150 mg/ℓ). Both runs were performed at 200 kPa

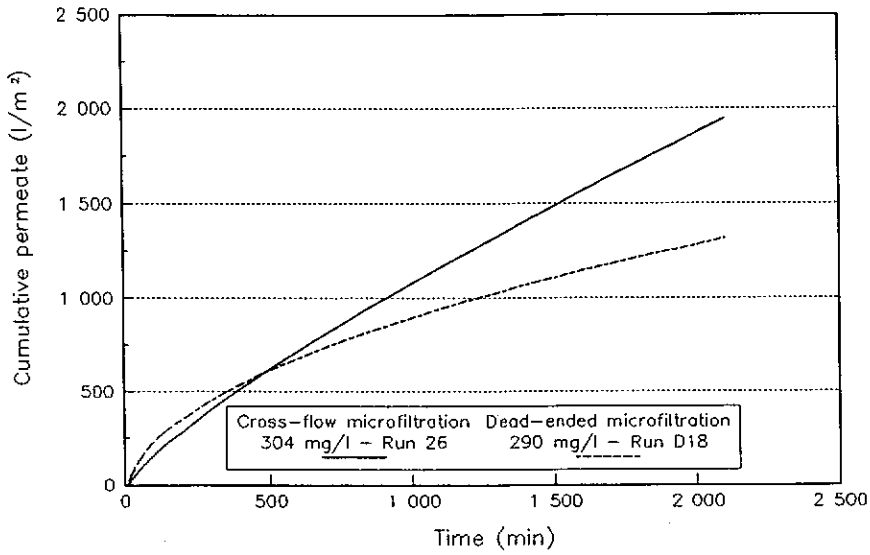

Figure 5.25 : Graph showing the cumulative volume of permeate produced vs time for the DEMF and the CFMF. The two runs were performed at similar concentrations (approximately 300 mg/ℓ). Both runs were performed at 200 kPa

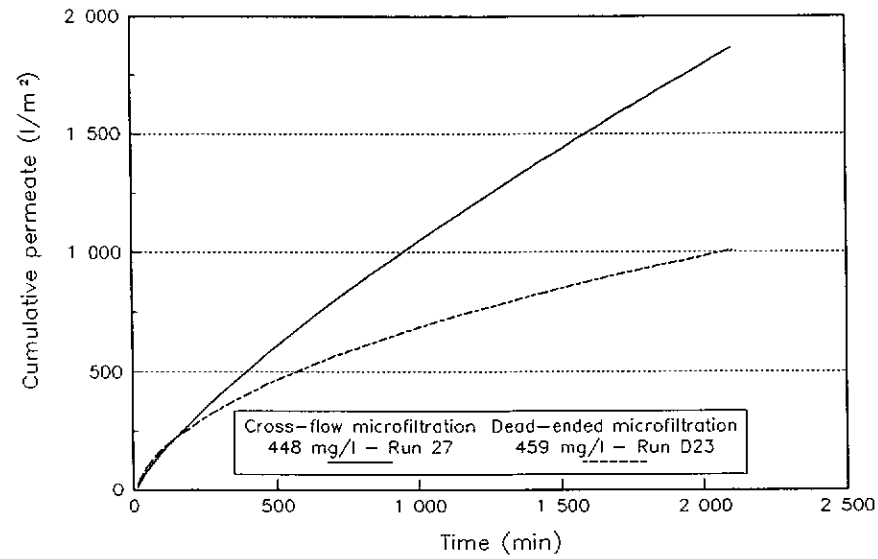

Figure 5.26 : Graph showing the cumulative volume of permeate produced vs time for the DEMF and the CFMF. The two runs were performed at similar concentrations (approximately 450 mg/ℓ). Both runs were performed at 200 kPa

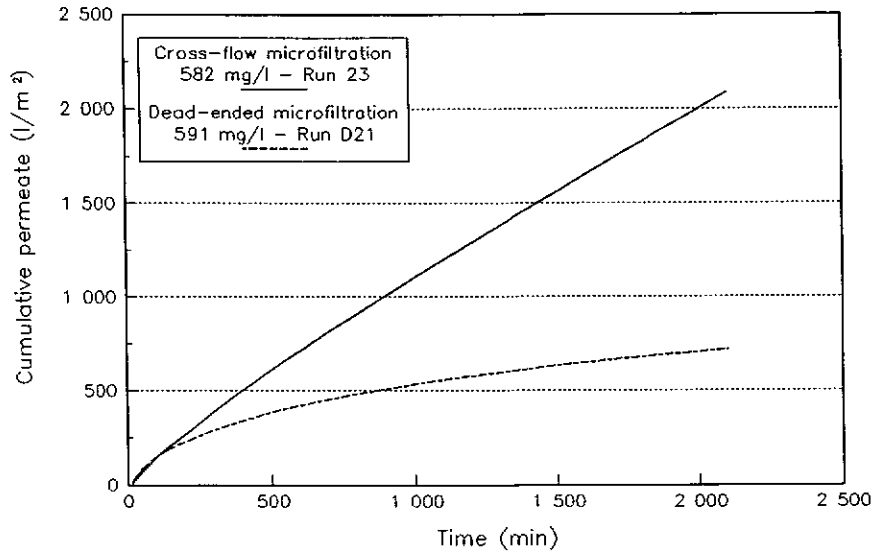

Figure 5.27 : Graph showing the cumulative volume of permeate produced vs time for the DEMF and the CFMF. The two runs were performed at similar concentrations (approximately 600 mg/ℓ). Both runs were performed at 200 kPa

The advantage given by operation in the DEMF mode as opposed to the CFMF mode can also be quantified by subtracting the cumulative volume plots in Figs. 5.23, 5.24, 5.25, 5.26 and 5.27. The difference can be expressed using a parameter $\Delta_{FLUX,t}$. Using this parameter, it is possible to obtain a theoretical maximum cycle time.

$$\Delta_{FLUX,t} = \int_{t_0}^{t} \mathbf{J}_{DEMF}\,dt - \int_{t_0}^{t} \mathbf{J}_{CFMF}\,dt \tag{5.4}$$

The function $\Delta_{FLUX,t}$ represents the difference in the quantity of permeate produced by the DEMF and the CFMF. The function is plotted against time in Fig. 5.28 for selected combinations of experiments.

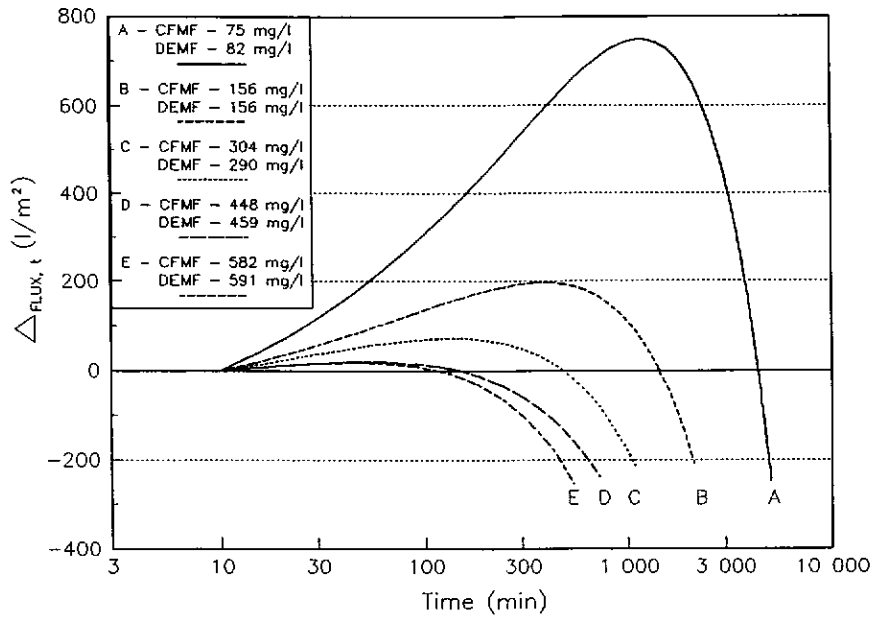

Figure 5.28 : **The function $\Delta_{FLUX,t}$ is plotted against time. All the experiments that were used to construct this curve were done at 200 kPa and all the CFMF runs were at 1,8 m/s. Note that the x-axis is plotted on a logarithmic scale. The experimental runs used to plot this figure are the same runs that were used in Figs. 5.23, 5.24, 5.25, 5.26 and 5.27.**

From Fig. 5.28 it can be seen that the DEMF produces more permeate than the CFMF up to the point where the curve intersects with the zero axis. At this point, the CFMF begins to produce more permeate than the DEMF. In essence, if cycle times less than the intersection time are chosen, the DEMF will be more favourable than the CFMF both in terms of power consumption and area cost. As was outlined earlier, the curves represent theoretical minimum times since the DEMF is compared against a hypothetical best case where the CFMF inlet concentration remains constant. In practise the DEMF will be more favourable for even longer periods since in reality the CFMF flux curves are further depressed by an increasing inlet concentration.

The parameter $\Delta_{FLUX,t}$ is expressed in units of (ℓ/m^2). It would be more useful to express the benefit obtained by operating in the DEMF mode by expressing $\Delta_{FLUX,t}$ as a percentage relative CFMF. In other words :

$$\Delta_{\%} = \frac{\Delta_{FLUX,t}}{\int_{t_0}^{t} J_{CFMF}\,dt} \qquad (5.5)$$

Fig. 5.29 shows the parameter $\Delta_{\%}$ plotted against time for the combinations of experiments used in Figs. 5.23, 5.24, 5.25, 5.26 and 5.27. From Fig. 5.29 it is clear that the relative percentage improvement that operation in the DEMF mode gives, is substantial. At the

low concentration range (approximately 75 mg/ℓ) operation in the DEMF mode over a period of 24 h gives a 47 % improvement in cumulative permeate volume (ℓ/m²) relative to operation in the CFMF mode. At the concentration of 150 mg/ℓ the $\Delta_{\%}$ drops to 33 % over an 8 h period.

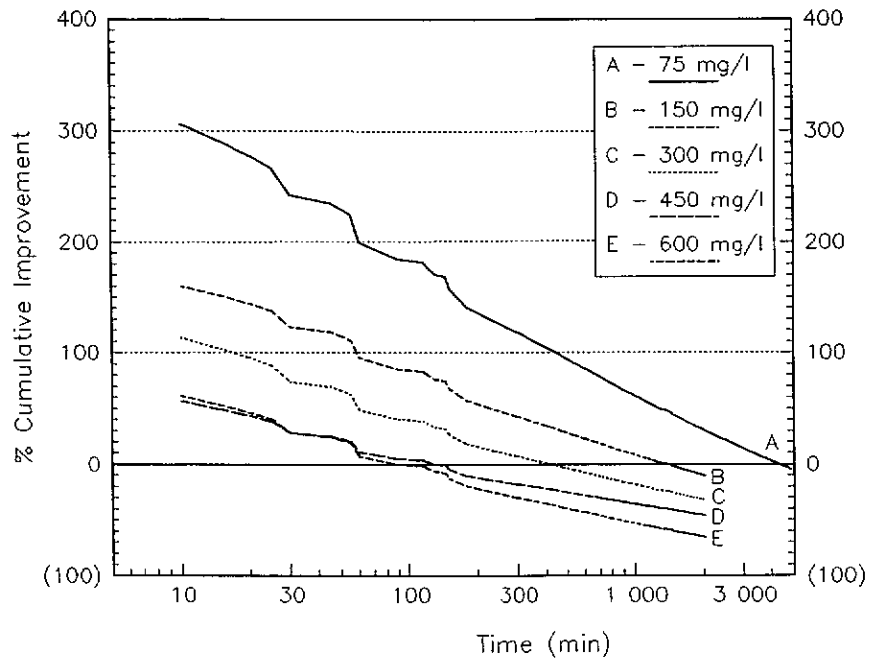

Figure 5.29 : The function $\Delta_{\%}$ is plotted against time. All the experiments that were used to construct this curve were done at 200 kPa and all the CFMF runs were at 1,8 m/s. Note that the x-axis is plotted on a logarithmic scale. The experimental runs used to plot this figure are the same runs that were used in Figs. 5.23, 5.24, 5.25, 5.26 and 5.27. The concentrations indicated are approximate concentrations, the actual concentrations of the individual runs have been indicated in the previous figures.

The intersection points on the zero axis are plotted in Fig. 5.30. It is clear from the curve that as the concentration is increased, operation in the CFMF mode becomes more favourable for longer cycle times.

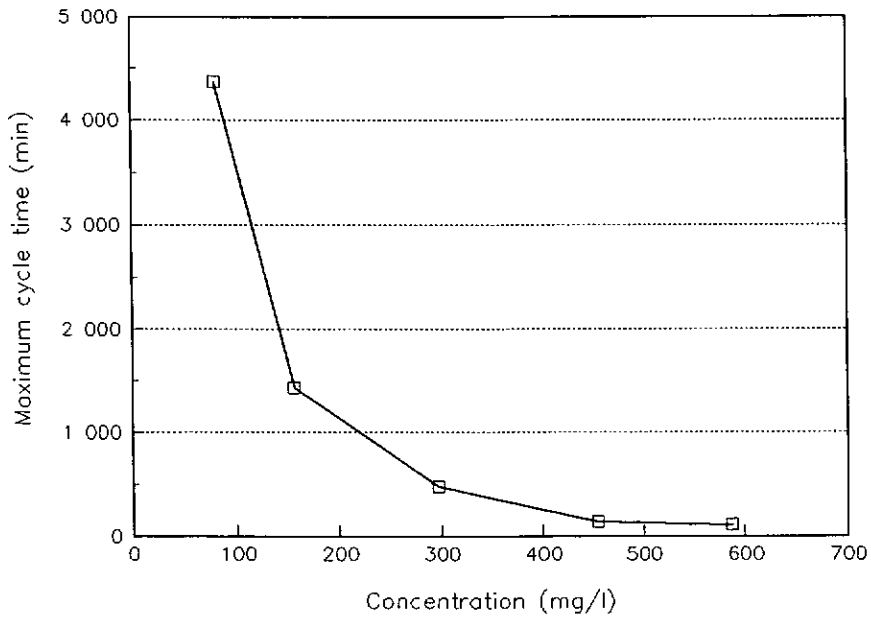

Figure 5.30 : The curve represents theoretical maximum cycle times before operation in the CFMF mode becomes more favourable. The concentrations used in this figure are approximate concentrations. The actual concentrations used for the individual experiments have been listed in previous figures.

The question that needs to be addressed is how the cycle time, t_c is chosen or determined. The choice of cycle time would be made on the basis of minimising both the area and the power cost. The optimisation would be a function of the operating mode and its determination would be dependent on the derivation of the function f_t. The choice of cycle time would also have to incorporate the wear on the fabric tubes. In practise the EXXFLOW system runs with cycle times which can vary from 4 h to 24 h. Thus, on the basis of Fig. 5.30, it would appear as if the DEMF might be more favourable than the CFMF for feed concentrations up to about 300 mg/ℓ based on current operational practises. For higher concentration ranges, the operation in the DEMF could possibly be justified for shorter production cycles though in all cases this would have to be weighed up against the relative percentage improvement that was being gained. The *cross-over* points together with $\Delta_{\%}$ at various cycle times is tabulated in Table 5.2. From Table 5.2 it is clear that operation in DEMF mode might be justified at a concentration of 300 mg/ℓ for cycle times less than 4 h while for lower concentrations operation could be justified for even longer periods. It is should also be noted that operation in the DEMF mode might even be justified for longer periods based on the relative power saving that operation in the DEMF mode gives. This has however not been evaluated.

Conc (mg/ℓ)	Cross-over Point (min)	$\Delta_{\%}$ 4h	8h	12h	16h	20h	24h
75	4 370	**141**	**103**	**81**	**67**	**56**	**47**
150	1 430	**57**	**33**	**20**	**11**	**5**	**0**
300	480	**18**	**0**	-10	-16	-21	-25
450	145	-10	-23	-29	-34	-37	-40
600	115	-20	-36	-45	-51	-55	-59

Table 5.2: Table showing the cross-over point tabulated against the approximate concentration. The function $\Delta_{\%}$ is also tabulated against concentration for different cycle times. A negative value indicates operation more favourable to CFMF. The actual concentrations and run numbers have been listed in Figs. 5.23, 5.24, 5.25, 5.26 and 5.27.

In summary, to determine the point at which one operational mode becomes more favourable than the next would require extensive modelling of the suspension in question. The model would have to incorporate profiles of the various variables down the fabric tubes and the various operational configurations would have to be taken into account. However, using the simplified model outlined above, certain definite trends have been established and it has been shown that operation in the precoated DEMF mode is more favourable from a power and an area cost at low concentrations. The choice of mode would be dependent on the optimum choice of cycle time, though using current practises, it would appear as if the precoated DEMF would be more favourable than the unprecoated CFMF to concentrations of about 300 mg/ℓ.

CHAPTER

SIX

Conclusions and Recommendations

The operation of fabric tube filters in a cross-flow mode (CFMF) has traditionally been used for the production of a high quality permeate from a turbid feed while operation in a dead-end mode (DEMF) has been used for the recovery of a spadeable cake. This study set out to investigate whether operation in a dead-end mode might be utilised for the production of a high quality permeate, thus making use of the lower power requirements associated with this mode of operation.

The experimental study has obtained flux and permeate quality data for the CFMF and the DEMF. A low suspended solids feed made up of equal mass proportions of bentonite and kaolin was used and experiments were conducted over a range of concentrations (<1 000 mg/ℓ).

To evaluate the economic favourability of one mode over the next would require the development of a comprehensive model which would allow the flux to be predicted at any point down the tube. The model would have to account for variations of pressure, concentration and velocity. Such a model would allow different CFMF configurations, both theoretical and commercial to be evaluated and the power and area costs determined. This study concerned itself with constant concentration experimental runs and the data was not extended into the formulation of a comprehensive model as outlined above.

Without the development of such a model, the full economic implications associated with each mode of operation could not be determined. It was possible however, with the data that were obtained, to illustrate particular peculiarities of the system and hence to show trends.

A problem that was encountered from the start was the permeate quality of the DEMF. It was found that unless the fabric tubes were precoated with limestone in a cross-flow mode before switching to the dead-ended operation, the permeate quality was both poor and unpredictable. The system was also found to be relatively insensitive to pressure with the pressure variation curves lying within the ± 6% error band. All experiments were thus conducted at a pressure of 200 kPa while the concentration was varied from approximately 75 mg/ℓ to approximately 600 mg/ℓ. The velocity, in the case of the CFMF, was varied between 1,3 and 2,3 m/s. Since

permeate turbidity of the CFMF fell below the accepted limit of 0,5 NTU, there was little need to precoat the CFMF tubes. All CFMF experiments were thus carried out in an unprecoated mode.

The use of precoats of fabric tubes is the subject of other current research and hence no attempt was made to optimise the use of precoats on the DEMF. Precoating the DEMF was also found to enhance the permeate flux and it might be possible that under certain precoating conditions the CFMF might also show enhanced fluxes.

The experimental results showed that initially operation in the DEMF mode gave higher fluxes up to a point which has been termed the *cross-over* point, after which the CFMF produces the higher flux. The *cross-over* point was found to be a strong function of concentration. As the feed concentration was decreased so the time for which the DEMF maintained the higher flux increased. This has a strong implication in the choice of the permeate production cycle. As the cycle time is increased a point is reached where the gain derived from operation in the dead-end mode is offset by the higher fluxes maintained by the CFMF after the *cross-over* point.

A simple model was developed which compares the DEMF against a hypothetical best performance CFMF. This was necessitated due to the restriction that constant concentration experimental runs posed. Using this model the cycle times derived are minimum cycle times, since in practise the inlet concentration in CFMF is not constant but increases. The CFMF flux profiles are thus depressed to a greater extent, making operation in the DEMF mode even more favourable. It was found using this model that operation in the DEMF would be more favourable than the CFMF, both in terms of area and power, for low concentrations. The restriction lies with the choice of cycle time. At concentrations of about 75 mg/ℓ it was shown that the DEMF would maintain the area advantage for a period of about 3 d before operation in the CFMF became more desirable. This maximum cycle time decreases to about 2 h at a concentration of about 600 mg/ℓ. Using the simplified model two parameters were introduced to evaluate the flux advantage given by operation in the DEMF, namely $\Delta_{FLUX,t}$ and $\Delta_{\%}$. The former quantified the advantage in terms of volume of permeate produced per square metre while the latter quantified the relative percentage improvement. Using the above parameters it is clear that the advantage given by DEMF was significant. Extended cycle times would have to evaluated by comparing the decrease in permeate volume against the power saving derived by operation in the DEMF mode.

The cycle time is clearly a parameter that would have to be optimised. What the advantage translates to in monetary terms has not been evaluated since it would require extensive assumptions and move into the design and optimisation phase of the commercial operation.

Recommendations

It is recommended that :

1. Further experiments should be performed on the system that was used in this study in order to collect sufficient data, which would allow for the determination of a comprehensive model, to predict the parameter profiles down the tubes of the curtain of a commercial filter.

   Experiments over a range of pressures would be required for both the DEMF and CFMF. The primary restriction of the data collected in this study was that the pressure was held constant over the majority of the experiments. Although the system was found to be largely insensitive to pressure it would have to be considered in the development of a comprehensive model.

   This would allow for the evaluation of each mode of operation as outlined in Sec. 2.3. and thus a more precise evaluation of the power and area costs would be possible.

2. Experimentation needs to be performed using a range of precoating materials and conditions for the CFMF and the DEMF. From the experimentation, the optimum precoating conditions for the CFMF and the DEMF needs to be identified and the benefits obtained from that operation should be evaluated. The use of precoats should then be incorporated in the model outlined in the first recommendation.

3. It is further recommended that theoretical work be undertaken to explain the mechanism behind the *cross-over* point. Once this is understood it might give further insight into how the filters might be manipulated in order to maximise the throughput and minimise the power consumption.

References

AHSAN, T., ALAERTS, G.J. and BUITEMAN, J.P. (1991), **Direct Horizontal-Flow Roughing Filtration : An Improved Pretreatment Process for Highly Turbid Water**, The Filtration Society Filtech '91 Conference, Karlsruhe, 15-17 October

ALTENA, F.W. and BELFORT, G. (1984), **Lateral Migration of Spherical Particles in Porous Flow Channels : Application to Membrane Filtration**, *Chemical Engineering Science*, **39**(2), pp. 343-355

ASTM 1888-78 (1990), **Standard Test Methods for Particulate and Dissolved Matter, Solids, or Residue In Water**, 1990 Annual Book of ASTM Standards, Volume 11.01, ASTM, Philadelphia, pp. 175-182

ASTM D 1889 - 88A (1990), **Standard Test Method for Turbidity of Water**, 1990 Annual Book of ASTM Standards, Volume 11.01, ASTM, Philadelphia, pp. 233-238

ASTM D 4189 - 82 (1990), **Standard Test Method for Silt Density Index (SDI) Of Water, 1990 Annual Book Of ASTM Standards**, Volume 11.01, ASTM, Philadelphia, pp. 223-224

BAKER R.J., FANE A.G., FELL C.J.D. and YOO B.H. (1985), **Factors Affecting Flux in Crossflow Filtration**, *Desalination*, **53**, pp. 81-93

BECKETT, R., NICHOLSON, G., HART, B.T., HANSEN, M. and GIDDINGS, J.C. (1988), **Separation and Size Characterization of Colloidal Particles in River Water by Sedimentation Field-Flow Fractionation**, *Water Research*, **22**(12), pp. 1535-1545

BELFORT, G. and NEGATA, N. (1985), **Fluid Mechanics and Cross-Flow Filtration : Some Thoughts**, *Desalination*, **53**, pp. 57-79

BHAVE, R.R. (1991), **Inorganic Membranes : Synthesis, Characteristics and Applications**, Van Nostrand Reinhold, New York

BINDOfF, A.M., TREFFRY-GOATLEY, K., FORTMANN, N.E., HUNT, J.W. and BUCKLEY, C.A. (1988), **The Application of Cross-flow Microfiltration Technology to the Concentration of Sewage Works Sludge Streams**, *Journal of the Institute of Water and Environmental Management*, 2(5), pp. 513-522

BLATT, W.F., DRAVID, A., MICHAELS, A.S. and NELSEN, L. (1970), **Solute Polarization and Cake Formation in Membrane Ultrafiltration : Causes, Consequences and Control Techniques**, Membrane Science and Technology, Plenum Press, New York, pp. 47-97

CLARK, J.G. (1990), **Select the Right Fabric for Liquid-Solid Separation**, *Chemical Engineering Progress*, November, pp. 45-50

COULSON, J.M., RICHARDSON, J.F. (1978), **Chemical Engineering**, 3ed, 2, Chap 9, pp. 323

CROWLEY, F.W., JACKSON, C.R. and HEARD, T.R. (1985), **Application of Science to Water Supply Projects in Developing Countries**, *Journal of the Institution of Water Engineers and Scientists*, 39(1), pp. 46-56

DAVIS, R.H. and LEIGHTON, D.T. (1987), **Shear-Induced Transport of a Particle Layer along a Porous Wall**, *Chem. Eng. Science*, 42(2), pp. 275-281

DAVIS, R.J. and BIRDSELL, S.A. (1987), **Hydrodynamic Model and Experiments for Crossflow Microfiltration**, *Chemical Engineering Communications*, 49, pp. 217-234

EPPLER, B., NEIS, U. and HAHN, H.H. (1975), **Engineering Aspects of the Coagulation of Colloidal Particles in Natural Waters**, *Progress in Water Technology*, 7(2), pp. 207-216

ERIKSSON, A. (1985), **Some Examples of the Use of Crossflow Filtration in the Downstream Processing in a Biochemical Industry**, *Desalination*, 53, pp. 259-263

FANE, A.G., FELL, C.J.D. and NOR, M.T. (1982), **Ultrafiltration in the Presence of Suspended Matter**, *I. Chem. E. Symposium Series*, 73, pp. C1-C12

FISCHER, E. and RAASCH, J. (1986), **Model Tests of the Particle Deposition at the Filter Medium in Cross-Flow Filtration**, Proceedings of the 4th World Filtration Congress, Ostend, 22-25 April 1986, Part III, pp. 11.11-11.17

FLEMMER, R.L.C., BUCKLEY, C.A. and GROVES, G.R. (1982), **An Analysis of the Performance of a Spiral-Wound Ultrafiltration Membrane with a Turbulence Promoting Net**, *Desalination*, 41, pp. 25-32

FORDHAM E.J. and LADVA H.K.J. (1989), **Cross-flow Filtration of Bentonite Suspensions**, *PhysicoChemical Hydrodynamics*, 11(4), pp. 411-439

GASSEL, T.J. and RIPPERGER, S. (1985), **Crossflow Microfiltration in the Process Industry**, *Desalination*, **53**, pp. 373-387

GREEN, G. and BELFORT, G. (1980), **Fouling of Ultrafiltration Membranes : Lateral Migration and the Particle Trajectory Model**, *Desalination*, **35**, pp. 129-147

HANEMAAIJER, J.H. (1985), **Microfiltration in Whey Processing**, *Desalination*, **53**, pp. 143-155

HENRY, J.D. (1972), Cross Flow Filtration, Recent Developments in Separation Science, 2, pp. 205-225

HOLDICH, R.G. and ZHANG, G.M. (1991), **Seawater Crossflow Filtration**, The Filtration Society Filtech '91 Conference, Karlsruhe, 15-17 October

HOOGLAND, M.R., FANE, A.G. and FELL, C.J.D. (1988), **Crossflow Filtration of Mineral Slurries with Ceramic Membranes**, *Paper G25*, International Membrane Technology Conference, Sydney, Australia

HUNT, J.W. (1987), **Mathematical Modelling of Cross-Flow Microfiltration**, MScEng Thesis, University of Natal, Durban

KEMP, H.P. (1963), **Geological Effects on Surface Waters in Natal**, *Nature*, **4911**, pp. 1085

KIM K., CHEN, V. and FANE, A.G. (1991), **Ultrafiltration of Colloidal Silver Particles: Flux, Rejection and Fouling**, In Print

KIRK, J.T. (1985), **Effects of Suspensoids (Turbidity) on Penetration of Solar Radiation in Aquatic Ecosystems**, *Hydrobiologia*, **125**, pp. 195-208

KLEIN, W. and HOELZ, W. (1982), **Crossflow Microfiltration in Chemical Processes**, *The Chemical Engineer*, pp. 369-373, October

KUWABARA, J.S. and HARVEY, R.W. (1990), **Application of a Hollow-Fiber, Tangential-Flow Device for Sampling Suspended Bacteria from Natural Waters**, *J. Environ. Qual.*, **19**, pp. 625-629

LE, M.S. (1987), **Recovery of Beer from Tank Bottoms with Membranes**, *J. Chem. Tech. Biotechnol.*, 37, pp. 59-66

LEGER, J.P. (1985), **Dynamic Membranes from Surface Water Imputities - A Study of Membrane Fouling By Rand Water Board Water**, MScEng Thesis, University of Natal, Durban, pp. 189-191

LEONARD and VASSILIEFF (1984), **The Deposition of Rejected Matter in Membrane Separation Processes**, *Chemical Engineering Communications*, 30, pp. 209-217

MACKAY, D. and SALUSBURY, T. (1988), **Choosing between Centrifugation and Crossflow Microfiltration**, *The Chemical Engineer*, pp. 45-50, April

MILISIC, V. and BERSILLON, J.L. (1986), **Anti-Fouling Techniques in Cross Flow Microfiltration**, Proceedings of the 4th World Filtration Congress, Ostend - Belgium, 22-25 April 1986, pp. 11.19-11.24

MURKES, J. (1986), **Cross-flow Filtration of Emulsions Combined with Coalescing. A New Filter-Coalescer Concept.**, The Proceedings of the 4th World Filtration Congress, Ostend - Belgium, 22-25 April 1986, pp. 11.35-11.41

MURKES, J. and CARLSSON, C.G. (1988), **Crossflow Filtration**, John Wiley and Sons, Great Britain

PERONA, J.J., ROM, A.M., HUTCHINS, J.D. and JOHNSON, J.S. (1974), **A Pilot Plant for Sewage Treatment by Cross-Flow Filtration**, Internal Document - Oak Ridge National Laboratories, pp. 1-20, Tennessee

PILLAY, V.L. (1992a), **Modelling of Turbulent Cross-Flow Microfiltration of Particulate Suspensions**, Phd Thesis, University of Natal, Durban

PILLAY, V.L. (1992b), **The Utilisation of Cross-flow Microfiltration to Improve Anaerobic Digestor Performance**, IMSTEC '92 Conference, Sydney, 10-12 November 1992

RAUTENBACH, R. and SCHOCK, G. (1988), **Ultrafiltration of Macromolecular Solutions and Cross-Flow Microfiltration of Colloidal Suspensions. A Contribution to Permeate Flux Calculations**, *Journal of Membrane Science*, **30**, pp. 231-242

RENCKEN, G.E. (1992), **Performance Studies of the Tubular Filter Press**, Phd Thesis, University of Natal, Durban

SABS 241-1984 (1984), **South African Standard - Specification for Water for Domestic Supplies**, The Council of the South African Bureau of Standards

SAW, C.B., ANDERSON, G.K., JAMES A. and LE, M.S. (1985), **A Membrane Technique for Biomass Retention in Anaerobic Waste Treatment Processes**, Proceedings of the 40th Industrial Waste Conference, Lafayette Indiana, May 1985

SCHNEIDER, K., KLEIN, W. (1982), **The Concentration of Suspensions by Means of Crossflow-Microfiltraion**, *Desalination*, **41**, pp. 263-275

SHACKLETON, R. (1987), **The Application of Ceramic Membranes to the Biological Industries**, *J. Chem. Tech. Biotechnol.*, **37**, pp. 67-69

SHEPPARD, J.D. and THOMAS, D.G. (1974), **Engineering Development of Hyperfiltration with Dynamic Membranes. Part II : Brackish Water Pretreatment Pilot Plant**, *Desalination*, **15**, pp. 307-323

SQUIRES, R.C. (1992), **Removal of Heavy Metals from Industrial Effluent by Crossflow Microfiltration**, *Water Science and Technology*, **25**(10), pp. 55-67

TANNY, G.B. and HAUK, D. (1980), **Filtration of Particulates and Emulsions with a Pleated, Thin Channel, Cross-Flow Module,** *Separation Science and Technology*, 15(3), pp. 317-337

TANNY, G.B., HAUK, D. and MERIN, U. (1982), **Biotechnical Applications of a Pleated Crossflow Microfiltration Module,** *Desalination*, 41, pp. 299-312

TARLETON E.S. and WAKEMAN R.J. (1991), **Factors Affecting the Fouling of Membranes in Crossflow Microfiltration,** Filtech Conference, Karlsruhe

TESELKIN, V.V., KOCHKODAN, V.M., REPETYUK, L.Y. and GORONOVSKII, I.T. (1988), **Determination of the Dispersion of Solids in Natural Water with a Laser Phototyndallimeter,** *Soviet Journal of Water Chemistry and Technology*, 10(1), pp. 105-108

TILLER, F.M. and YEH, C.S. (1985), **The Role of Porosity in Filtration Part X : Deposition of Compressible Cakes on External Radial Surfaces,** *Journal of the American Institution of Chemical Engineers*, 31(8), pp. 1241-1248

TREFFRY-GOATLEY, K., BUCHAN, M.I., RENCKEN, G.E., VOORTMAN W.J. and BUCKLEY C.A. (1987), **The Dewatering of Sludges Using a Tubular Filter Press,** *Desalination*, 67, pp. 467-479

VAN DER HORST, H.C. and HANEMAAIJER, J.H. (1990), **Cross-Flow Microfiltration in the Food Industry. State of the Art,** *Desalination*, 77, pp. 235-258

VILJOEN, F.C. (1992), **Risks, Criteria and Water Quality,** *Water Sewage and Effluent*, 12(2), pp. 11-20

VLASOVA, O.L., BEZRUKOVA, A.G., MCHEDLISHVILI, B.V., KOLIKOV, V.M., NERODA, L.M. and NIKIFOROVA, T.V. (1989), **Use of Superturbidimetry to Analyze Mineral Suspended Solids in Natural Water Bodies,** *Soviet Journal of Water Chemistry and Technology*, 11(3), pp. 57-60

WALL, G.J. and WILDING, L.P. (1976), **Mineralogy and Related Parameters of Fluvial Suspended Sediments in Northwestern Ohio,** *Journal of Environmental Quality*, 5(2), pp. 168-173

WATER RESEARCH COMMISSION (1991), **Project 274 - The Technical Support for the Application of Dynamic Membrane Plants for the Treatment of Industrial Effluents,** Pretoria

WORLD HEALTH ORGANIZATION (1984), *Guidelines for Drinking-Water Quailty*, V1 & 2, World Health Organization, Belgium

ZAIDI, A., BUISSON, H., SOURIRAJAN, S. and WOOD, H. (1992), **Ultra- and Nano- Filtration in Advanced Effluent Treatment Schemes for Pollution Control in the Pulp and Paper Industry,** *Water Science and Technology*, 25(10), pp. 263-276

ZYDNEY, A.L. and COLTON, C.K. (1986), **A Concentration Polarisation Model for the Filtrate Flux in Cross-Flow Microfiltration of Particulate Suspensions,** *Chemical Engineering Communications*, **47**, pp. 1-21

Appendix A

Operating Mode Derivations

A-1. Cross-flow with Continuous Purge (Eqn. 2.21)

Fig. 2.4 has been reproduced for convenience.

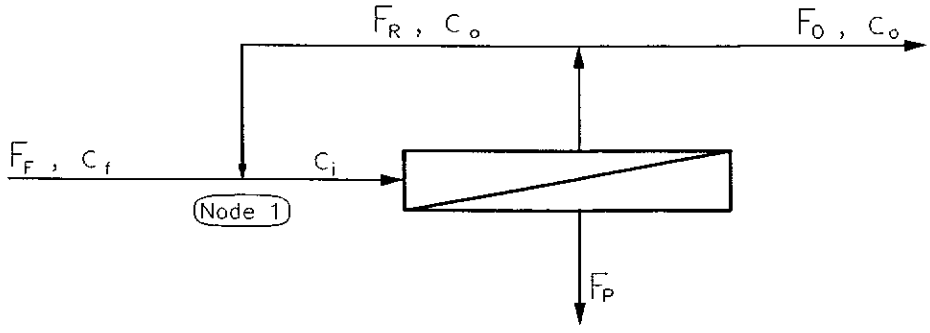

Symbol	Description
F	Flow rate
c	Concentration

Subscript	Description
F, f	Feed
O, o	Purge
P	Permeate
R	Recycle
i	Inlet

Figure 2.4 : A schematic diagram of a CFMF showing a recycle and a continuous purge

An overall material balance yields :

$$F_F = F_O + F_P \tag{A.1}$$

If it is assumed that the suspended matter in the permeate and the mass of solids deposited in the tube is negligible, a balance of the solid suspended matter yields :

$$F_F c_f = F_O c_o \tag{A.2}$$

Substituting Eqn. (A.1) into Eqn. (A.2) and writing in terms of c_o :

$$c_o = \frac{(F_P + F_o)}{F_o} c_f \tag{A.3}$$

If a material balance is now performed around node 1 :

$$(F_F + F_R)c_i = F_F c_f + F_R c_o \tag{A.4}$$

Substituting Eqn. (A.1) into Eqn. (A.4) yields :

$$(F_P + F_O + F_R)c_i = (F_P + F_O)c_f + F_R c_o \tag{A.5}$$

Writing the equation in terms of c_i and substituting in Eqn. (A.3) for c_o yields :

$$c_i = \left[\frac{F_P + F_O}{F_P + F_O + F_R}\right] c_f + \left[\frac{F_P + F_O}{F_P + F_O + F_R}\right] \frac{F_R}{F_O} c_f \tag{A.6}$$

Re-arranging the Eqn. (A.6) yields the final result, Eqn. 2.21 :

$$c_i = c_f \times \left[\frac{F_P + F_O}{F_P + F_R + F_O}\right] \cdot \left[1 + \frac{F_R}{F_O}\right] \tag{2.21}$$

A-2. Cross-flow operated in a Batch Mode (Eqn. 2.24)

Fig. 2.5 has been reproduced for convenience.

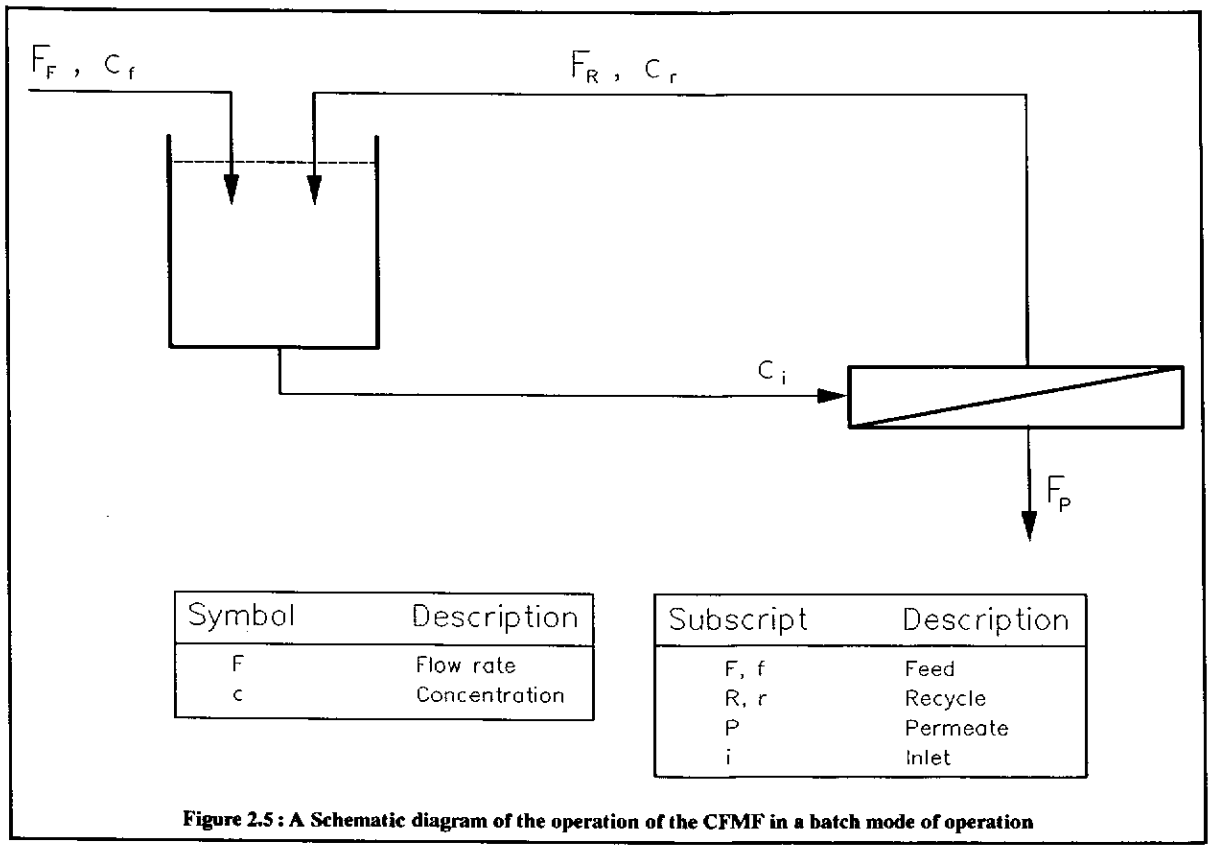

Figure 2.5 : A Schematic diagram of the operation of the CFMF in a batch mode of operation

In the above system, the feed to the tank is controlled such that the volume in the tank is maintained at a volumetric capacity of V_t . Initially the concentration in the tank and the tube inlet will be the same namely :

$$c_i = c_f$$

If it is assumed that the concentration of solids in the permeate and deposited solids in the tube is negligible, and that the permeate production capacity (F_p) is a fixed external design parameter then after a given cycle time of t_c the mass of solids in the tank would have increased to :

$$Total\ Solids = V_t c_f + F_p c_f t_c \qquad (A.7)$$

This would give an inlet concentration of :

$$c_i = \frac{V_i c_f + F_p c_f t_c}{V_i} \tag{A.8}$$

Re-arranging Eqn. (A.8) yields Eqn. (2.24) :

$$c_i = c_f \times \left[1 + \frac{F_p \ t_c}{V_i} \right] \tag{2.24}$$

Appendix B

Particle Size Analysis

The bentonite / kaolin slurry used in this study was passed through a HIAC/ROYCO Particle Counter. Below is the particle population distribution curve obtained from the raw data outputed by the counter.

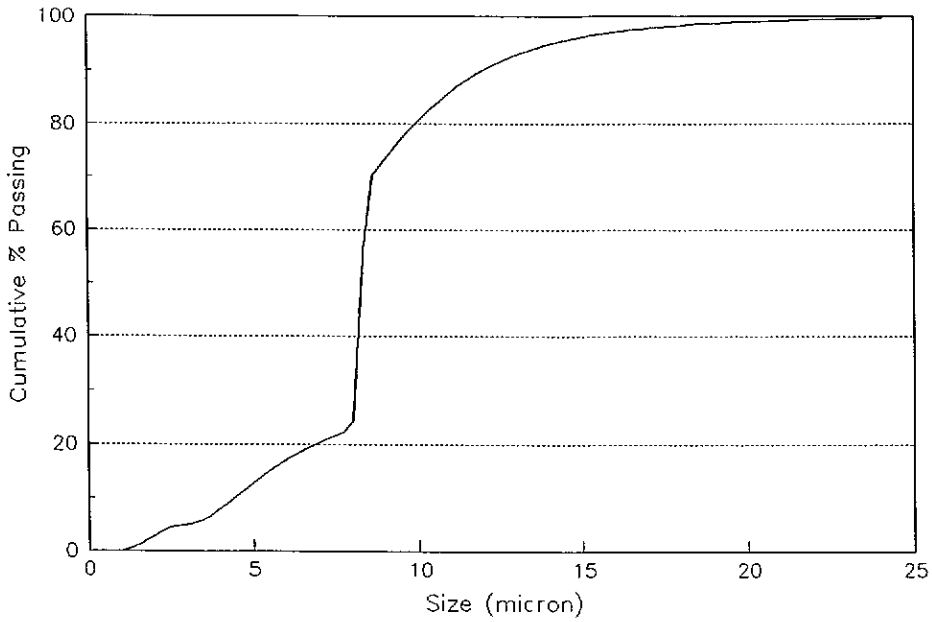

Figure B.1 : Cumulative % passing curve of the bentonite / kaolin slurry used

The instrument calculated the following means :

Arithmetic mean : 8,46 µm

Volume mean : 9,81 µm

Appendix C

Turbidity Calibration

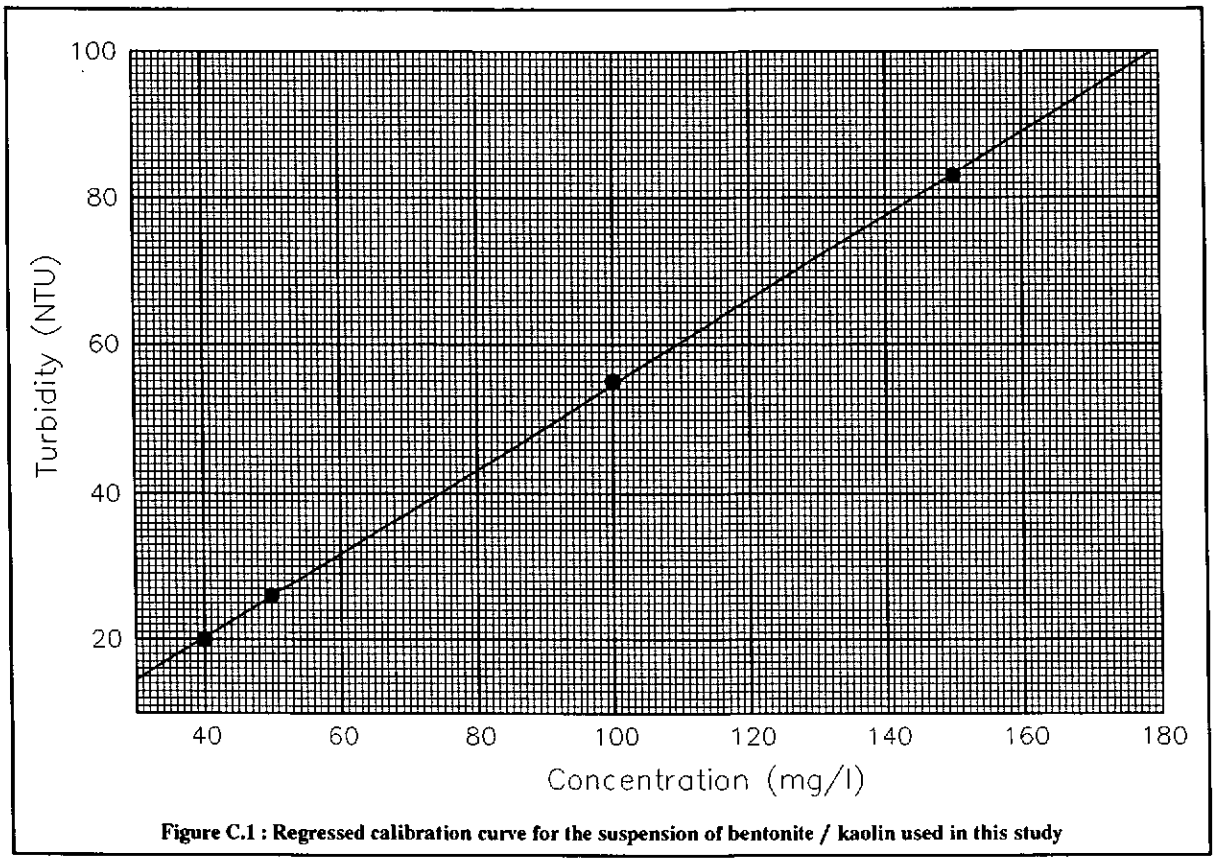

Figure C.1 : Regressed calibration curve for the suspension of bentonite / kaolin used in this study

The following equation was fitted to the data by regression :

$$Turbidity = 0,573 \cdot Concentration - 2,682$$

The sample coefficient of determination was found to be 0,99989

The concentration of samples that fell outside the limits of the turbidity or concentration range was determined by serial dilution.

Appendix D

Experimental Results

Below are listed the experimental raw data for both the CFMF and the DEMF. The flux and turbidity results are presented together with the experimental conditions. Experiments which were abandoned or the results discarded have been omitted. The regressed constants for each flux curve are also presented.

1. CFMF Results

The CFMF results listed below show 4 constants : A, B, C and D. These correspond to the regressed curve (Eqn. 4.2) discussed in Sec. 4.7.4. The form is presented below :

$$\frac{dV_a}{dt} = \frac{A}{\sqrt{t+C}} + B + \frac{D}{t}$$

The raw data below was regressed against the above equation and the 4 constants obtained. The regressed curve was plotted in all graphs presented in the main body of this dissertation.

CFMF - Run 8	
Inlet concentration (mg/ℓ)	76
Superficial inlet velocity (m/s)	1,8
Outlet pressure (kPa)	200
Temperature (°C)	30
Tube area (m^2)	0,0684
Constant A	831,5435
Constant B	36,0945
Constant C	138,6192
constant D	613,1414

Time from start-up (min)	Permeate flux (ℓ/m^2h)	Permeate turbidity (NTU)
4	252,6	1,20
10	169,3	0,35
17	143,0	0,25
25	128,9	0,26
35	118,4	0,26
60	102,6	0,20
75	97,4	0,25
154	86,0	0,25
211	82,5	0,26
269	78,1	0,28
415	75,0	0,26
605	74,3	0,20
1 324	57,9	0,18
1 506	56,7	0,20
1 712	55,3	-
1 897	53,8	0,17

CFMF - Run 9	
Inlet concentration (mg/ℓ)	82
Superficial inlet velocity (m/s)	1,8
Outlet pressure (kPa)	300
Temperature (°C)	30
Tube area (m^2)	0,0684
Constant A	307,2615
Constant B	52,4895
Constant C	17,8566
Constant D	508,5106

Time from start-up (min)	Permeate flux (ℓ/m^2h)	Permeate turbidity (NTU)
4	244,7	22
9	170,2	0,93
14	142,1	-
23	121,9	0,39
33	111,4	0,25
38	107,9	0,17
79	88,6	0,18
170	78,9	0,20
444	68,4	0,18
525	67,1	-
721	63,6	-
1 215	61,4	-

CFMF - Run 10	
Inlet concentration (mg/ℓ)	310
Superficial inlet velocity (m/s)	1,8
Outlet pressure (kPa)	200
Temperature (°C)	30
Tube area (m^2)	0,0684
Constant A	716,77
Constant B	26,8746
Constant C	102,1693
Constant D	350,3534

Time from start-up (min)	Permeate flux (ℓ/m^2h)	Permeate turbidity (NTU)
5	164,5	1,2
11	129,8	0,47
16	114,0	0,26
21	107,9	0,22
30	100,9	0,18
45	92,9	0,25
75	85,1	-
105	79,8	0,18
232	67,5	0,23
310	63,5	0,23
368	61,4	0,16
1 445	45,2	0,13
1 656	44,5	0,16
1 753	43,4	0,15

CFMF - Run 11	
Inlet concentration (mg/ℓ)	314
Superficial inlet velocity (m/s)	1,8
Outlet pressure (kPa)	300
Temperature (°C)	30
Tube area (m^2)	0,0684
Constant A	590,2528
Constant B	27,5263
Constant C	84,0873
Constant D	348,2659

Time from start-up (min)	Permeate flux (ℓ/m^2h)	Permeate turbidity (NTU)
5	155,3	2,1
10	124,6	0,56
15	114,9	0,30
20	102,6	0,25
30	93,0	0,38
40	88,2	0,24
50	84,6	0,17
60	82,0	0,31
90	77,6	0,19
195	64,9	0,20
390	55,3	0,24
1 017	45,3	-

CFMF - Run 12	
Inlet concentration (mg/ℓ)	162
Superficial inlet velocity (m/s)	1,8
Outlet pressure (kPa)	200
Temperature (°C)	30
Tube area (m^2)	0,0684
Constant A	824,0977
Constant B	29,7469
Constant C	166,4007
Constant D	562,5819

Time from start-up (min)	Permeate flux (ℓ/m^2h)	Permeate turbidity (NTU)
5	204,4	4,4
10	149,1	1,6
20	120,2	0,55
25	110,5	0,34
35	102,6	0,31
45	98,2	0,34
60	94,7	0,33
106	86,0	0,23
151	79,4	-
381	66,4	0,23
525	61,7	0,22
1 236	53,2	-
1 548	49,4	0,24

CFMF - Run 13	
Inlet concentration (mg/ℓ)	163
Superficial inlet velocity (m/s)	2,3
Outlet pressure (kPa)	200
Temperature (°C)	30
Tube area (m^2)	0,0684
Constant A	839,0638
Constant B	33,7628
Constant C	226,0661
Constant D	514,1356

Time from start-up (min)	Permeate flux (ℓ/m^2h)	Permeate turbidity (NTU)
5	185,1	0,92
10	144,7	0,48
20	116,7	0,40
30	104,4	0,33
40	96,5	0,32
50	94,7	0,27
70	87,7	0,27
90	86,0	0,39
315	70,6	0,26
672	64,5	0,34
1 406	55,7	0,28
1 532	53,7	0,28
1 728	52,2	0,27

CFMF - Run 14	
Inlet concentration (mg/ℓ)	610
Superficial inlet velocity (m/s)	2,3
Outlet pressure (kPa)	200
Temperature (°C)	30
Tube area (m^2)	0,0684
Constant A	485,7217
Constant B	32,9505
Constant C	146,5925
Constant D	180,0713

Time from start-up (min)	Permeate flux (ℓ/m^2h)	Permeate turbidity (NTU)
5	105,3	1,1
10	90,4	0,73
15	85,1	0,62
20	79,8	0,44
30	75,9	0,34
40	72,8	0,36
50	70,6	0,35
65	69,3	0,26
123	63,6	0,28
220	59,1	0,24
400	54,4	0,44
1 414	45,3	0,25
1 574	45,0	0,30
2 000	43,3	0,24
2 164	43,2	0,23

CFMF - Run 15	
Inlet concentration (mg/ℓ)	158
Superficial inlet velocity (m/s)	1,8
Outlet pressure (kPa)	200
Temperature (°C)	30
Tube area (m^2)	0,0665
Constant A	782,4967
Constant B	31,027
Constant C	109,0478
Constant D	613,3132

Time from start-up (min)	Permeate flux (ℓ/m^2h)	Permeate turbidity (NTU)
5	217,4	1,2
10	166,0	0,37
15	144,4	0,39
20	135,3	0,43
25	124,5	0,31
30	118,2	0,37
35	113,7	0,44
45	106,5	0,27
50	103,8	0,27
60	100,2	0,29
75	95,6	0,33
106	90,2	0,29
160	83,0	0,27
235	75,3	0,30
282	73,1	0,30
365	69,5	0,28
676	60,0	0,34
1 285	52,8	0,36
1 512	51,0	0,30
1 622	49,6	0,32

CFMF - Run 16	
Inlet concentration (mg/ℓ)	156
Superficial inlet velocity (m/s)	1,8
Outlet pressure (kPa)	200
Temperature (°C)	30
Tube area (m^2)	0,0665
Constant A	622,2925
Constant B	33,9383
Constant C	98,4712
Constant D	575,2467

Time from start-up (min)	Permeate flux (ℓ/m^2h)	Permeate turbidity (NTU)
5	197,6	1,2
10	155,2	0,66
15	133,5	0,37
20	121,8	0,35
25	113,7	0,36
30	107,4	0,35
40	100,2	0,34
282	67,2	0,26
365	64,5	0,27
466	61,4	0,33
498	60,5	0,34
563	59,1	0,43
660	57,3	-
1 219	52,8	0,36
1 308	51,9	0,37
1 441	49,6	-
1 515	49,3	-
1 656	48,7	0,41

CFMF - Run 17	
Inlet concentration (mg/ℓ)	158
Superficial inlet velocity (m/s)	1,8
Outlet pressure (kPa)	200
Temperature (°C)	30
Tube area (m^2)	0,0665
Constant A	731,4155
Constant B	31,6467
Constant C	109,1622
Constant D	475,0772

Time from start-up (min)	Permeate flux (ℓ/m^2h)	Permeate turbidity (NTU)
5	189,5	1,2
10	148,9	0,36
15	133,5	0,39
20	120,0	0,41
25	113,7	-
30	108,3	0,27
40	102,0	0,36
50	99,2	0,40
60	95,6	0,40
80	90,2	0,34
128	83,0	-
338	67,2	0,35
476	63,6	-
845	56,4	0,44
1 443	50,5	0,19
1 609	49,2	0,36

CFMF - Run 19	
Inlet concentration (mg/ℓ)	617
Superficial inlet velocity (m/s)	1,3
Outlet pressure (kPa)	200
Temperature (°C)	30
Tube area (m^2)	0,0665
Constant A	780,9624
Constant B	12,8999
Constant C	82,8127
Constant D	256,5777

Time from start-up (min)	**Permeate flux** (ℓ/m^2h)	**Permeate turbidity** (NTU)
5	147,1	1,1
10	120,0	0,40
15	109,2	0,34
20	104,7	0,33
25	97,4	0,31
30	95,6	0,27
40	88,4	0,30
50	85,7	0,25
60	82,6	0,31
121	69,0	-
184	61,8	-
328	53,2	-
480	46,5	0,22
1 288	34,3	0,20
1 445	32,7	-
1 932	30,5	-

CFMF - Run 20	
Inlet concentration (mg/ℓ)	164
Superficial inlet velocity (m/s)	1,3
Outlet pressure (kPa)	200
Temperature (°C)	30
Tube area (m^2)	0,0665
Constant A	867,9707
Constant B	25,4274
Constant C	74,0976
Constant D	560,3019

Time from start-up (min)	Permeate flux (ℓ/m^2h)	Permeate turbidity (NTU)
5	233,7	0,85
10	175,9	0,35
15	157,0	0,28
20	142,6	0,29
25	136,2	0,26
30	130,0	0,27
41	120,0	0,23
50	113,7	0,23
60	109,2	0,25
122	89,3	0,24
149	86,6	0,20
202	81,2	-
352	69,9	0,23
497	64,1	-
585	60,9	0,29
747	56,4	-
1 313	48,3	0,24

CFMF - Run 21	
Inlet concentration (mg/ℓ)	167
Superficial inlet velocity (m/s)	2,3
Outlet pressure (kPa)	200
Temperature (°C)	30
Tube area (m^2)	0,0665
Constant A	806,4196
Constant B	37,055
Constant C	170,2012
Constant D	492,5585

Time from start-up (min)	Permeate flux (ℓ/m^2h)	Permeate turbidity (NTU)
5	180,5	0,84
10	149,8	0,43
15	132,6	0,26
20	121,8	0,31
25	115,5	0,24
30	112,8	0,25
40	105,6	0,22
50	102,0	0,32
60	96,5	-
110	88,4	-
130	86,6	0,34
414	72,2	0,31
871	63,2	-
1 517	56,8	-
1 730	55,6	0,23

CFMF - Run 22	
Inlet concentration (mg/ℓ)	75
Superficial inlet velocity (m/s)	1,3
Outlet pressure (kPa)	200
Temperature (°C)	30
Tube area (m^2)	0,0665
Constant A	668,2737
Constant B	33,9682
Constant C	46,1777
Constant D	486,5574

Time from start-up (min)	Permeate flux (ℓ/m^2h)	Permeate turbidity (NTU)
5	226,5	0,40
10	177,7	0,35
15	155,2	0,26
20	142,6	0,28
25	131,7	0,25
30	125,4	0,25
40	116,4	0,23
50	108,3	0,25
60	103,8	0,26
90	92,9	0,30
140	86,6	-
216	78,5	0,30
292	74,4	-
395	69,5	-
543	65,0	0,17
1 300	53,3	0,28
1 863	46,9	-

CFMF - Run 23	
Inlet concentration (mg/ℓ)	582
Superficial inlet velocity (m/s)	1,8
Outlet pressure (kPa)	200
Temperature (°C)	30
Tube area (m^2)	0,0665
Constant A	582,1695
Constant B	38,4899
Constant C	84,4488
Constant D	281,2687

Time from start-up (min)	Permeate flux (ℓ/m^2h)	Permeate turbidity (NTU)
5	155,2	1,1
10	129,0	0,64
15	118,2	0,36
20	111,0	0,35
25	104,7	0,32
30	99,2	-
40	96,5	-
80	87,5	-
112	81,7	0,3
172	76,2	-
238	72,5	-
385	67,7	0,22
640	60,9	-
1 373	53,2	0,26

CFMF - Run 24	
Inlet concentration (mg/ℓ)	615
Superficial inlet velocity (m/s)	1,8
Outlet pressure (kPa)	200
Temperature (°C)	30
Tube area (m^2)	0,0665
Constant A	545,6614
Constant B	28,6614
Constant C	77,4869
Constant D	206,1617

Time from start-up (min)	Permeate flux (ℓ/m^2h)	Permeate turbidity (NTU)
5	129,0	-
10	109,2	0,77
15	100,2	0,44
25	90,2	0,31
30	88,4	0,31
40	83,7	-
50	81,2	0,33
65	76,2	-
143	67,1	0,35
238	60,5	-
448	53,7	0,20
540	51,4	-
579	50,1	-
1 158	43,8	0,21
1 618	42,2	0,20

CFMF - Run 25	
Inlet concentration (mg/ℓ)	82
Superficial inlet velocity (m/s)	1,8
Outlet pressure (kPa)	200
Temperature (°C)	30
Tube area (m^2)	0,0665
Constant A	489,1805
Constant B	42,8537
Constant C	46,8349
Constant D	519,311

Time from start-up (min)	**Permeate flux** (ℓ/m^2h)	**Permeate turbidity** (NTU)
5	216,5	0,64
10	163,3	0,43
15	143,5	0,31
20	130,8	-
25	120,9	0,27
30	114,6	-
40	104,7	-
50	98,3	-
151	79,8	-
205	76,7	0,22
274	72,5	-
403	70,7	-
441	69,5	-
1 443	54,6	0,27
1 545	54,1	-

CFMF - Run 26	
Inlet concentration (mg/ℓ)	304
Superficial inlet velocity (m/s)	1,8
Outlet pressure (kPa)	200
Temperature (°C)	30
Tube area (m^2)	0,0665
Constant A	790,4498
Constant B	26,9671
Constant C	88,4823
Constant D	370,977

Time from start-up (min)	Permeate flux (ℓ/m^2h)	Permeate turbidity (NTU)
5	182,3	0,58
10	145,3	0,35
15	128,1	0,27
20	120,9	-
25	116,4	-
30	111,9	-
40	107,4	0,27
50	101,1	-
60	97,4	-
96	89,3	-
181	77,1	-
276	69,5	0,23
786	54,5	-
1 615	46,2	0,22

CFMF - Run 27	
Inlet concentration (mg/ℓ)	448
Superficial inlet velocity (m/s)	1,8
Outlet pressure (kPa)	200
Temperature (°C)	30
Tube area (m^2)	0,0665
Constant A	753,0522
Constant B	25,3256
Constant C	62,0132
Constant D	311,836

Time from start-up (min)	**Permeate flux** (ℓ/m^2h)	**Permeate turbidity** (NTU)
5	178,6	1,1
10	146,2	0,47
15	132,6	0,33
20	124,5	0,35
25	118,2	-
30	113,7	0,24
40	108,3	-
50	102,9	-
60	97,4	0,25
115	84,8	-
245	70,8	-
537	59,1	-
637	56,4	0,22
881	52,3	-
1 549	45,6	-

CFMF - Run 28	
Inlet concentration (mg/ℓ)	591
Superficial inlet velocity (m/s)	1,3
Outlet pressure (kPa)	200
Temperature (°C)	30
Tube area (m^2)	0,0665
Constant A	628,3727
Constant B	17,7378
Constant C	82,349
Constant D	197,5961

Time from start-up (min)	Permeate flux (ℓ/m^2h)	Permeate turbidity (NTU)
5	123,6	0,82
10	103,8	0,50
15	97,4	0,35
20	90,2	0,24
25	85,7	0,33
30	83,0	-
40	79,4	0,26
50	74,9	0,44
61	72,6	-
135	61,4	0,23
252	53,7	-
547	43,8	-
670	41,1	0,21
1 257	34,6	-

CFMF - Run 29	
Inlet concentration (mg/ℓ)	608
Superficial inlet velocity (m/s)	2,3
Outlet pressure (kPa)	200
Temperature (°C)	30
Tube area (m^2)	0,0665
Constant A	743,8308
Constant B	40,9136
Constant C	235,9266
Constant D	185,7543

Time from start-up (min)	**Permeate flux** (ℓ/m^2h)	**Permeate turbidity** (NTU)
5	125,4	1,1
10	106,5	0,48
15	102,0	0,30
20	97,4	-
25	94,7	0,29
30	92,0	0,32
40	90,2	-
85	83,5	0,23
172	78,5	-
452	70,4	-
890	63,6	-
1 387	59,1	0,19

CFMF - Run 30	
Inlet concentration (mg/ℓ)	80
Superficial inlet velocity (m/s)	2,3
Outlet pressure (kPa)	200
Temperature (°C)	30
Tube area (m^2)	0,0665
Constant A	331,7167
Constant B	49,6431
Constant C	45,1951
Constant D	676,3908

Time from start-up (min)	Permeate flux (ℓ/m^2h)	Permeate turbidity (NTU)
5	229,2	1,6
10	165,1	1,1
15	134,4	-
20	128,1	0,50
25	117,3	-
30	111,0	0,22
40	102,0	0,21
50	96,5	0,41
60	91,1	-
144	77,1	-
330	70,4	0,30
475	68,1	-
1 215	59,5	-
1 305	58,6	0,21
1 446	57,7	-

2. DEMF Results

The DEMF results listed below show 3 constants : X, Y, Z. The constants represent the value for the regressed parameters for Eqn. 4.1. The theoretical basis for the above equation was outlined in Sec. 4.7.4. Eqn. 4.1 has been reproduced below :

$$\frac{dV_a}{dt} = \frac{X}{\sqrt{t+Z}} + Y$$

The raw data listed below was used to regress against Eqn. 2.10 to obtain the constants X, Y and Z. The regressed curve was plotted in all graphs presented in the main body of the dissertation.

DEMF - Run D1		
Inlet concentration (mg/ℓ)	132	
Precoated (Yes/No)	No	
Outlet pressure (kPa)	300	
Temperature (°C)	30	
Tube area (m^2)	0,0493	
Constant X	1247,8746	
Constant Y	10,1872	
Constant Z	2,7557	
Time from start-up (min)	**Permeate flux** (ℓ/m^2h)	**Permeate turbidity** (NTU)
5	458,8	7,8
75	145,5	5,2
135	124,1	3,8
215	98,6	1,7
265	90,1	0,95
315	73,0	0,77
745	57,2	0,32
1 425	42,6	0,22
1 785	40,2	0,21
2 035	37,7	0,19

DEMF - Run D2		
Inlet concentration (mg/ℓ)	132	
Precoated (Yes/No)	No	
Outlet pressure (kPa)	300	
Temperature (°C)	30	
Tube area (m^2)	0,0493	
Constant X	1481,2794	
Constant Y	5,709	
Constant Z	8,4003	
Time from start-up (min)	**Permeate flux** (ℓ/m^2h)	**Permeate turbidity** (NTU)
5	410,1	5,4
75	166,7	3,5
135	132,7	2,8
195	109,5	1,2
510	69,4	0,36
1 210	47,5	0,28
1 675	42,6	0,19

DEMF - Run D3		
Inlet concentration (mg/ℓ)	132	
Precoated (Yes/No)	No	
Outlet pressure (kPa)	200	
Temperature (°C)	30	
Tube area (m^2)	0,0551	
Constant X	1111,0096	
Constant Y	3,571	
Constant Z	11,7868	
Time from start-up (min)	**Permeate flux** (ℓ/m^2h)	**Permeate turbidity** (NTU)
5	279,9	5,2
77	117,6	0,23
122	101,3	0,30
255	74,0	0,28
695	42,5	0,17
1 380	34,8	0,19

DEMF - Run D4	
Inlet concentration (mg/ℓ)	132
Precoated (Yes/No)	No
Outlet pressure (kPa)	200
Temperature (°C)	30
Tube area (m^2)	0,0551
Constant X	977,9304
Constant Y	9,2719
Constant Z	5,2742

Time from start-up (min)	Permeate flux (ℓ/m^2h)	Permeate turbidity (NTU)
5	315,8	20
48	139,4	5,1
75	117,6	3,8
198	80,6	0,27
528	52,3	0,23
745	44,9	-
1096	38,5	-
1523	33,8	0,25

DEMF - Run D5		
Inlet concentration (mg/ℓ)	137	
Precoated (Yes/No)	No	
Outlet pressure (kPa)	300	
Temperature (°C)	30	
Tube area (m^2)	0,0551	
Constant X	1044,443	
Constant Y	8,6192	
Constant Z	8,4	
Time from start-up (min)	**Permeate flux** (ℓ/m^2h)	**Permeate turbidity** (NTU)
4	307,1	9,9
60	128,5	2,3
140	92,6	1,1
180	86,0	0,87
230	79,5	1,1
275	70,2	0,93
590	47,9	0,33
875	43,6	-
1 245	38,1	0,23
1 383	37,0	0,25

DEMF - Run D6		
Inlet concentration (mg/ℓ)	132	
Precoated (Yes/No)	No	
Outlet pressure (kPa)	400	
Temperature (°C)	30	
Tube area (m^2)	0,0551	
Constant X	1362,911	
Constant Y	3,8916	
Constant Z	37,0749	
Time from start-up (min)	**Permeate flux** (ℓ/m^2h)	**Permeate turbidity** (NTU)
7	280,9	12
102	118,7	1,5
179	98,0	1,1
260	84,9	0,9
513	59,9	0,6
1 345	40,3	0,31
1 518	38,1	0,29
1 639	38,1	0,27

DEMF - Run D7		
Inlet concentration (mg/ℓ)	132	
Precoated (Yes/No)	No	
Outlet pressure (kPa)	200	
Temperature (°C)	30	
Tube area (m^2)	0,0551	
Constant X	896,4826	
Constant Y	18,3283	
Constant Z	5,6718	
Time from start-up (min)	**Permeate flux** (ℓ/m^2h)	**Permeate turbidity** (NTU)
5	292,9	8,0
55	132,8	1,0
145	91,5	0,60
365	65,3	0,26
1 145	44,6	0,25

DEMF - Run D8	
Inlet concentration (mg/ℓ)	263
Precoated (Yes/No)	No
Outlet pressure (kPa)	200
Temperature (°C)	30
Tube area (m^2)	0,0551
Constant X	848,0608
Constant Y	4,2481
Constant Z	17,5727

Time from start-up (min)	Permeate flux (ℓ/m^2h)	Permeate turbidity (NTU)
5	184,0	6,8
45	108,9	0,75
85	87,1	0,31
120	78,4	0,29
680	37,0	0,23
1 445	26,1	0,23

DEMF - Run D9		
Inlet concentration (mg/ℓ)	263	
Precoated (Yes/No)	No	
Outlet pressure (kPa)	400	
Temperature (°C)	30	
Tube area (m^2)	0,0551	
Constant X	970,937	
Constant Y	5,7358	
Constant Z	9,4208	
Time from start-up (min)	**Permeate flux** (ℓ/m^2h)	**Permeate turbidity** (NTU)
5	261,3	17
55	126,3	-
115	93,6	3,2
592	45,5	-
1 135	31,6	0,14
1 540	30,5	0,11
2 715	29,4	0,13
4 120	26,1	0,11
4 360	18,5	0,11

DEMF - Run D10	
Inlet concentration (mg/ℓ)	270
Precoated (Yes/No)	No
Outlet pressure (kPa)	300
Temperature (°C)	30
Tube area (m^2)	0,0551
Constant X	917,5257
Constant Y	4,1795
Constant Z	7,3318

Time from start-up (min)	Permeate flux (ℓ/m^2h)	Permeate turbidity (NTU)
5	274,4	30
40	122,0	5,5
105	91,5	9,5
170	76,2	5,7
340	54,4	1,2
445	47,9	0,98
1 215	32,7	0,18
1 420	29,4	0,13
1 585	28,3	0,11
2 660	21,8	0,11
3 325	18,5	0,11

DEMF - Run D12		
Inlet concentration (mg/ℓ)	76	
Precoated (Yes/No)	No	
Outlet pressure (kPa)	200	
Temperature (°C)	30	
Tube area (m^2)	0,0539	
Constant X	1050,249	
Constant Y	17,6656	
Constant Z	-0,0325	
Time from start-up (min)	**Permeate flux** (ℓ/m^2h)	**Permeate turbidity** (NTU)
7	420,8	16
33	188,1	6
97	122,4	2,5
165	103,5	1,3
275	82,4	0,45
360	75,7	0,38
558	65,7	0,27
720	56,8	0,27
1 315	44,5	0,25
1 728	42,3	0,25

DEMF - Run D13		
Inlet concentration (mg/ℓ)	266	
Precoated (Yes/No)	No	
Outlet pressure (kPa)	200	
Temperature (°C)	30	
Tube area (m^2)	0,0539	
Constant X	827,999	
Constant Y	1,4217	
Constant Z	5,9908	
Time from start-up (min)	**Permeate flux** (ℓ/m^2h)	**Permeate turbidity** (NTU)
5	253,8	32
48	109,1	6,6
133	71,2	2,3
203	56,8	0,32
382	44,5	0,26
1 388	30,1	0,24
2 743	15,6	0,34

DEMF - Run D14		
Inlet concentration (mg/ℓ)	147	
Precoated (Yes/No)	No	
Outlet pressure (kPa)	200	
Temperature (°C)	30	
Tube area (m^2)	0,0539	
Constant X	977,295	
Constant Y	6,4177	
Constant Z	2,1083	
Time from start-up (min)	**Permeate flux** (ℓ/m^2h)	**Permeate turbidity** (NTU)
4	413,0	3,8
9	289,4	3,0
17	224,9	1,7
25	190,4	1,3
37	167,0	1,1
51	139,1	1,0
85	113,5	0,77
120	98,0	0,61
610	45,6	0,36
1 330	33,0	0,30

DEMF - Run D15	
Inlet concentration (mg/ℓ)	580
Precoated (Yes/No)	No
Outlet pressure (kPa)	200
Temperature (°C)	30
Tube area (m^2)	0,0539
Constant X	665,8562
Constant Y	-0,5676
Constant Z	6,8041

Time from start-up (min)	Permeate flux (ℓ/m^2h)	Permeate turbidity (NTU)
5	195,9	44
20	125,8	13
35	100,2	5,5
190	47,3	0,68
250	41,2	0,40
1 141	18,9	0,30
1 345	18,2	0,31
1 615	16,5	0,30
2 635	11,9	0,32

DEMF - Run D16	
Inlet concentration (mg/ℓ)	148
Precoated (Yes/No)	Yes
Outlet pressure (kPa)	200
Temperature (°C)	30
Tube area (m^2)	0,0539
Constant X	1137,645
Constant Y	-0,794
Constant Z	-1,3917

Time from start-up (min)	Permeate flux (ℓ/m^2h)	Permeate turbidity (NTU)
4	694,6	0,47
9	418,6	0,35
15	316,1	0,40
25	237,1	0,45
35	200,4	0,38
67	140,3	0,40
165	91,3	0,34
200	70,7	0,43
367	59,6	0,42
1 370	30,8	0,36

DEMF - Run D17		
Inlet concentration (mg/ℓ)	146	
Precoated (Yes/No)	Yes	
Outlet pressure (kPa)	200	
Temperature (°C)	30	
Tube area (m^2)	0,0539	
Constant X	1267,018	
Constant Y	0,9445	
Constant Z	-0,6508	
Time from start-up (min)	**Permeate flux** (ℓ/m^2h)	**Permeate turbidity** (NTU)
3	819,3	0,34
9	449,7	0,32
14	354,0	0,33
24	267,2	0,38
39	207,1	0,34
69	152,5	0,37
99	129,1	0,35
159	99,1	0,38
262	77,4	-
890	41,2	0,39
1 144	40,1	-
1 394	35,8	0,10
1 687	31,8	-

DEMF - Run D18	
Inlet concentration (mg/ℓ)	290
Precoated (Yes/No)	Yes
Outlet pressure (kPa)	200
Temperature (°C)	30
Tube area (m^2)	0,0539
Constant X	989,5905
Constant Y	-2,7047
Constant Z	-0,9054

Time from start-up (min)	**Permeate flux** (ℓ/m^2h)	**Permeate turbidity** (NTU)
4	551,0	0,2
9	355,1	0,1
14	278,3	0,1
23	209,3	0,13
33	171,4	0,16
43	150,3	0,16
53	134,7	0,12
83	104,6	0,12
114	90,2	0,14
174	69,0	0,13
223	64,6	0,14
1 333	24,0	0,11
1 488	23,6	0,12

DEMF - Run D19	
Inlet concentration (mg/ℓ)	295
Precoated (Yes/No)	Yes
Outlet pressure (kPa)	200
Temperature (°C)	30
Tube area (m^2)	0,0539
Constant X	907,5605
Constant Y	0,246
Constant Z	-0,6821

Time from start-up (min)	Permeate flux (ℓ/m^2h)	Permeate turbidity (NTU)
4	495,4	0,28
10	300,1	0,26
15	243,8	0,22
20	207,1	0,19
30	167,0	0,23
40	144,7	-
50	130,2	0,27
75	105,8	0,27
371	46,8	0,23
607	36,2	0,23
1 164	26,9	0,25
1 363	24,9	0,24
1 618	22,9	0,30
1 975	20,9	0,28

DEMF - Run D20	
Inlet concentration (mg/ℓ)	156
Precoated (Yes/No)	Yes
Outlet pressure (kPa)	200
Temperature (°C)	30
Tube area (m^2)	0,0539
Constant X	1227,824
Constant Y	0,9074
Constant Z	-0,8369

Time from start-up (min)	Permeate flux (ℓ/m^2h)	Permeate turbidity (NTU)
5	598,9	0,35
10	408,5	0,21
15	329,5	0,23
20	283,9	0,25
30	229,3	0,21
40	198,1	0,25
50	174,8	0,24
96	126,9	0,31
184	90,2	0,32
298	71,8	0,30
1 160	36,3	0,29
1 457	33,4	0,32
1 633	31,7	0,27

DEMF - Run D21	
Inlet concentration (mg/ℓ)	591
Precoated (Yes/No)	Yes
Outlet pressure (kPa)	200
Temperature (°C)	30
Tube area (m^2)	0,0539
Constant X	705,5384
Constant Y	-8,175
Constant Z	-0,235

Time from start-up (min)	Permeate flux (ℓ/m^2h)	Permeate turbidity (NTU)
5	335,1	0,21
10	209,3	0,22
15	168,1	0,26
20	144,7	0,25
30	118,0	0,27
40	100,2	0,22
50	88,5	0,24
60	80,7	0,18
100	62,9	0,20
162	50,1	0,19
475	28,2	0,22
640	23,7	0,22
1 480	9,2	0,42

DEMF - Run D22	
Inlet concentration (mg/ℓ)	76
Precoated (Yes/No)	Yes
Outlet pressure (kPa)	200
Temperature (°C)	30
Tube area (m^2)	0,0539
Constant X	1769,33
Constant Y	-0,3347
Constant Z	-0,9895

Time from start-up (min)	Permeate flux (ℓ/m^2h)	Permeate turbidity (NTU)
5	878,3	0,32
10	594,4	0,32
15	475,3	0,28
20	406,3	0,27
25	361,8	0,29
30	327,3	0,31
40	281,6	0,26
50	252,7	0,35
60	229,3	0,33
90	185,9	0,26
136	153,6	0,27
270	108,0	0,35
491	78,5	0,32
1 220	49,4	0,32
1 740	43,0	0,30

DEMF - Run D23	
Inlet concentration (mg/ℓ)	459
Precoated (Yes/No)	Yes
Outlet pressure (kPa)	200
Temperature (°C)	30
Tube area (m^2)	0,0539
Constant X	747,5309
Constant Y	-1,5942
Constant Z	-0,5305

Time from start-up (min)	Permeate flux (ℓ/m^2h)	Permeate turbidity (NTU)
5	350,6	0,29
10	243,8	0,37
15	194,8	0,24
20	168,1	0,25
25	149,2	0,24
30	135,8	0,33
40	116,8	-
50	104,6	0,24
65	92,4	0,30
105	71,2	0,23
175	55,7	0,23
330	39,0	0,37
516	31,5	0,37
1 215	19,4	0,33
1 400	18,4	0,35
1 660	17,1	0,35

DEMF - Run D24	
Inlet concentration (mg/ℓ)	306
Precoated (Yes/No)	Yes
Outlet pressure (kPa)	200
Temperature (°C)	30
Tube area (m^2)	0,0539
Constant X	897,1777
Constant Y	-1,2008
Constant Z	-0,7097

Time from start-up (min)	Permeate flux (ℓ/m^2h)	Permeate turbidity (NTU)
4	488,7	0,24
10	298,3	0,36
15	238,2	0,35
20	204,8	0,24
25	181,4	0,18
30	165,9	0,20
40	141,4	0,34
50	126,9	0,38
60	114,7	0,35
115	81,3	-
191	62,9	0,36
324	49,0	0,38
665	33,0	0,19
1 457	22,7	-

DEMF - Run D25	
Inlet concentration (mg/ℓ)	76
Precoated (Yes/No)	Yes
Outlet pressure (kPa)	200
Temperature (°C)	30
Tube area (m^2)	0,0539
Constant X	2007,962
Constant Y	-1,3786
Constant Z	-1,3397

Time from start-up (min)	Permeate flux (ℓ/m^2h)	Permeate turbidity (NTU)
5	1040,8	0,39
10	685,7	0,38
15	542,1	0,40
20	466,4	0,36
25	415,2	0,36
30	377,4	0,22
40	323,9	0,35
50	288,3	0,35
60	260,5	-
108	190,4	0,20
210	136,9	-
312	111,3	0,35
545	82,9	0,25
775	70,1	-
1 370	53,4	-
1 575	50,1	-

DEMF - Run D26	
Inlet concentration (mg/ℓ)	155
Precoated (Yes/No)	No
Outlet pressure (kPa)	200
Temperature (°C)	30
Tube area (m^2)	0,0539
Constant X	1074,29
Constant Y	6,9686
Constant Z	0,3812

Time from start-up (min)	Permeate flux (ℓ/m^2h)	Permeate turbidity (NTU)
5	483,1	7,7
10	335,1	5,0
15	275,0	3,3
20	240,4	2,3
25	216,0	1,6
30	198,1	1,1
40	174,8	0,17
50	158,1	0,16
60	145,8	0,30
75	133,6	0,22
149	97,4	-
437	60,7	-
546	54,0	0,26
660	49,9	-
1 437	34,5	0,22
1 949	30,5	-

DEMF - Run D27	
Inlet concentration (mg/ℓ)	451
Precoated (Yes/No)	No
Outlet pressure (kPa)	200
Temperature (°C)	30
Tube area (m^2)	0,0539
Constant X	767,3001
Constant Y	-1,213
Constant Z	3,8194

Time from start-up (min)	Permeate flux (ℓ/m^2h)	Permeate turbidity (NTU)
5	257,1	5,3
10	202,6	3,5
15	177,0	3,1
20	154,7	1,8
25	142,5	-
30	132,5	2,6
40	115,8	1,2
50	104,6	0,73
60	94,6	0,60
70	88,5	0,61
80	82,4	0,55
90	77,9	0,46
181	55,1	0,22
326	41,2	0,28
430	35,1	-
585	29,8	-
1 150	21,0	0,18
1 376	19,4	-
1 675	18,1	-

DEMF - Run D28	
Inlet concentration (mg/ℓ)	73
Precoated (Yes/No)	No
Outlet pressure (kPa)	200
Temperature (°C)	30
Tube area (m^2)	0,0539
Constant X	1102,15
Constant Y	22,958
Constant Z	1,2597

Time from start-up (min)	Permeate flux (ℓ/m^2h)	Permeate turbidity (NTU)
5	484,2	9,5
10	338,4	6,5
15	288,3	5,7
20	254,9	-
25	237,1	4,4
30	216,0	3,9
40	193,7	2,8
50	178,1	2,3
60	163,6	1,8
70	155,8	1,3
88	142,5	0,61
100	134,7	0,36
346	87,9	0,27
803	64,0	-
1 455	50,5	-
1 656	48,2	0,25

DEMF - Run D29	
Inlet concentration (mg/ℓ)	280
Precoated (Yes/No)	No
Outlet pressure (kPa)	200
Temperature (°C)	30
Tube area (m^2)	0,0539
Constant X	711,5296
Constant Y	6,5478
Constant Z	5,4861

Time from start-up (min)	Permeate flux (ℓ/m^2h)	Permeate turbidity (NTU)
5	242,7	26
10	183,7	16
15	157,0	8,5
20	142,5	5,4
25	130,2	3,7
30	120,2	2,8
40	112,4	2,1
50	105,8	2,1
80	89,6	1,2
235	56,8	0,28
959	28,9	0,21
1 067	27,7	-

DEMF - Run D30	
Inlet concentration (mg/ℓ)	608
Precoated (Yes/No)	No
Outlet pressure (kPa)	200
Temperature (°C)	30
Tube area (m^2)	0,0539
Constant X	675,3866
Constant Y	-0,8677
Constant Z	6,3146

Time from start-up (min)	Permeate flux (ℓ/m^2h)	Permeate turbidity (NTU)
5	200,4	3,6
10	167,0	0,76
15	143,6	0,35
20	130,2	0,27
25	119,1	0,30
30	112,4	0,28
40	98,0	0,33
50	90,1	-
60	82,4	0,34
118	60,7	-
200	46,2	0,28
295	37,8	-
451	30,1	0,27
1 210	18,4	-
1 756	15,4	-

DEMF - Run D31	
Inlet concentration (mg/ℓ)	144
Precoated (Yes/No)	No
Outlet pressure (kPa)	200
Temperature (°C)	30
Tube area (m^2)	0,0539
Constant X	953,5562
Constant Y	9,6092
Constant Z	6,943

Time from start-up (min)	Permeate flux (ℓ/m^2h)	Permeate turbidity (NTU)
5	316,1	16
10	239,3	9,4
15	204,8	8,0
20	185,9	5,5
25	168,1	-
30	158,1	4,0
40	142,5	2,9
50	133,6	2,5
60	126,9	2,1
91	108,0	1,1
108	101,3	0,79
125	95,2	-
150	89,6	0,50
209	79,0	-
305	67,3	-
514	53,4	0,22
646	47,9	-
1 231	35,3	-
1 703	31,2	0,22